



The temperature dependence of the forbidden-hyperfine spectrum of rare earth S-state ions in cubic crystals
by Don Kay Worsencroft

A thesis submitted to the Graduate Faculty in partial fulfillment of the requirements for the degree of
DOCTOR OF PHILOSOPHY in Physics
Montana State University
© Copyright by Don Kay Worsencroft (1970)

Abstract:

The temperature dependence of the intensities of the electron paramagnetic resonance (E.P.R.) spectrum for one percent Eu^{++} impurities in fluorite crystals has been investigated. This temperature dependence has been analyzed and has been shown to result from crystal expansion due to anharmonic terms of the lattice vibrations and from the harmonic terms which modulate the crystal-field as seen by the paramagnetic electrons.

It was determined that the relative intensities between forbidden and allowed hyperfine lines varied with temperature as [formula not captured by OCR] Good agreement between the predicted temperature dependence and the experiment were found; however, the value of C based on point charge calculations was subject to some question because of crystal-field parameter values.

In the analysis of the hyperfine spectrum as it depends on spatial orientation with respect to the magnetic field, certain "forbidden" hyperfine lines, heretofore not identified, were cataloged.

THE TEMPERATURE DEPENDENCE OF THE FORBIDDEN-
HYPERFINE SPECTRUM OF RARE EARTH
S-STATE IONS IN CUBIC CRYSTALS

by

DON KAY WORSENCROFT

A thesis submitted to the Graduate Faculty in partial
fulfillment of the requirements for the degree

of

DOCTOR OF PHILOSOPHY

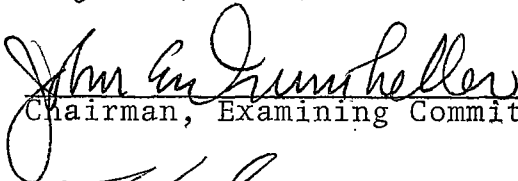
in

Physics

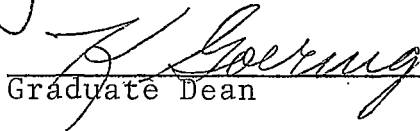
Approved:



Head, Major Department



Chairman, Examining Committee



Graduate Dean

MONTANA STATE UNIVERSITY
Bozeman, Montana

August, 1970

ACKNOWLEDGEMENTS

The author wishes to thank his government, the people of the United States and specifically the State of Montana for his educational opportunities. A traineeship from the National Aeronautics and Space Administration, the National Defense Education Act fellowship and financial assistance and equipment from the National Science Foundation were instrumental in this effort. To his advisor, Dr. J. E. Drumheller, special thanks are extended for knowledgeable instruction, wise administration and warm friendship. Thanks to Dr. David H. Dickey who constructed the machine and for the many helpful discussions. Thanks are extended to Fred Blankenburg for help with the electronics equipment and to Cecil Badgley for machine work. For the numerous acquisitions of equipment and the dependable liquid nitrogen supply, many thanks to Dr. Roy Wiegand. The writer extends appreciation to Mrs. Sheila Hight for the typescript and wonderful attention to the details in this thesis. Finally to his patient wife and children much appreciation for this wonderful opportunity.

TABLE OF CONTENTS

Chapter	Page
LIST OF TABLES	vi
LIST OF FIGURES	vii
ABSTRACT	ix
I INTRODUCTION	1
II SPLITTING OF THE $8s_{7/2}$ GROUND STATE OF Eu IN FLUORITE CRYSTALS	9
<u>Crystal Field Theory</u>	9
<u>Group Theory</u>	12
<u>Operator Equivalence</u>	17
<u>The Spin Hamiltonian</u>	20
<u>Fine Structure</u>	25
<u>Angular Dependence of Fine Structure</u>	29
III THE E.P.R. EXPERIMENT AND THE HYPERFINE INTERACTION	38
<u>Magnetic Resonance</u>	38
<u>The Hyperfine Splitting</u>	44
<u>The Calculation of the Core Hyperfine Field</u>	45
IV THE ORBIT-LATTICE INTERACTION	66
<u>Necessary Approximations</u>	66
<u>Symmetry Reduction</u>	74
<u>Crystal-Field Energy Shift Due to</u> <u>Orbit-Lattice Interaction</u>	86
V EXPERIMENTAL RESULTS	98
Corrections Due to Lattice Expansion	98

Table of Contents Continued

	Page
<u>Phonon Contribution</u>	100
APPENDIX	115
APPENDIX A. <u>GROUP THEORY</u>	115
APPENDIX B. EXPERIMENTAL EQUIPMENT	127
APPENDIX C. PHONONS	131
APPENDIX D. MECHANISM OF THE HYPERFINE INTERACTION .	139
LIST OF LITERATURE CITED	145

LIST OF TABLES

Table	Page
2.1 Operator Transformations	32
2.2 Form of Operators O_n^m	34
3.2 Analytic Form of $ P_{mm}(\mu) ^2$	59
3.3 The Line Position of $\Delta M = 3/2 \leftrightarrow 1/2$ Spectrum	65
5.1 Ratio of Forbidden to Allowed Intensities at Various Temperatures	107
A.1 Double O_h Group	121
A.2 Spherical Functions	126

LIST OF FIGURES

Figure	Page
1.1 Crystallography of CaF_2	8
2.1 X-band Spectrum of 0.1% Eu- CaF_2 at 78° Kelvin	211
2.2 Fine Structure Splitting Eu- CaF_2	23
2.3 Zero Field Matrix for Crystal-Field	26
2.4 Zero Field Splitting	27
2.5 Non-zero Field Matrix With Crystal-Field	30
2.6 The Angular Dependence of the Fine Structure	37
3.1 The Direct Absorption at X-band for $\Delta M = \frac{1}{2} \leftrightarrow -\frac{1}{2}$	43
3.2 Phase Detected Absorption $\Delta M = \frac{1}{2} \leftrightarrow -\frac{1}{2}$	43
3.3 Hyperfine Spectrum $\Delta M = \frac{1}{2} \leftrightarrow -\frac{1}{2}$ at Different Crystal Orientations.	58
3.4 Effective Field for Different M States	60
3.6 $\Delta M = \frac{1}{2} \leftrightarrow -\frac{1}{2}$ with both Eu^{151} and Eu^{153} . in Crystal	62
3.7 Forbidden Hyperfine Lines in $\Delta M = 3/2 \leftrightarrow 1/2$	64
4.1 Functional Cell of XY_8	80
4.2 Polarization Vectors in Spherical Coordinates	89
5.1 b_4 vs. Nearest Neighbor Distance	101
5.2 Thermoexpansivity of CaF_2	102

List of Figures Continued

Figure	Page
5.3 b_4 vs. Lattice Expansion	103
5.4 Ratio of Forbidden to Allowed Intensities vs. Temperature	104
5.5 Ratio of Forbidden to Allowed Intensities vs. $T \int_0^{\theta/T} x^5 (\exp x - 1)^{-1} dx$	106
B.1 Block Diagram of a Superheterodyne Spectrometer	129

ABSTRACT

The temperature dependence of the intensities of the electron paramagnetic resonance (E.P.R.) spectrum for one percent Eu^{+2} impurities in fluorite crystals has been investigated. This temperature dependence has been analyzed and has been shown to result from crystal expansion due to anharmonic terms of the lattice vibrations and from the harmonic terms which modulate the crystal-field as seen by the paramagnetic electrons.

It was determined that the relative intensities between forbidden and allowed hyperfine lines varied with temperature as

$$I_f/I_a = (I_f/I_a)_{T=0} \left(1 - CT^6 \int_0^{\Theta/T} \chi^5 [\exp \chi - 1]^{-1} d\chi \right).$$

Good agreement between the predicted temperature dependence and the experiment were found; however, the value of C based on point charge calculations was subject to some question because of crystal-field parameter values.

In the analysis of the hyperfine spectrum as it depends on spatial orientation with respect to the magnetic field, certain "forbidden" hyperfine lines, heretofore not identified, were cataloged.

CHAPTER I

INTRODUCTION

The research problem in this thesis is the investigation of the temperature dependence of the intensities of the E. P. R. spectrum lines of paramagnetic europium impurities in those cubic crystals which are, for the most part, bound by coulomb forces i.e. ionic binding.

Investigations made on Eu^{++} in CaF_2 were at first concentrated on measuring the fine structure parameters and hyperfine structure parameters, (Baker, Bleaney, and Hayes, 1958 and Lacroix, 1957). The early interest also sought to give reason for the crystal-field splitting of an S-state by an electro-static field. The theories did not give numerical agreement with experiment, but did propose possible mechanisms for the splitting (Abragam and Pryce, 1951). The spin Hamiltonian of Chapter II was introduced to account for the nature of the splitting.

These parameters were measured not calculated (Pryce, 1950).

Temperature dependent effects between paramagnetic ions and the crystal environment in which they may be placed were first studied theoretically. Waller (1932) in his paper "Über die Magnetisierung von Paramagnetischen Kristallen in Wechselfeldern," proposed two methods of

paramagnetic relaxation, spin-spin and the spin-lattice interactions. Fierz (1938), Kronig (1939) and Van Vleck (1939, 1940) developed this theory but found poor agreement between susceptibility experiments and the theory. The failure of the explanation by Van Vleck has been attributed to the chemistry of the alums to which he applied the theory (Manenkov and Orbach, 1966).

The advent of electron paramagnetic resonance (E.P.R.) experiments, introduced by Zavoisky (1945, 1946) and developed mainly by the Clarendon Laboratory at Oxford, gave a new tool to relaxation measurements. A renewed interest in this field was a result of a paper by Finn, Orbach, and Wolf (1961). They proposed an additional process, the Orbach process, for relaxation. Van Vleck (1940) had considered the "direct" process for spin-lattice relaxation and a "Raman" process. The direct process refers to a first order effect involving a single phonon exchange between excited and ground state configurations of paramagnetic ions. The Raman process is a second order effect involving two phonons and a virtual process which allows the entire phonon spectrum to interact between two paramagnetic states. Orbach's process was simply a resonance fluorescence type process of two phonons which unlike the Raman

process includes conservation of energy.

Finn, Orbach, and Wolf's work revived an interest in spin-lattice relaxation which led to the consideration of other temperature dependent effects between phonons and the paramagnets. Blume and Orbach (1962) applied the method to S-state paramagnets and developed an orbit-lattice interaction for S-state transition metal ions. In this work they also proposed a form for the ground state splitting by a crystal field which allowed them to predict phonon contributions to the temperature dependence of crystal field splitting. The crystal field splitting in S-state transition metal ions is small while the hyperfine splitting is large. The crystal field splitting of rare-earth S-state ions is large. Eu^{++} in fluorite crystals exhibits both a large crystal field splitting and large hyperfine splitting making this ion ideal for a study of temperature dependent effects.

Temperature dependent effects of crystal field parameters have been measured by Rewaj (1968) and Horai (1964). Rewaj assumed the dependence to be due solely to lattice expansion and predicted the dependence of the parameter b_4 to be

$$b_4 = KR^{-16.3} (\text{CaF}_2: \text{Eu}^{++}) \quad 1,1$$

where R is the nearest neighbor ion separation.. Walsh, Jeener, and Bloembergen (1965) examined the dependence of iron-group S-state ion parameters both as to temperature dependence and their dependence on R directly by subjecting the crystal to hydrostatic pressure. Because of the small value of b_4 it was not possible to tell if orbit-lattice effects contributed to the temperature dependence. Hurren, Nelson, Larson, and Gardner (1969), made similar hydrostatic pressure measurements for the crystal field parameter of $\text{CaF}_2: \text{Eu}^{++}$ and found

$$b_4 = KR^{-8.9} \quad 1.2$$

The difference between Rewaj's results and Hurren, et.al., suggest an orbit-lattice contribution to b_4 .

In this work the dependence of b_4 on the orbit-lattice interaction was examined by measuring the temperature dependence of the intensities of the hyperfine spectrum. A similar investigation for the iron-group S-state ion was undertaken by Shrivastava and Drumheller (1969). Bir, Bulikov, and Sochara (1965) have shown the angular dependence of the hyperfine intensities depend quadratically on the crystal field parameter. In Bir's method the hyperfine transitions depend on the strong magnetic field

at the nucleus created not so greatly by the laboratory magnet but by the electronic state of the 4f shell of spin 7/2. This field, the effective field is

$$H_{\text{eff}} = \frac{A}{g_n \beta_n} \langle \Psi_e | \vec{S} | \Psi_e \rangle . \quad 1.3$$

A is the experimentally measured hyperfine coupling constant $g_n \beta_n$ is the nuclear magneton, $|\Psi_e\rangle$ are the electronic wave functions and \vec{S} the spin operator for the electrons. In Chapter II the wave functions Ψ_e will be developed. Then in Chapter III the induced field method of Bir will be developed for the Eu^{++} ion in fluorite crystals. During this investigation some transitions predicted by the theory but heretofore not reported were examined. The results of this investigation are included at the end of Chapter III.

The orbit-lattice interaction was largely developed by Menne, Ames, and Lee (1968). Menne used the interaction to explain the temperature dependence of the hyperfine coupling constant A. Chapter IV will be devoted to expounding the orbit-lattice interaction and applying it to predict the temperature dependence of the hyperfine spectrum.

The results displayed in Chapter V include corrections

for crystal expansion extracted from the hydrostatic pressure measurements of Hurren. Very clear spectra were obtained in this investigation due to using the single isotope Eu^{151} . The sample obtained from A. E. C. was 96.67% Eu^{151} and 3.33% Eu^{153} with trace amounts of rare earth and other metal ions present. The crystals were grown by Optovac, Inc.

The crystal structure chosen to produce a cubic environment for the paramagnetic ion was fluorite. Examples of a fluorite crystal are CaF_2 , BaF_2 , and SrF_2 . The unit cell of fluorite is face-centered cubic. The basis is usually an alkaline earth-halide molecule of the form ab_2 . The cation a of the basis is located at (0,0,0) corner of the cube. An anion b is located at each position $(1/4, 1/4, 1/4)$ and $(3/4, 3/4, 3/4)$ on the diagonal of the cube.

The fluorite structure is referred to as eight-coordinated because each cation is situated in an environment of eight nearest neighbors, all anions being located at the eight corners of a cube (See Fig. 1). The crystal structure is also referred to as XY_8 to include in the reference structures of this type where the bonding may not be ionic and the X's and Y's can be a molecular

structure such as water.

Europium ions were chosen for the paramagnetic impurity because the doubly ionized atoms replace the cation of XY_8 without requiring a charge compensation elsewhere in the crystal which would change the environment of some sites from cubic to axial. The triple ionized gadolinium ion would also have an $^8S_{7/2}$ ground state such as europium but presented charge compensation problems.

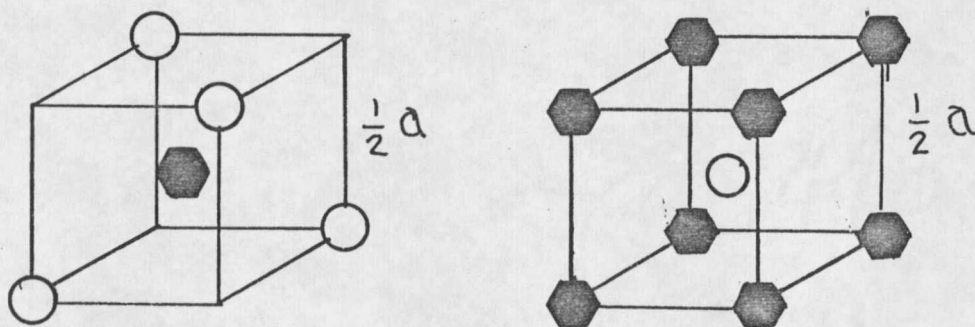
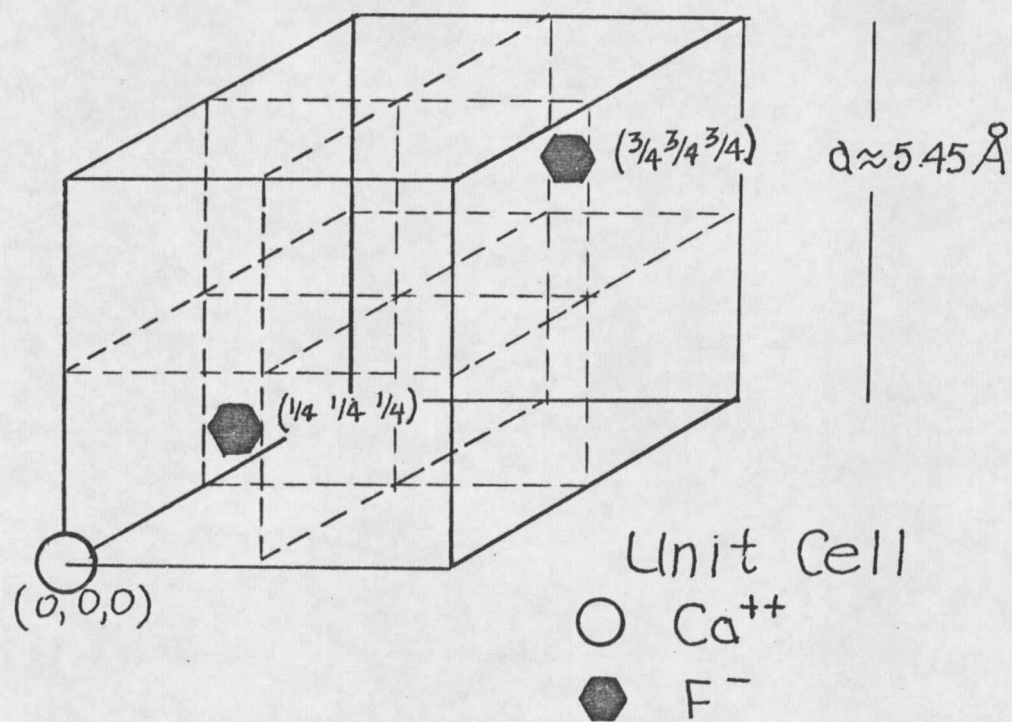


Figure 1.1

Crystallography of CaF_2 with functional cell of F and Ca ion shown.

CHAPTER II
SPLITTING OF THE $^8S_{7/2}$ GROUND STATE OF
Eu IN FLUORITE CRYSTAL

Crystal Field Theory

The electric field at the paramagnetic electrons of Eu ions in a crystal is the field from all sources in the crystal. The strongest influence results from the nearest neighbor ions. A first order effect can be calculated by considering only these nearest neighbors. In order to make this calculation a very simple model is devised for the nearest neighbor interaction. First, the source ions are considered to be point sources. This assumption is much better for rare earth paramagnets than for the transition element groups because overlap of the electron wave function of the deep-seated f electron with the electronic wave function of the anion is less. The anion will henceforth be fluorine F. Second, the fluorine ions will at first be considered to be in a fixed position. This will neglect vibrations and use a time average position for the fluorine as if in a rigid lattice. Third, a semi-classical theory will be used where the electric field is calculated classically, then used as a quantum operator. Of course, any variance of this theory with an experiment

will point up the weakness of this theory and also will point to corrections which may be made to the theory (Griffith, 1961, page 65).

The Hamiltonian of the ion in a crystal including only kinetic and coulomb energies and spin-orbit effects

is

$$H = \sum_{k=1}^n \left\{ \frac{p_k^2}{2m} - \frac{Ze^2}{r_k} + \xi(r_k) \vec{l}_k \cdot \vec{S}_k + V(\vec{r}_k) \right\} + \sum_{k>\lambda} \frac{e^2}{r_{k\lambda}}$$

The term $V(\vec{r}_k)$ is the potential energy of the k^{th} electron in the electrostatic crystal field. The other terms are the same as for the free ion. When $V(\vec{r}_k)$ is small, the Hamiltonian can be written as

$$H = H_0 + V_1$$

where V_1 is a small correction due to the Stark interaction of the electrostatic field with the ion. This form of H allows a perturbation type calculation to find the energy levels relative to the ground state free atom, and the wave function in terms of the free atom wave functions.

Using the model of Fig. 1.1 the electrostatic field at the site of a paramagnetic electron can be calculated classically considering the fluorine ions to be point sources. In this way the field point is in a charge-free region and the electric field results from a solution of

Laplace's equation

$$\nabla^2 V(\mathbf{r}) = 0 . \quad 2.1$$

The potential energy $V(\vec{r})$ of the paramagnetic electron is then

$$V(\vec{r}) = \int \frac{e\rho(\vec{R})d\tau}{|\vec{R}-\vec{r}|} . \quad 2.2$$

Choosing the paramagnetic ion as the center of the coordinate system, \vec{R} is the location of the field source, i.e. the fluorine ions, and \vec{r} is the location of the field point, the electrons. In rare earth atoms the assumption $\vec{R} > \vec{r}$ is valid.

$$|\vec{R}-\vec{r}| = (R^2 + r^2 - 2rR \cos \gamma)^{\frac{1}{2}}$$

Using a binomial expansion for the function $1/|\vec{R}-\vec{r}|$, $V(\vec{r})$ is

$$V(\vec{r}) = \int \frac{e\rho(\vec{R})}{R} \sum_{\ell=0}^{\infty} \left(\frac{r}{R}\right)^{\ell} P_{\ell}(\cos \gamma) d\tau . \quad 2.3$$

γ is the angle between \vec{R} and \vec{r} and the expansion coefficients are the Legendre polynomials. (Arfken, 1966, page 418).

In spherical coordinate systems the angle γ can be expressed in terms of the two different directions of \vec{r}

and \vec{R} as

$\cos \gamma = \cos \theta_1 \cos \theta_2 + \sin \theta_1 \sin \theta_2 \cos(\phi_1 - \phi_2)$,
 ϕ 's are azimuthal angles and θ 's polar angles. The Legendre polynomial P_ℓ can be expanded in terms of spherical harmonics by the addition theorem (Arfken, 1966, page 450-453)

$$P_\ell(\cos \gamma) = \frac{4\pi}{2\ell+1} \sum_{m=-\ell}^{\ell} (-1)^m Y_{\ell}^m(\theta_1, \phi_1) Y_{\ell}^{-m}(\theta_2, \phi_2). \quad 2.4$$

(Also see Messiah I, 1961 Appendix B).

$$V(\vec{r}) = 4\pi \int \frac{e\rho(R) d\tau_2}{R} \sum_{\ell=0}^{\infty} \left(\frac{r}{R}\right)^\ell \frac{1}{2\ell+1} \times$$

$$\sum_{m=-\ell}^{\ell} (-1)^m Y_{\ell}^m(\theta_1, \phi_1) Y_{\ell}^{-m}(\theta_2, \phi_2). \quad 2.5$$

Group Theory

The point group symmetry of XY_8 is O_h . O_h refers to the point group operations performed on a cube which cannot be distinguished from the unaffected cube. The set of elements of this group contains an identity, the unchanged cube; a 180° rotation about an axis perpendicular to each face of the cube and passing through the center of the cube; a 180° rotation about each axis passing through the midpoint of an edge and the center of the cube;

two 120° rotations, clockwise and counter-clockwise, about each of the cube diagonals; and two 90° rotations about each face axis, clockwise and counter-clockwise. Also included in O_h are the improper rotations or each of the proper rotations mentioned above followed by an inversion.

The elements of the O_h point group can be grouped as classes, these being the identity class, the 120° rotation class of which there are eight elements, the two 180° rotation classes, the face centered class of three elements, and the edge centered class of six elements; the six 90° elements form a class as do the improper rotations associated with each class above. If the elements are represented by rotation matrices, the elements of the same class all have the same trace. The trace is called the character of the class and the point group.

There is only a finite number of ways in which a finite abstract group can be made to represent the group in terms of concrete mathematical entities. Any one way is called a "representation" of the group and the number of irreducible representations equals the number of classes. A representation is said to be irreducible if it cannot be expressed as the outer product of representation

of lesser dimensionality. A character table for O_h is given in Appendix A. An irreducible representation in terms of the characters of the classes is given for the possible matrix representations of the group.

The abstract group of rotations has been represented by rotation matrices. These matrices transform functions within a finite dimensional subspace among themselves and if no set of functions within this manifold, apart from the whole subspace, were to transform among themselves by the group operations, the subspace would be irreducible (Gel'fand, Minlos, and Shapiro, 1963, page 16. Also see Appendix A). The basis functions which are transformed by the group elements, form a Euclidean space. Writing these functions analytically can be accomplished an infinite number of ways. The functions can be, however, an orthogonal set. The functions are a "basis" of the representation chosen and must transform distinctly among themselves by the operations of the group. Given any function as one of the basis functions all the basis for the other representations can be generated orthogonal to one another (Tinkham, 1964, page 41).

The set of all rotations is an infinite group and the set of spherical harmonics form a set of basis functions.

for the full rotation group. The spherical harmonics of the same order ℓ are

$$Y_{\ell}^m(\theta, \phi) = (-1)^m \left[\frac{(2\ell+1)(\ell-m)!}{4\pi(\ell+m)!} \right] P_{\ell}^m(\cos \theta) e^{im\phi}$$

where θ is the polar angle and ϕ the azimuthal angle in spherical coordinates. P_{ℓ}^m are associated Legendre polynomials, and $-\ell \leq m \leq \ell$ (Messiah, 1961, page 495). A transformation by a spatial rotation transforms the Y_{ℓ}^m 's of order ℓ among themselves.

$$Y_{\ell}^{m'} = \sum_{n=-\ell}^{\ell} C_{mn}^{\ell} Y_{\ell}^n, \quad 2.6$$

then the C_{mn}^{ℓ} 's are matrix elements as calculated in Appendix A. By the definition of an irreducible representation, any set of $2\ell+1$ spherical harmonic of order ℓ form a basis for the full rotation group since they transform among themselves.

The crystalline field transforms according to its own identity representation (Γ_{1g}) for O_h . Only $D^{(0)}$, $D^{(4)}$, $D^{(6)}$, $D^{(8)}$... contain Γ_{1g} when reduced under O_h . Thus in the crystal field expansion in terms of spherical harmonics (Eq. 2.5) only the $\ell = 0, 4, 6, 8, \dots$ need be kept. The 4f electrons of Eu^{2+} will have spherical functions of $\ell = 3$. Non-zero matrix elements will result from direct products

$D^{(3)} \times D^{(2)} \times D^{(3)}$; $D^{(\ell)}$ being the matrix of the crystal field. It can be seen that

$$D^{(3)} \times D^{(\ell)} \times D^{(3)} = D^{(\ell)} \times [D^{(6)} + D^{(5)} + D^{(4)} + D^{(3)} + D^{(2)} + D^{(1)} + D^{(0)}]$$

thus no non-zero matrix will result for $\ell > 6$, since only $D^{(6)} \times D^{(6)}$ contain $D^{(0)}$.

The $\ell = 0$ spherical functions are not angular dependent and only add a constant to the potential energy term $V(\vec{r})$. Then

$$V(\vec{r})_{\text{cubic}} = \sum_{\ell=0}^{\infty} \sum_{m=-\ell}^{\ell} r^{\ell} \gamma_{\ell}^{\ell m} Y_{\ell}^m \quad 2.7$$

where from eq. 2.2 and 2.5

$$\gamma_{\ell}^{\ell m} = \frac{4\pi e}{(2\ell+1)R^{\ell+1}} \int Y_{\ell}^{-m}(\theta, \phi) d\tau_2 \rho(R).$$

Eq. 2.7 becomes

$$V(\vec{r})_{\text{cubic}} = r^4 \left[\sum_{m=-4}^4 \gamma_{4}^{4m} Y_{4}^m \right] + r^6 \left[\sum_{m=-6}^6 \gamma_{6}^{6m} Y_{6}^m \right].$$

The rotation about the z axis of $\pi/2$ transforms the coordinate system as:

$$x \rightarrow y, \quad y \rightarrow -x, \quad \text{and } z \rightarrow z.$$

The spherical functions Y_4^0 , Y_4^4 , and Y_4^{-4} are the only

invariants of order 4 under this transformation. Y_6^0 and $Y_6^{\pm 4}$ are the only order 6 invariants. (Low, 1960, Table II).

Considering point charges and XY_8

$$V(\vec{r}) = \frac{-Ze^2 r^4}{R^5} \frac{4\pi}{9} \left[\frac{28}{9} Y_4^0 + \frac{2}{9} \sqrt{70} (Y_4^4 + Y_4^{-4}) \right] \\ + \frac{Ze^2 r^6}{R^7} \frac{4\pi}{13} \left[\frac{16}{9} Y_6^0 + \frac{8}{9} \sqrt{14} (Y_6^4 + Y_6^{-4}) \right]$$

which may be written as

$$V(\vec{r}) = B_4 (O_4^0 + 5O_4^4) + B_6 (O_6^0 - 21O_6^4) \quad 2.8$$

O_ℓ^m is the sum $Y_\ell^m + Y_\ell^{-m}$ in which any common numerical factors have been taken out and included in B (Jones, Baker and Pope, 1959 and Stevens, 1952).

Operator Equivalence

A vector \vec{T} can be defined as a vector of type "T" following Condon and Shortley (1935), with respect to a general angular momentum \vec{j} when it meets the following commutation relations:

$$[j_\ell, T_m] = ih T_n \epsilon_{\ell mn}$$

$\epsilon_{\ell mn}$ is the Levi-Civita tensor density (Goldstein, 1959, page 129), defined to be zero if any two of the indices ℓ, m, n are equal, and either +1 or -1 otherwise, according

as (λ, m, n) is an even or odd permutation of (x, y, z) . Two excellent expositions of the subject of angular momentum in quantum mechanics can be found in Chapter II of J. S. Griffith's The Theory of Transition-Metal Ions (1961) and Chapter XII of A. Messiah's Quantum Mechanics, Volume II (1962).

The replacement theorem follows from the Wigner-Eckart theorem and says that if \vec{T}_1 and \vec{T}_2 are both type T with respect to \vec{j} then $\langle \alpha' j m | \vec{T}_1 | \alpha'' j m' \rangle = \gamma \langle \alpha' j m | \vec{T}_2 | \alpha'' j m' \rangle$ where $\gamma = \gamma(\alpha', \alpha'', j)$ independent of m and m' . A corollary to the replacement theorem is:

For any vector \vec{T} of type T with respect to \vec{j} , the relation

$$\langle \alpha' j m | \vec{T} | \alpha'' j m' \rangle = \gamma \langle \alpha' j m | \vec{j} | \alpha'' j m' \rangle \quad 2.9$$

holds with $\gamma = \gamma(\alpha', \alpha'', j)$. Note on the right side of the equation the quantum numbers j and α' are the same for both bra and ket. This results because any component of \vec{j} can only generate functions within the manifold of $2j+1$ eigenstates belonging to j and α' . The manner of using this theorem and the corollary would be to evaluate γ for any one matrix element then use the replacement theorem.

The replacement theorem allows the crystal field operator in terms of the spherical functions Y_{ℓ}^m to be

replaced by angular momentum operators. If the spherical functions are written in terms of their cartesian equivalents, each of the components x, y, and z can be replaced by operator equivalents in j_x , j_y , and j_z . These operators are to be expressed in a standard representation whose basis vectors are the set $|\alpha jm\rangle$, that is in the normalized

$$\begin{aligned} j_1 &= \frac{1}{\sqrt{2}} (j_x + ij_y) = \frac{1}{\sqrt{2}} j_+ \\ j_0 &= j_z \\ j_{-1} &= \frac{1}{\sqrt{2}} (j_x - ij_y) = \frac{1}{\sqrt{2}} j_- \end{aligned} \quad 2.10$$

Because of the noncommuting nature of the operators, mixed products such as xy must be symmetrized when replaced by operator equivalents, for example:

$$xy \rightarrow 1/2 (xy + yx) \rightarrow 1/2 (j_x j_y + j_y j_x).$$

The crystal field written in operator equivalent form is from eq. 2.8,

$$V(\vec{r}) = B_4(O_4^0 + 5O_4^4) + B_6(O_6^0 - 21O_6^4) \quad 2.11a$$

$$O_4^0 = 35j_z^4 - 30j(j+1)j_z^2 + 25j^2 - 6j(j+1) + 2j^2(j+1)^2,$$

$$O_4^4 = \frac{1}{2} [j_+^4 + j_-^4] \quad 2.11b$$

$$\begin{aligned}
0_6^0 &= 231 j_z^6 + 315j(j+1) j_z^4 + 105j^2(j+1)^2 j_z^2 \\
&+ 525j(j+1)j_z^2 + 294j_z^2 + 5j^3(j+1)^3 + 40j^2(j+1)^2 \\
&+ 60j(j+1)
\end{aligned}
\tag{2.11c}$$

$$\begin{aligned}
0_6^4 &= \frac{1}{4} \left[(j_+^4 + j_-^4) \{11j_z^2 + j(j+1) - 38\} \right. \\
&\left. + \{11j_z^2 + j(j+1) - 38\} (j_+^4 + j_-^4) \right] .
\end{aligned}
\tag{2.11d}$$

(Jones, Baker, and Pope, 1959, Table 3).

The Spin Hamiltonian

The angular momentum of the europium ion is $\vec{J} = \vec{L} + \vec{S} = \vec{S}$. The shells are all closed with respect to orbital angular momentum. In the above notation then, replace \vec{j} with \vec{S} . A difficulty results since \vec{S} is not a T type vector with respect to \vec{L} . The result of this is to nullify the replacement theorem. Physically, this result states that the Stark effect cannot split a system which has a closed electron shell.

Group theory, which explains the type of splitting allowed if the mechanism were present, predicts a crystal field splitting of three levels. The O_h group must now be a double group to account for the nature of half integral angular momentum systems where a twofold rotation

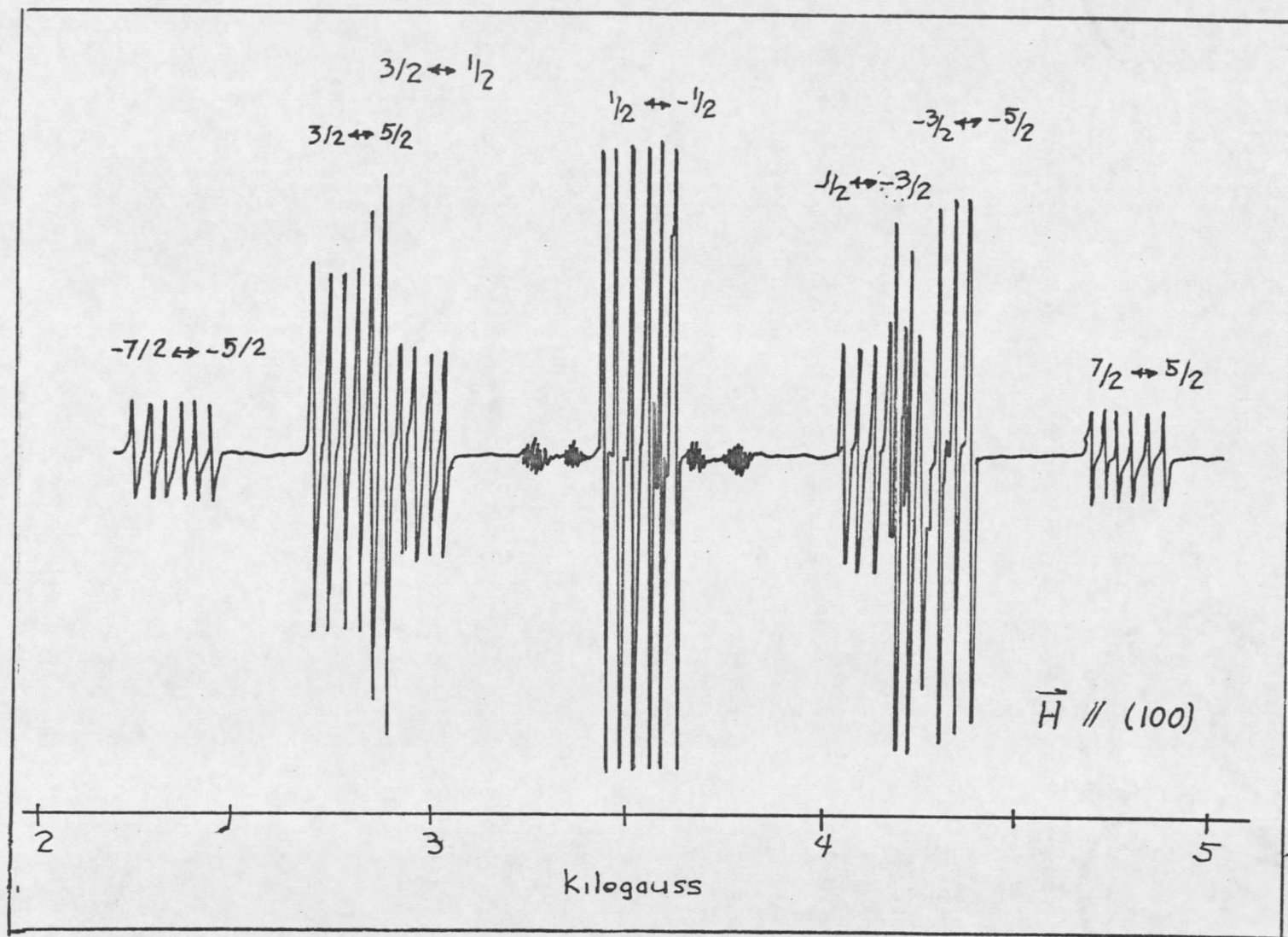


Figure 2.1 X-band spectrum 0.1% Eu - CaF₂ at 78°K.

is single valued. The zero magnetic field splitting of a $J = 7/2$ system is calculated in Appendix A.

Experimental evidence clearly shows there is a crystal field interaction. Fig. 2.1 shows the splitting of the ground state by a Zeeman effect. The fine structure spectrum can only be explained if a crystal field interaction exists. This splitting will be calculated below and the energy level diagram of Fig. 2.2 shows the zero field splitting.

An explanation of the S-state splitting by Van Vleck and Penney (1934) concluded that an orbit-spin coupling mixed in excited states in which L is not zero. Abragam and Pryce (1951) considered the spin-spin interaction between dipoles which depends on spin variables and position variables

$$H_{\text{spin-spin}} = \left| \vec{S}_j \cdot \vec{S}_k / r_{jk}^3 - \frac{3(\vec{r}_{jk} \cdot \vec{S}_j)(\vec{r}_{jk} \cdot \vec{S}_k)}{r_{jk}^5} \right|. \quad 2.12$$

The crystal field distorts the orbits which are coupled to other spins resulting in a net distortion of the ground state. The distorted S-state can interact with the electric field.

An acceptable theory which shows good agreement with

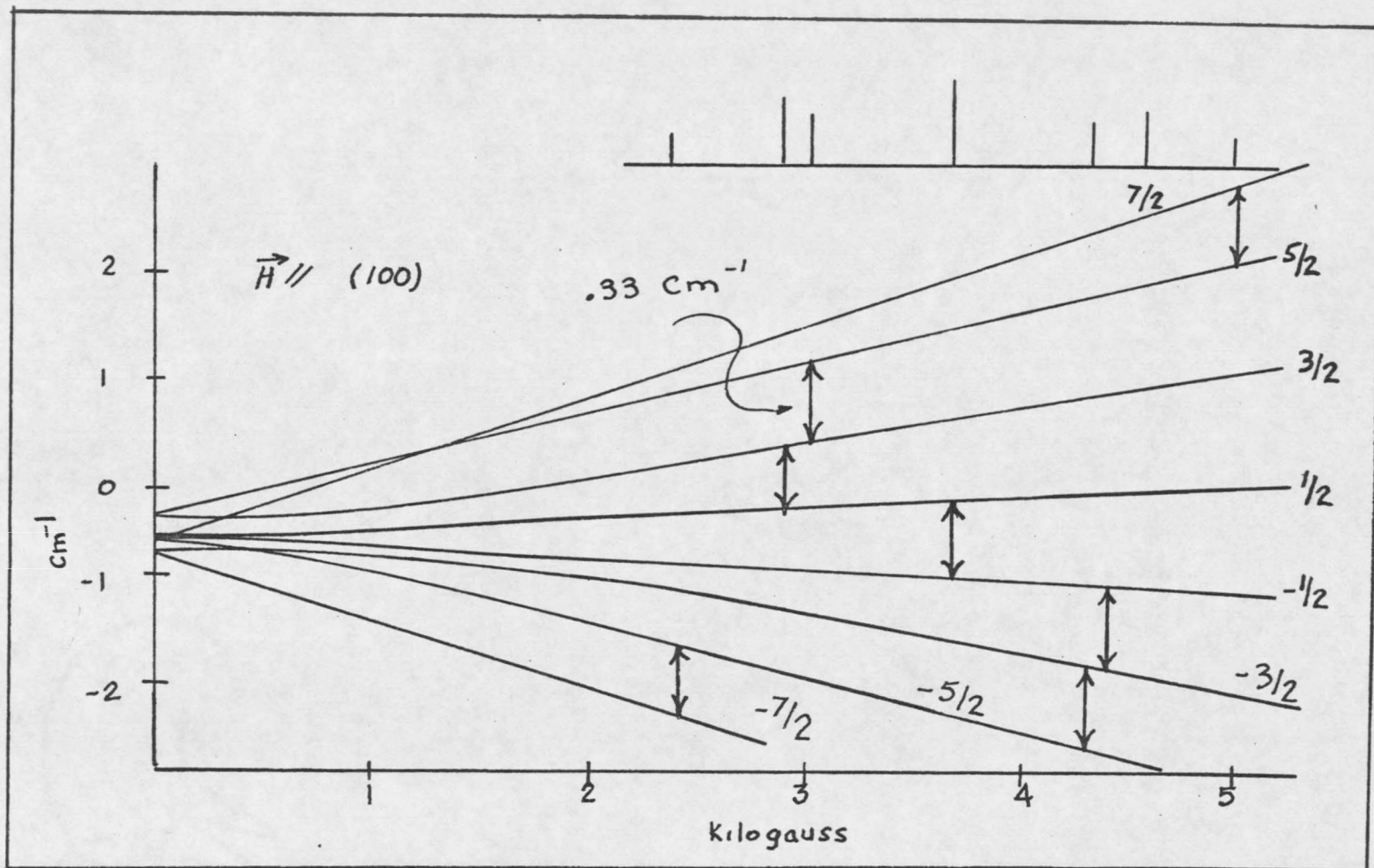


Figure 2.2 Fine structure splitting Eu - CaF₂ as a function of magnetic Field.

the experiments on S-states has not been developed to date. An heuristic Hamiltonian can be proposed in which the coefficients B_4 and B_6 of eq. 2.8 are measured experimentally. This is the "Spin Hamiltonian" for S-state ions.

$$H = g\beta\vec{H}\cdot\vec{S} + B_4(O_4^0 + 5O_4^4) + B_6(O_6^0 - 21O_6^4) + \vec{I}\cdot\vec{A}\cdot\vec{S} + g_N\beta_N\vec{H}\cdot\vec{I}. \quad 2.13$$

$g\beta\vec{H}\cdot\vec{S}$ is the Zeeman effect of a magnetic dipole $g\beta\vec{S} = \vec{\mu}_e$ in a magnetic field. There is also a nuclear Zeeman term $g_N\beta_N\vec{H}\cdot\vec{I}$ which is small compared to other spin Hamiltonian terms but is kept in order to devise nuclear wave functions required to explain the hyperfine interaction (see Chapter III).

An interaction between the electrons and the nucleus is called the hyperfine interaction. This interaction is essentially a spin-spin interaction as eq. 2.12. An s electron has a finite probability of being within the nuclear volume giving rise to the Fermi contact term

$$(8\pi/3) g\beta g_N\beta_N \delta(\vec{r}_e - \vec{r}_n) \vec{I}\cdot\vec{S}.$$

F. J. Milford (1960) has a simple derivation of this term in the American Journal of Physics.

The spin-spin term of the hyperfine interaction does not predict as large a hyperfine coupling tensor \vec{A} , which

is a constant for Eu, as is measured in experiments. William Hayes (1963) accounts for the hyperfine interaction as resulting mostly from the Fermi contact term of unpaired s electrons density at the nucleus. In Eu all the s electrons are paired, thus no hyperfine splitting should occur. It is thought, however, that the unfilled paramagnetic shell will polarize the s electrons by exchange interactions such that one of the pair will have a greater electron density in the nucleus than the other. The hyperfine interaction is included as a spin Hamiltonian term and A is measured by experiment (Baker, Bleaney, and Hayes, 1958).

Fine Structure

Taking the Hamiltonian

$$H = g \vec{H} \cdot \vec{S} + B_4 \left(O_4^0 + 5 O_4^4 \right) + B_6 \left(O_6^0 - 21 O_6^4 \right),$$

the crystal field dominates when \vec{H} is small and group theory predicts a zero field splitting. Replacing the operators O by spin operators in a standard representation as given in Table II, and evaluating matrix elements between the basis of the representation, $|SM_s\rangle$, an eight by eight matrix results. The matrix has four distinct diagonal elements. $\langle S, M | H_{cf} | S, M \rangle = \langle S, -M | H_{cf} | S, -M \rangle$, a

result which stems from Kramer's theorem (Tinkham, 1964, page 143.) For any half-integral angular momentum system an electric field of any symmetry can at best remove degeneracy such that each new level is of even degeneracy. This is because an electric field results from a time reversal symmetry. The matrix can be written as two four by four matrices along the diagonal. The cubic field operators 0 only have off-diagonal elements between M and $M \pm 4$ by virtue of the terms S_+^4 and S_-^4 . By an interchange of rows and columns the 4×4 matrix becomes two 2×2 matrices along the diagonal.

Figure 2.3

	$\pm 7/2$	$\pm 1/2$		
$\pm 7/2$	$(7b_4 + b_6)$	$35(b_4 - 3b_6)$	0	0
$\pm 1/2$	$35(b_4 - 3b_6)$	$(9b_4 - 5b_6)$	0	0
$\pm 5/2$	0	0	$(-13b_4 - 5b_6)$	$3(5b_4 + 7b_6)$
$\pm 3/2$	0	0	$3(5b_4 + 7b_6)$	$(-3b_4 + 9b_6)$

where $b_4 = 60B_4$ and $b_6 = 120B_6$ of eq. 2.13.

By diagonalizing the above matrix the eigenvalues of energy are

$$E_1 = 14b_4 - 20b_6, \quad M = \pm 5/2,$$

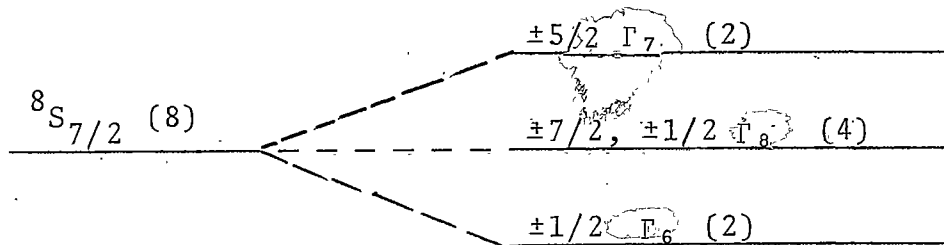
$$E_2 = 2b_4 + 16b_6, \quad M = \pm 7/2,$$

$$E_3 = 2b_4 + 16b_6, \quad M = \pm 3/2,$$

and $E_4 = -18b_4 - 12b_6, \quad M = \pm 1/2,$

The E_2 and E_3 levels are degenerate, and since each level is twofold degenerate because of Kramer's degeneracy, two twofold degenerate levels and a four fold level are split by a zero magnetic field Hamiltonian.

Figure 2.4
Zero Field Splitting



If a magnetic field is introduced such that the field is directed along the z axis of the crystal field ($\pm x, \pm y, \pm z$ are equivalent z axes) the spin Hamiltonian is

$$H = g \vec{H} \cdot \vec{S} + \frac{b_4}{60} \begin{pmatrix} 0 & \\ & 4 \end{pmatrix} + 50 \begin{pmatrix} 4 & \\ & 4 \end{pmatrix} + \frac{b_6}{1260} \begin{pmatrix} 0 & \\ & 6 \end{pmatrix} - 210 \begin{pmatrix} 4 & \\ & 6 \end{pmatrix}$$

when the magnetic field is small the states are perturbed

by $H_1 = g\beta H S_z$ which removes the remaining degeneracy.

In the strong field region, the crystal field term is the perturbation and the eigenfunctions belonging to S_z are perturbed by

$$V_{cf} = \frac{b_4}{60} (0_4^0 + 50_4^4) + \frac{b_6}{1260} (0_6^0 + 210_6^4). \quad 2.14$$

Figure 2.2 displays the splitting as a function of the field strength H .

The eigenvalues of H when considering eq. 2.14 as a small H_1 , $H_1 \ll g\beta H$ are

$$E_M = E_M^0 + \langle M | H_1 | M \rangle + \sum_{M'} \frac{\langle M | H_1 | M' \rangle \langle M' | H_1 | M \rangle}{E_M^0 - E_{M'}^0} \quad 2.15$$

with

$$E_M^0 = \langle M | g\beta H S_z | M \rangle = g\beta H M.$$

The eigenfunctions belonging to S_z are $|\alpha SM\rangle$. These are shortened to $|M\rangle$ within the manifold $S = 7/2$ for Eu ions; $-7/2 \leq M \leq 7/2$. The resulting levels are

$$E_{\pm 7/2} = \pm g\beta H (7/2) + 7b_4 + b_6 \pm \frac{35(b_4 - 3b_6)^2}{4g\beta H} \quad 2.16a$$

$$E_{\pm 5/2} = \pm g\beta H (5/2) + 13b_4 - 5b_6 \pm \frac{3(5b_4 + 7b_6)^2}{4g\beta H} \quad 2.16b$$

$$E_{\pm 3/2} = \pm g\beta H(3/2) - 3b_4 + 9b_6 \pm \frac{3(5b_4 + 7b_6)^2}{4g\beta H} \quad 2.16c$$

and

$$E_{\pm 1/2} = \pm g\beta H(1/2) + 9b_4 - 5b_6 \pm \frac{35(b_4 - 3b_6)^2}{4g\beta H} \quad 2.16d$$

Angular Dependence of Fine Structure.

When the coordinates x , y , and z of the crystalline field do not coincide with the vector external magnetic field, the vector products of eq. 2.13 must be written in a common coordinate system. In eq. 2.13 it is implied that the coordinate system chosen is along the three equivalent crystal axes. Maintaining this coordinate system, the scalar product $\vec{H} \cdot \vec{S}$ becomes

$$\vec{H} \cdot \vec{S} = H(S_x \sin\theta \cos\phi + S_y \sin\theta \sin\phi + S_z \cos\theta).$$

In the experiment the magnetic field \vec{H} was always at right angles to a (100) axis of the crystal. In the calculations the rotations are always in the x, z plane; thus the azimuthal angle ϕ is zero. The terms of the matrix of figure 2.5 times $g\beta H$ are the matrix elements of H of eq. 2.13. b'_4 and b'_6 are respectively $b_4/g\beta H$ and

	-7/2	-5/2	-3/2	-1/2	1/2	3/2	5/2	7/2
$-\frac{7}{2}$	$\frac{7b_4+b_6}{-7/2\cos\theta}$	$\sqrt{7/2}\sin\theta$	0	0	$\frac{\sqrt{35}}{(b_4-3b_6)}$	0	0	0
$-\frac{5}{2}$	$\sqrt{7/2}\sin\theta$	$\frac{-13b_4-5b_6}{-5/2\cos\theta}$	$\sqrt{3}\sin\theta$	0	0	$\frac{\sqrt{75}}{(b_4+7/5b_6)}$	0	0
$-\frac{3}{2}$	0	$\sqrt{3}\sin\theta$	$\frac{-3b_4+9b_6}{-3/2\cos\theta}$	$\frac{\sqrt{15}\sin\theta}{2}$	0	0	$\frac{\sqrt{75}}{(b_4+7/2b_6)}$	0
$-\frac{1}{2}$	0	0	$\frac{\sqrt{15/2}\sin\theta}{\sin\theta}$	$\frac{9b_4-5b_6}{-1/2\cos\theta}$	$2\sin\theta$	0	0	$\frac{\sqrt{35}}{(b_4-3b_6)}$
$\frac{1}{2}$	$\frac{\sqrt{35}}{(b_4-3b_6)}$	0	0	$2\sin\theta$	$\frac{9b_4-5b_6}{1/2\cos\theta}$	$\frac{\sqrt{15}\sin\theta}{2}$	0	0
$\frac{3}{2}$	0	$\frac{\sqrt{75}}{(b_4+7/5b_6)}$	0	0	$\frac{75\sin\theta}{2}$	$\frac{-3b_4+9b_6}{+3/2\cos\theta}$	$\sqrt{3}\sin\theta$	0
$\frac{5}{2}$	0	0	$\frac{\sqrt{75}}{(b_4+7/5b_6)}$	0	0	$\sqrt{3}\sin\theta$	$\frac{-13b_4-5b_6}{5/2\cos\theta}$	$\frac{\sqrt{7}\sin\theta}{2}$
$\frac{7}{2}$	0	0	0	$\frac{\sqrt{35}}{(b_4-3b_6)}$	0	0	$\frac{\sqrt{7}\sin\theta}{2}$	$\frac{7b_4+b_6}{+7/2\cos\theta}$

Figure 2.5

$b_6/g\beta H$, the angle θ is the angle between a (100) axis of the crystal, chosen as the z axis of the coordinate system, and the magnetic field H . The resulting matrix is displayed in Fig. 2.5,

An approximate diagonalization of this matrix using perturbation techniques can be used when $H \ll 60$ gauss. Using a much larger field, H_0 , it is possible to treat the crystal field as a perturbation as in eq. 2.16; however, a representation written with the z axis along the H_0 direction is then necessary. In this case the crystal field operators O written in the cartesian form for the spherical harmonics will transform as

$$x \rightarrow x \sin \theta \rightarrow S_x \sin \theta \rightarrow \frac{S_+ + S_-}{2} \sin \theta$$

and

$$z \rightarrow z \cos \theta \rightarrow S_z \cos \theta$$

where again all products of S_z , S_+ , and S_- must be symmetrized. This has been done for the operators O_4^0 , O_4^4 , O_6^0 , O_6^4 of eq. 13, (Stevens, 1951 and Jones, Baker, and Pope).

Table 2.1

Jones, Baker, and Pope (1959)

$$O_4^0 \rightarrow \frac{3}{8} O_4^0 + \frac{5}{2} O_4^2 + \frac{35}{8} O_4^4$$

$$O_4^2 \rightarrow \left(-\frac{1}{8} O_4^0 + \frac{1}{2} O_4^2 + \frac{7}{8} O_4^4 \right) \cos 2\phi + i \left(\frac{1}{2} O_4^1 + \frac{7}{2} O_4^3 \right) \sin 2\phi$$

$$O_4^4 \rightarrow \left(\frac{1}{8} O_4^0 - \frac{1}{2} O_4^2 + \frac{1}{8} O_4^4 \right) \cos 4\phi - i (O_4^1 - i O_4^3) \sin 4\phi$$

$$O_4^4 \rightarrow -\frac{5}{16} O_6^0 - \frac{105}{32} O_6^2 - \frac{63}{16} O_6^4 - \frac{231}{32} O_6^6$$

$$O_6^2 \rightarrow \left(\frac{1}{16} O_6^0 + \frac{17}{32} O_6^2 + \frac{3}{16} O_6^4 - \frac{33}{32} O_6^6 \right) \cos 2\phi \\ - i \left(\frac{1}{4} O_6^1 + \frac{9}{8} O_6^3 + \frac{33}{8} O_6^5 \right) \sin 2\phi$$

$$O_6^4 \rightarrow \left(-\frac{1}{16} O_6^0 - \frac{5}{32} O_6^2 + \frac{13}{16} O_6^4 - \frac{11}{32} O_6^6 \right) \cos 4\phi \\ + i \left(\frac{1}{2} O_6^1 + \frac{5}{4} O_6^3 - \frac{11}{4} O_6^5 \right) \sin 4\phi$$

$$O_6^6 \rightarrow \left(\frac{1}{16} O_6^0 - \frac{15}{32} O_6^2 + \frac{3}{16} O_6^4 - \frac{1}{32} O_6^6 \right) \cos 6\phi \\ - i \left(\frac{3}{4} O_6^1 - \frac{5}{8} O_6^3 + \frac{3}{8} O_6^5 \right) \sin 6\phi$$

The Hamiltonian with an angle θ between the crystal axis and the magnetic field (chosen to be the z axis of coordinate system) rotated about the y axis is

$$\begin{aligned}
H = & g\beta H S_z + \frac{b_4}{60} \left\{ \frac{3}{8} O_4^0 + \frac{5}{8} O_4^2 + \frac{35}{8} O_4^4 + 5 \left[\left(\frac{1}{8} O_4^0 - \frac{1}{2} O_4^2 \right. \right. \right. \\
& \left. \left. \left. + \frac{1}{8} O_4^4 \right) \cos 4\theta - i \left(O_4^1 - i O_4^3 \right) \sin 4\theta \right] \right\} + \frac{b_6}{1260} \\
& \times \left\{ -\frac{5}{16} O_6^0 - \frac{105}{32} O_6^2 - \frac{63}{16} O_6^4 - \frac{231}{32} O_6^6 - 21 \left[\left(-\frac{1}{16} O_6^0 \right. \right. \right. \\
& \left. \left. \left. + \frac{13}{16} O_6^4 - \frac{11}{16} O_6^6 \right) \cos 4\theta + i \left(\frac{1}{2} O_6^1 + \frac{5}{4} O_6^3 \right. \right. \right. \\
& \left. \left. \left. - \frac{11}{4} O_6^5 \right) \sin 4\theta \right] \right\} \quad 2.17
\end{aligned}$$

Tables giving the values of the matrix elements of the O_m^n 's are given by Low (1960) and Drumheller (1969).

A concluding note to give further insight into the transformation of the O_m^n 's follows. The O_m^n 's are a linear combination of O_m^{n+} and O_m^{n-} which are spherical harmonics written in symmetrized operator equivalent form. The common numerical coefficients are not included. On rotation the spherical harmonics Y_ℓ^m are transformed into linear combinations of the spherical harmonics belonging to the same manifold ℓ :

$$Y_\ell^m(\theta', \phi') = \sum_n C_{mn}^\ell Y_\ell^n(\theta, \phi). \quad 2.6$$

The transformation matrix whose elements are the C_{mn}^ℓ 's is unitary. This matrix is the operator

$$e^{-i\phi(\vec{J} \cdot \vec{\mu})} |\ell m\rangle = R(\phi) |\ell m\rangle \quad 2.18$$

Table 2.2

Jones, Baker, and Pope (1959)
Baker, Bleaney, and Hayes (1951)

Form of Operators O_n^m

$$O_4^0 = 35s_z^4 - \{30s(s+1) - 25\}s_z^2 - 6s(s+1) + 3s^2(s+1)^2$$

$$O_4^2 = \frac{1}{4}[\{7s_z^2 - s(s+1) - 5\}(s_+^2 + s_-^2) + (s_+^2 + s_-^2)\{7s_z^2 - s(s+1) - 5\}]$$

$$O_4^4 = \frac{1}{2}(s_+^4 + s_-^4)$$

$$O_6^0 = 231s_z^6 - 105\{3s(s+1) - 7\}s_z^4 + \{105s^2(s+1)^2 - 525s(s+1) + 294\}s_z^2 - 5s^3(s+1)^3 = 40s^2(s+1)^2 - 60s(s+1)$$

$$O_6^2 = \frac{1}{4}[\{33s_z^4 - [18s(s+1) + 123]s_z^2 + 10s(s+1) + 102\}(s_+^2 + s_-^2) + (s_+^2 + s_-^2)\{33s_z^4 - \text{etc.}\}]$$

$$O_6^4 = \frac{1}{4}[\{11s_z^2 - s(s+1) - 38\}(s_+^4 + s_-^4) + (s_+^4 + s_-^4)\{11s_z^2 - s(s+1) - 38\}]$$

$$O_6^6 = \frac{1}{2}(s_+^6 + s_-^6)$$

$$O_4^3 = \left(\frac{1}{4}\right)\{s_z(s_+^3 + s_-^3) + (s_+^3 + s_-^3)s_z\}$$

$$O_6^3 = \frac{1}{4}[\{11s_z^3 - 3s(s+1)s_z - 59s_z\}(s_+^3 + s_-^3) + (s_+^3 + s_-^3)\{11s_z^3 - 3s(s+1)s_z - 59s_z\}]$$

$$O_6^2 = \frac{1}{4}[\{35s_z^5 - s_z^3\langle 30s(s+1) - 15 \rangle + s_z\langle 5s^2(s+1)^2 - 105(s+1) + 12 \rangle\}(s_+ + s_-) + (s_+ + s_-)\{35s_z^5 - s_z^3\langle 30s(s+1) - 15 \rangle + s_z\langle 5s^2(s+1)^2 - 105(s+1) + 12 \rangle\}]$$

$$O_4^1 = \frac{1}{4}[\{75s_z^3 - 35(s+1)s_z - s_z\}(s_+ + s_-) + (s_+ + s_-)\{7s_z^3 - 35(s+1)s_z - s_z\}]$$

ϕ is the angle of rotation, \vec{J} , the angular momentum operator and $\vec{\mu}$ a unit vector acting as the axis of rotation. (Messiah, 1964 Appendix D, Section 10 and Chapter XIII). Gelfand, Minlos, and Shapiro (1963) derive this operator in terms of Euler angles. The solution is the Generalized Spherical Functions which are also used in Chapter III to explain the hyperfine interaction. The function is derived in Appendix A.

Baker, Bleaney, and Hayes (1958) have used first order perturbation calculations to find the angular dependence of the fine structure energy levels. In eq. 2.16 the following substitutions are made to show this dependence (Bleaney, Baker, and Hayes, 1958):

$$b_4 \rightarrow b_4 p; \quad b_6 \rightarrow b_6 q, \quad 2.19$$

where

$$p = 1 - 5(\ell^2 m^2 + m^2 n^2 + n^2 \ell^2)$$

and

$$q = \frac{21}{2} \{ 11 \ell^2 m^2 n^2 - (\ell^2 m^2 + m^2 n^2 + n^2 \ell^2) + \frac{2}{21} \}. \quad 2.20$$

In eq. 2.20 (ℓ, m, n) are the direction cosines to the (x, y, z) axis. In spherical coordinates

$$\begin{aligned} \ell &= \sin \theta \cos \phi \\ m &= \sin \theta \sin \phi \end{aligned}$$

and

$$n = \cos \theta,$$

Since the rotations of the experiment are made in the x-z plane, the azimuthal angle ϕ is $\pi/2$ thus

$$p = 1 - \frac{5}{4} \sin^2 \theta \cos^2 \theta = 1 - \frac{5}{16} \sin^2 2\theta$$

$$q = 1 - \frac{21}{8} \sin^2 2\theta.$$

The angular dependence of the difference between adjacent levels (since transitions between these levels were the measured quantities in the experiment, the differences $\Delta M \pm 1$ are plotted rather than the energy levels themselves) is plotted in Fig. 2.6.

When θ is zero the fine structure transitions of eq. 16 are plotted in Fig. 2.2 when the energy difference between $\Delta M \pm 1$ levels is 0.33 cm^{-1} in energy (the 10 GHz microwave energy). This figure shows the location of the high field splitting of the fine structure levels which result from eq. 2.16.

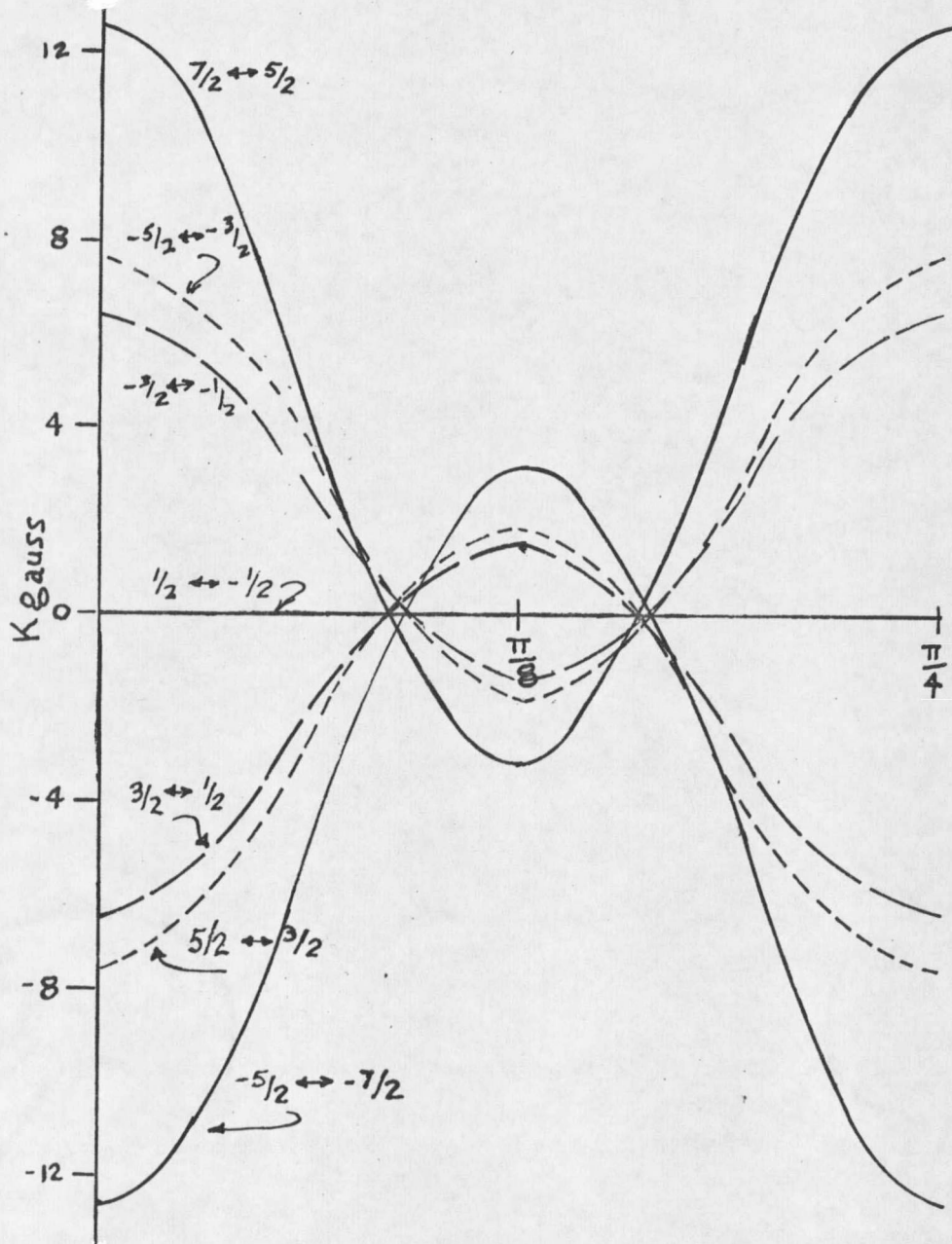


Figure 2.6 The angular dependence of the fine-structure spectrum rotated about a (100) axis.

CHAPTER III

THE E. P. R. EXPERIMENT AND THE HYPERFINE INTERACTION

Magnetic Resonance

The principle of magnetic resonance experiments is the Zeeman effect. In this experiment a gyromagnetic top is placed in a magnetic field. The interaction between the magnetic moment

$$\vec{\mu} = \gamma \hbar \vec{J} \quad 3.1$$

and the magnetic field causes a Larmor precession of the top. $\hbar \vec{J}$ is the angular momentum of the top. The torque on a magnetic moment $\vec{\mu}$ in a magnetic field is

$$\vec{T} = \vec{\mu} \times \vec{H}$$

From mechanics $\vec{T} \hat{=} \frac{d\hbar \vec{J}}{dt}$, thus

$$\frac{d}{dt} \left[-\frac{1}{\gamma} \vec{\mu} \right] = \vec{\mu} \times \vec{H} \quad 3.2$$

The solution to this equation, where \vec{H} is constant and the angle between $\vec{\mu}$ and \vec{H} nonzero, is a precession of frequency

$$\vec{\omega}_0 = \gamma \vec{H}_0 \quad 3.3$$

The energy levels of the paramagnets of eq. 3.2 are fixed, depending on the component of $\vec{\mu}$ in the direction of

\vec{H} .

$$\vec{E} = -\vec{\mu} \cdot \vec{H}. \quad 3.4$$

If \vec{H} is not a constant but is perturbed by a weaker magnetic field at right angles to \vec{H}_0 , the perturbing field \vec{H}_1 will appear to average to zero from a reference frame rotating at the Larmor frequency. When \vec{H}_1 is also rotated, it will have an average life-time as an effective field when the rotation is close to the Larmor frequency. When the two frequencies are the same, resonance occurs giving rise to the name magnetic resonance. From the view of the rotating reference frame, when \vec{H}_1 is in resonance, the field \vec{H}_0 appears to be zero and \vec{H}_1 now will cause a precession of $\vec{\mu}$ about \vec{H}_1 changing the eigenstates of \vec{J} to other combinations within the manifold of $2J + 1$. These transitions both absorb and emit energy to the system maintaining \vec{H}_1 .

The coordinate system is selected such that z is along the magnetic field H_0 and the perturbing field is the magnetic component of sinusoidal microwave radiation. The Hamiltonian is

$$H = H_0 + H_1 \quad 3.5$$

where H_0 is the spin Hamiltonian, which for the present discussion will be the electronic Zeeman term.

$$H_0 = g\beta\vec{H}\cdot\vec{S} = g\beta H_0 S_z \quad 3.6$$

in the representation of Chapter II.

$$H_1 = g\beta\vec{H}_1\cdot\vec{S} \quad 3.7$$

and

$$\vec{H}_1 \rightarrow \vec{H}_1 \cos \omega t. \quad 3.8$$

The probability per unit time that a paramagnet initially in state $|m\rangle$ will be in state $|m'\rangle$ from time dependent perturbation theory is

$$w_{mm'} = q^2 \beta^2 H_1^2 |S_x^{mm'}|^2 g(\nu) \quad 3.9$$

If the spin-lattice relaxation mechanism keeps an excess of the paramagnets in the lower energy states the distribution function $g(\nu)$ will be Lorentzian,

$$g(\nu) = \frac{n 2T_2}{1 + T_2^2 (2\pi)^2 (\nu_0 - \nu)^2} \quad 3.10$$

where T_2 is the characteristic spin-lattice relaxation time introduced into the Bloch equation (Pake, 1962).

In a sample with a large number of paramagnets, and given a time long compared to the relaxation times, the probable number of paramagnets at an energy $E_m = \vec{\mu}_m \cdot \vec{H}$ is governed by Boltzmann statistics,

$$\frac{N}{N_0} = \frac{e^{-E_m/kT}}{e^{-Em/kT}} ; \quad -S \leq m \leq S \quad 3.11$$

when

$$E_n \ll kT; \quad \frac{N_m}{N_0} = \frac{1 - g\beta H_m/kT}{2S + 1} \quad 3.12$$

Then

$$\frac{\Delta N}{N_0} = \frac{N + 1}{N_0} - \frac{N}{N_0} = \frac{-g\beta H}{2kT(S + 1)} \quad 3.13$$

From eq. 3.9 the operator

$$S_x = \frac{1}{2} (S_+ + S_-) \quad 3.14$$

requires selection rules $\Delta M = \pm 1$. That is the only transitions between energy levels differing by $|\Delta M| = 1$ will be stimulated by the microwave radiation. Since the lower states are more populous

$$\Delta N = N_0 g\beta H / 2(S + 1)kT, \quad 3.15$$

more simulated absorption will occur than stimulated emission. If the microwave power is low enough to prevent saturation, the line shape of eq. 3.10 will occur. Saturation occurs when the radiation is intense enough to equally populate both levels. When this occurs the ratio between microwave power absorbed by the sample and power

available is not linearly related to the population of paramagnets occupying the energy levels. The intensity of a resonance line will be controlled by the matrix

$$\langle M' | S_x | M \rangle .$$

An accurate measure of the intensity will be the area under the curve $w_{MM'}$,

$$I = g^2 \beta^2 H_1^2 |S_x^{MM'}|^2 \int_{-\infty}^{\infty} g(\nu) d\nu ,$$

$$I = [g\beta H_1 |S_x^{MM'}|^2] . \quad 3.16$$

Figure 3.1 is an actual plot of the absorption of microwave power versus the magnetic field for Eu^{++} in CaF_2 . The six large lines are the $\Delta M = 1/2 \leftrightarrow -1/2$ transition when a (100) crystal field axis is along H_0 . The small satellite-lines adjacent to the six major lines are the mutual spin flip with fluorine nuclei discussed by Baker, Hayes, and O'Brien (1960). The overlap of these lines is virtually eliminated at very low temperatures since the more uniform local fields sharpen the line shape function $g(\nu)$. The existence of six lines depict the further splitting of the $M = 1/2$ and $M = -1/2$ levels by the

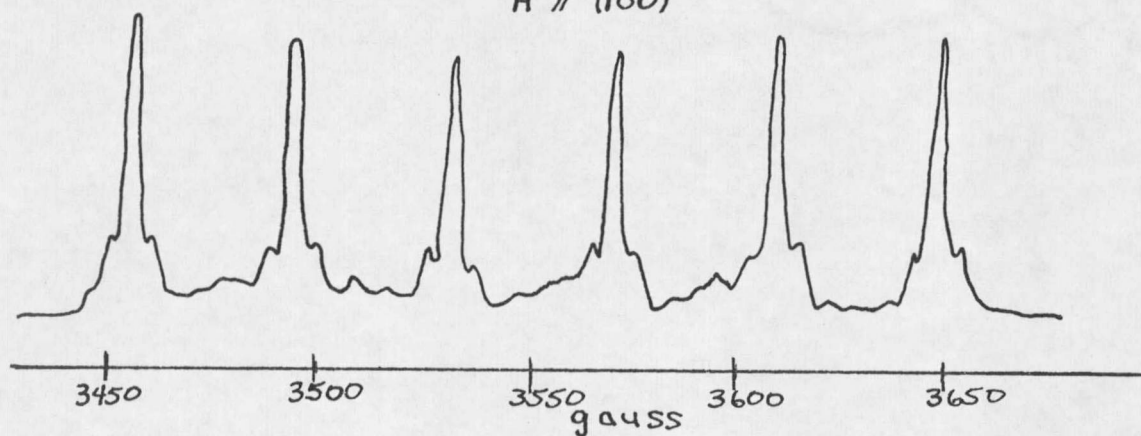
$\vec{H} \parallel (100)$ 

Figure 3.1

The direct absorption at X-band for $\Delta M = 1/2 \leftrightarrow -1/2$.

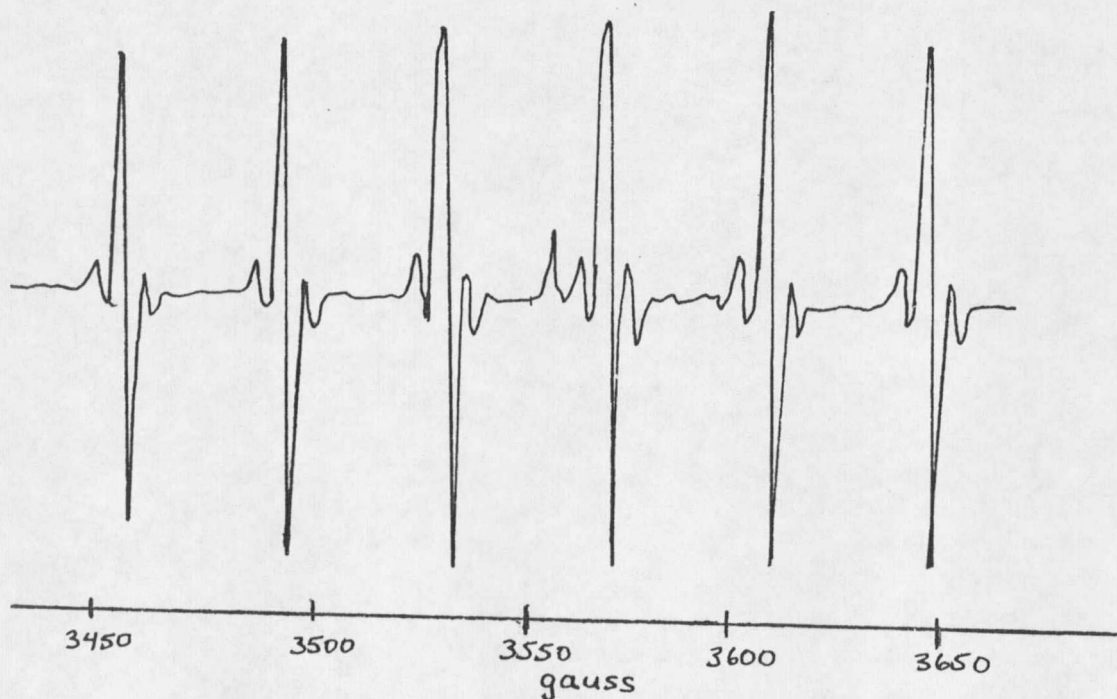
 $\vec{H} \parallel (100)$ 

Figure 3.2

The phase detected $\Delta M = 1/2 \leftrightarrow -1/2$ absorption with field modulation.

hyperfine interaction, which will be explained later in this chapter.

The method for producing the microwave frequency magnetic field H_1 perpendicular to H_0 and of detecting absorption is detailed in Appendix B. It is noted, however, that the spectrometer measures the derivative of the absorption lines not the lines of Fig. 3.1. Figure 3.2 is a display of the microwave absorption detected in this manner for the same $\Delta M = 1/2 \leftrightarrow -1/2$ spectrum.

The Hyperfine Splitting

The smallest energy splitting measured in the experiment was the hyperfine interaction. The Hamiltonian of an electron in a magnetic field \vec{H} , is derived from a vector potential. This discussion of the hyperfine interaction is well-treated by Milford, 1960, and is reproduced in Appendix D. Another spin Hamiltonian term is introduced into the phenomenological Hamiltonian of Chapter II

$$H(\text{Hyperfine}) = \vec{I} \cdot \vec{A} \cdot \vec{S} \quad 3.17$$

where \vec{A} is a symmetric tensor of order 2. For Eu impurities in fluorine crystals, \vec{A} is also isotropic and

$$H_{\text{hf}} = A \vec{I} \cdot \vec{S} \quad 3.18$$

The spin Hamiltonian is now

$$H = g\beta\vec{H}\cdot\vec{S} + \frac{b_4}{60} \left(0\begin{smallmatrix} 0 \\ 4 \end{smallmatrix} + 50\begin{smallmatrix} 4 \\ 4 \end{smallmatrix} \right) + \frac{b_4}{1260} \left(0\begin{smallmatrix} 0 \\ 6 \end{smallmatrix} - 210\begin{smallmatrix} 4 \\ 6 \end{smallmatrix} \right) + A\vec{I}\cdot\vec{S} + g_n\beta_n \vec{I}\cdot\vec{H} \quad 3.19$$

the last term being the nuclear Zeeman term.

For Eu the basis functions now included the nuclear function belonging to I^2 and I_z . Note, the nuclear spin I is $5/2$ for both isotopes 151 and 153 which occur in abundance.

$$I = 5/2; \quad -5/2 \leq m \leq 5/2 \quad 3.20$$

If a product wave function

$$\Psi = \Psi_e \Psi_n = |\gamma SM\rangle |Im\rangle$$

is used as a basis with respect to some common z axis, $\Psi = |M, m\rangle$ S and I implied, the matrix formed from H of eq. 3.10 and the $|M, m\rangle$'s having selected a coordinate system, would be an $8 \times 6 = 48$ matrix.

Calculation of Core Hyperfine Field

The 48 by 48 matrix can be diagonalized numerically for specific orientations of the crystal axes. The difficulty of this method can be reduced when the crystal field parameter is small relative to the Zeeman term.

Drumheller and Rubins (1964) have used perturbation theory to approximate the diagonalization when B_4 is very small.* For rather large B_4 such as is found in Eu^{++} in cubic crystals, this method may only be successful for very high external magnetic fields. It was found that a microwave frequency of 55 GHz was too great to allow clear resolution of forbidden transitions of Eu^{++} hyperfine lines in fluorite crystals. Perturbation techniques can be used to diagonalize the electronic 8 by 8 matrix when the wave functions of the spin Hamiltonian is written in a representation of the product of the eigenfunctions of I and S.

$$\psi_{M, m} = \psi_M^e \phi_m \quad (3.21)$$

For this purpose the Hamiltonian 3.19 is written as

$$H = H^e + H^n + H^{en} \quad (3.22)$$

where the electronic hamiltonian is

$$H^e = g\beta\vec{H} \cdot \vec{S} + \frac{b_4}{60} \left(0 \begin{smallmatrix} 0 \\ 4 \end{smallmatrix} + 50 \begin{smallmatrix} 4 \\ 4 \end{smallmatrix} \right) \quad (3.23)$$

In eq. 3.23 the order six terms of eq. 3.19 have been left off. The terms are small and need only be included when energy levels are being computed. The nuclear Hamiltonian

* b_4 about 1/2 when A is about $100 \times 10^{-4} \text{ cm}^{-1}$.

having eigenfunctions $\phi_m^{(M)}$ is

$$H'_n = g_n \beta_n \vec{H} \cdot \vec{I}. \quad 3.24$$

In eq. 3.24 quadrupolar terms are also left off. The term which couples the eigenfunctions of H^e and H^n is the hyperfine term

$$H^{en} = A \vec{I} \cdot \vec{S}. \quad 3.25$$

It is because of the coupling term eq. 3.25 that the nuclear wave functions $\phi_m^{(M)}$ are written as dependent on the electronic state indexed M. The fine structure levels of Chapter II are the

$$E_M^e \delta_{MM'} = \langle \Psi_M^e | H^e | \Psi_{M'}^e \rangle \quad 3.26$$

of eq. 2.19 with the angular correction of eq. 2.20 included. The Ψ_M^e 's are the functions which diagonalize H^e .

Using the representation of eq. 3.21,

$$\begin{aligned} \langle \Psi_{Mm}^e | H | \Psi_{M'm'}^e \rangle &= E_M^e \delta_{MM'} \\ &+ A \langle \Psi_M^e | \vec{S} | \Psi_{M'}^e \rangle \cdot \langle \phi_m^{(M)} | \vec{I} | \phi_{m'}^{(M)} \rangle \\ &+ g_n \beta_n \vec{H} \cdot \langle \phi_m^{(M)} | \vec{I} | \phi_{m'}^{(M)} \rangle \end{aligned} \quad 3.27$$

If A is small such that $A(E_{M'}^e - E_M^e)$ is much less than one, it is possible to set $M = M'$ in eq. 3.37 and not lose

accuracy in the hyperfine term.* Thus the spirit of the calculation implies accuracy to 1%. Then to find the eigenvalues of nuclear energy $E_m^{(M)}$ and the eigenfunctions $\phi_m^{(M)}$, the $2I + 1$ matrix of H'_n must be diagonalized. The prime of H'_n refers to the dependence of the set $\{\phi_m^{(M)}\}$ on the electronic states.

The second term in eq. 3.27

$$H_{MM',m'm}^n = A \langle \psi_M^e | \vec{S} | \psi_{M'}^e \rangle \cdot \langle \phi_m^{(M)} | \vec{I} | \phi_{m'}^{(M)} \rangle \quad 3.28$$

and the last term of eq. 3.27

$$H_{MM',m'm}^n = g_n \beta_n \vec{H} \cdot \langle \phi_m^{(M)} | \vec{I} | \phi_{m'}^{(M)} \rangle \quad 3.29$$

can be combined to a single nuclear term where $M = M'$.

Thus eqs. 3.28 and 3.29 become

$$\langle \phi_m^{(M)} | (g_n \beta_n \vec{H} + A \langle \psi_M^e | \vec{S} | \psi_M^e \rangle) \cdot \vec{I} | \phi_m^{(M)} \rangle.$$

The $\frac{A}{g_n \beta_n} \langle \psi_M^e | \vec{S} | \psi_M^e \rangle$ has units of magnetic field. It is termed variously as the "induced" field, the core hyperfine field and Bir's effective field after G. L. Bir (1964) who originally developed the theory. The "effective"

*For Eu^{++} in CaF_2 , $A = 34 \times 10^{-4} \text{ cm}^{-1}$ and $E_M^e - E_M^e$ is about 0.3 cm^{-1} .

field as seen by the nucleus then is

$$H_{\text{eff}}^{(m)} = \frac{A}{g_n \beta_n} \langle \psi_e | \vec{S} | \psi_e \rangle \cdot \vec{I} \quad (1) \quad 3.30$$

The field direction and magnitude depend on the electronic states ψ_M which have an angular dependence in this representation on the crystal field orientation. Physically one views this field as being the magnetic field the nucleus sees because of the orbital electrons. The total field at the nucleus is $\vec{H}_j = \vec{H}_{\text{eff}} + \vec{H}_0$, the vector sum of the external field and the effective field. For $A = 34 \times 10^{-4} \text{ cm}^{-1}$ and nuclear magneton $\beta_n = 5.03538 \times 10^{-24} \mu\text{g/G}$ and the spectroscopic splitting factor g_n is 1.44 for Eu^{151} and 0.637 for Eu^{153} , we have then $H_{\text{eff}} = 92,700 \vec{S}_{M,M}$ gauss for Eu^{151} and $44,500 \vec{S}_{M,M}$ gauss for Eu^{153} . When the experiment on Eu^{151} is done at X-band ($\nu = 10 \text{ GHz}$) the external magnetic field is about 3,600 gauss for the transitions $M = 1/2 \leftrightarrow -1/2$ which are of most importance to the experiment. Thus the external field is less than 4% of the induced field. In this case the induced field will dominate as the quantization axis of the nuclear Zeeman effect.

When an electronic transition occurs the effective field changes both magnitude and direction such as to

rotate the effective quantization axis $(H_{\text{eff}} + H) / |H_{\text{eff}} + H| = z$. The eigenfunctions in the rotated system can be expressed as a linear combination of the set $\{\phi_m^{(M)}\}$ belonging to the manifold of I. The unitary transformation matrix which represents a rotation is

$$[T_{mm}^I(\alpha, \beta, \gamma)] = T$$

and transforms the set of orthonormal ϕ_m 's as

$$\phi_m = \sum_{m'} T_{mm'}^I(\alpha, \beta, \gamma) \phi_{m'} \quad 3.31$$

The specific form for this matrix $T_{mm'}^I$, is the operator

$$R_{\vec{u}}(\theta) = \exp[-i\theta \vec{J} \cdot \vec{u}] = e^{-i\gamma J_z} e^{-i\beta J_x} e^{-i\alpha J_z} \quad 3.32$$

\vec{u} is the unit vector defining the axis of rotation in 3-space, θ is the angle of rotation about the axis and \vec{J} is the angular momentum operator. Expressing the arbitrary rotation in terms of Euler's angles, α is a rotation about the z axis, β a second rotation about the new x axis then γ a rotation about the z axis of the previous system. These three rotations can be made equivalent to a single rotation θ about \vec{u} (Messiah, 1962). Gel'fand, Minlos, and Shapiro (1963) have found an expression for this matrix and expresses $e^{-\beta J_x}$ of eq. 3.32 as the matrix

$$R_x = R(\beta) = [P_{mm'}^I(\mu)] \quad 3.33$$

where μ is the cosine of β , I indexes the manifold of the $2I + 1$ matrix.

The matrix of eq. 3.32, $e^{-i\gamma J_z}$ and $e^{-i\alpha J_z}$, can be shown to be simply

$$e^{-i\gamma J_z} |M\rangle = e^{-i\gamma M} |M\rangle \quad (\text{Messiah, 1962}) \quad 3.34$$

The derivation of the matrix $[P_{mm}^I(\mu)]$ is shown in Appendix A. The nuclear eigenfunctions in the representation which has the quantization axis shifted by differing electron spin states then becomes

$$\phi_m^{(M)} = \sum_{M'} P_{mm'}^I(\mu) \phi_{m'}^{(M)} \quad 3.35$$

In eq. 3.35 the function $\cos \theta = \mu$ depend on the angle between the electronic states M, M' .

$$= \cos(\vec{H}_M, \vec{H}_{M'})$$

(see eq. 3.30). This dependence then accounts for the angular dependence of the hyperfine coupling; that is, while $P_{mm'}^I(\mu)$ is a rotation matrix in the space spanned by the nuclear eigenfunctions $\phi_m^{(M)}$, its argument depends on the electronic eigenfunction Ψ_m^e . Actually μ depends on the transition between the eigenfunctions Ψ_M^e .

From eq. 3.27 the energy eigenvalues are

$$E_m^\mu = E_e^{MM} + g_n \beta_n [\vec{H}_{\text{eff}} + \vec{H}] \cdot \vec{I} \quad 3.36$$

The effective field can be substituted for the total field in the nuclear Zeeman term, thus

$$E_n^M = g_n \beta_n^m H_{\text{eff}}^{(M)} \quad 3.37$$

The field $H^{(M)}$ can be calculated from eq. 3.30 and becomes

$$\begin{aligned} \text{a) } H_x^{(M)} &= \frac{A}{g_n \beta_n} \langle \Psi_M^e | \frac{S_+ + S_-}{2} | \Psi_M^e \rangle \\ \text{b) } H_y^{(M)} &= \frac{A}{g_n \beta_n} \langle \Psi_M^e | \frac{S_+ - S_-}{2} | \Psi_M^e \rangle \\ \text{c) } H_z^m &= \frac{A}{g_n \beta_n} \langle \Psi_M^e | S_z | \Psi_M^e \rangle \end{aligned} \quad 3.38$$

From Chapter II when the crystal axes are rotated in the x-z plane by an angle θ , the electronic wave functions become

$$\begin{aligned} |\Psi_M^e\rangle &= |M\rangle + \sum_{M'}' \frac{\langle M | V_1 | M' \rangle}{E_M^0 - E_{M'}^0} |M'\rangle \\ &+ \sum_k' \sum_\ell' \left[\frac{\langle k | V_1 | \ell \rangle \langle \ell | V_1 | M \rangle}{(E_M^0 - E_k^0)(E_M^0 - E_\ell^0)} \right. \\ &\left. + \frac{\langle M | V_1 | M \rangle \langle k | V_1 | M \rangle}{(E_M^0 - E_k^0)^2} \right] |k\rangle \end{aligned} \quad 3.39$$

where V_1 is the crystal field interaction of the fourth order spherical harmonics.

$$V_1 = \frac{b_4}{60} \left\{ \left(\frac{3}{8} + \frac{5}{8} \cos 4\theta \right) O_4^0 + \left(\frac{5}{2} - \frac{5}{2} \cos 4\theta \right) O_4^2 \right. \\ \left. + \left(\frac{35}{8} + \frac{5}{8} \cos 4\theta \right) O_4^4 + 5i \sin 4\theta (O_4^1 - iO_4^2) \right\} \quad 3.40$$

The sixth order harmonics are not included because of the small value of b_6^* . In eq. 3.39 the $|M,m\rangle$'s are the $|M\rangle$'s which are the eigenfunctions of S_z when the magnetic field is selected as the z direction.

In order to calculate the energy levels directly from perturbation theory the entire spin Hamiltonian of eq. 3.19 is used with product wave functions $|M,m\rangle$ used as the representation. In this calculation the perturbation V_1 is the crystal field plus the hyperfine interaction. Again as in the induced field method the nuclear Zeeman term is left off. With the hyperfine term written as

$$H_{hf} = A \vec{I} \cdot \vec{S} = A \{ I_z S_z \} + \frac{A}{2} (S_+ I_- + S_- I_+), \quad 3.41$$

and the crystal field interaction as eq. 3.40, the energy levels are calculated from second order perturbation theory

$$E_{M,m} = E_{M,m}^0 + \langle M,m | H_1 | M,m \rangle + \sum_{M',m'} \frac{|\langle M',m' | H_1 | M,m \rangle|^2}{E_{M,m}^0 - E_{M',m'}^0}$$

* $b_6 = 0.5 \times 10^{-4} \text{ cm}^{-1}$, $b_4 = 55 \times 10^{-4} \text{ cm}^{-1}$ or $b_6/b_4 = 0.99\%$.

With $H_1 + H_{\text{eff}} + H_{\text{hf}}$ from eqs. 3.40 and 3.41 the energy levels of eq. 2.16, M, m levels become;

$$\begin{aligned} \text{a) } E_{\pm 7/2, m} &= \pm \frac{7}{2} g \beta H + \frac{7}{8} b_4 (3 + 5 \cos \theta) + b_6 \pm \frac{7}{2} A m \\ &+ \frac{35}{4} \frac{b_4^2}{g \beta H_0} \pm \frac{A^2}{4 g \beta H_0} [7 (\frac{35}{4} \mp m^2 \pm m)] \end{aligned}$$

$$\begin{aligned} \text{b) } E_{\pm 5/2, m} &= \pm \frac{5}{2} g \beta H + \frac{13}{8} b_4 (3 + 5 \cos \theta) + 5 b_6 \pm \frac{5}{2} A m \\ &+ \frac{75}{4} \frac{b_4^2}{g \beta H_0} [5 (\frac{35}{4} \mp m^2) \pm 19 m] \end{aligned}$$

$$\begin{aligned} \text{c) } E_{\pm 3/2, m} &= \pm \frac{3}{2} g \beta H + \frac{3}{8} b_4 (3 + 5 \cos 4\theta) + 9 b_6 \pm \frac{75 b_4^2}{4 g \beta H_0} \\ &+ \frac{3}{2} A m \pm \frac{A^2}{4 g \beta H} [3 (\frac{35}{4} \mp m^2) \pm 27 m] \end{aligned}$$

$$\begin{aligned} \text{d) } E_{\pm 1/2} &= \pm \frac{1}{2} g \beta H + \frac{9}{8} b_4 (3 + 5 \cos 4\theta) + 5 b_6 \pm \frac{35 b_4^2}{4 g \beta H} \\ &\pm \frac{1}{2} A m \pm \frac{A^2}{4 g \beta H_0} [\frac{35}{4} \mp m^2 \pm 31 m] \end{aligned} \quad 3.42$$

In the above expressions terms of order $\frac{b_4 b_6}{g \beta H}$, $\frac{b_6^2}{g \beta H}$ and $\frac{b_4^2}{g \beta H} \sin^2 4\theta$ are not included in the second order calculation. The above energy levels are accurate to the order of perturbation for $\theta \leq 5^\circ$ which is adequate for the measurements discussed in Chapter IV.

In the E.P. R. experiment the energy of the photon

exciting transitions between the levels of eq. 3.42 is fixed and the resonance condition is achieved by varying the external field H_0 . For the hyperfine transition, excluding a perturbation equal to or higher than $\Delta M = \pm 2$, the field where the transition occurs is called the line position. These transitions are:

$$\begin{aligned}
 \text{a) } \bar{H}_{\pm 7/2, \pm 5/2}^{mm'} &= H_0 \pm 20b_4q \pm 6b_6 \mp \frac{1}{4H_0} [35(b_4q \mp 3b_6)^2 \\
 &\quad \mp 3(5b_4q \mp 7b_6)^2 \mp \frac{A}{2}(7m \mp 5m') \mp \frac{A^2}{4H_0} \\
 &\quad \times \{7(\frac{35}{4} \mp m^2) \mp 5(\frac{35}{4} \mp m'^2) \pm (7m - 19m')\}] \\
 \text{b) } \bar{H}_{\pm 5/2, \pm 3/2}^{mm'} &= H_0 \pm b_4q \pm 14b_6 \mp \frac{A}{2}(5m \mp 3m') \mp \frac{A^2}{4H_0} \\
 &\quad \times \{5(\frac{35}{4} \mp m^2) \mp 3(\frac{35}{4} \mp m'^2) \pm (19m - 27m')\}] \\
 \text{c) } \bar{H}_{\pm 3/2, \pm 1/2}^{mm'} &= H_0 \pm 12b_4q \pm 14b_6 \mp \frac{1}{4H_0} [3(5b_4q \mp 7b_6)^2 \\
 &\quad \mp 35(b_4q \mp 3b_6)^2] \mp \frac{A}{2}(3m \mp m') \mp \frac{A^2}{4H_0} \\
 &\quad \times \{3(\frac{35}{4} \mp m^2) \mp \frac{35}{4} \mp m'^2 \pm (27m - 31m')\}] \\
 \text{d) } \bar{H}_{\pm 1/2, \pm 1/2}^{mm'} &= H_0 \mp \frac{35}{2} (b_6q \mp 3b_6)^2 \mp \frac{A}{2}(m \mp m') \mp \frac{A^2}{4H_0} \\
 &\quad \times \{ \frac{35}{4} \mp m^2 \mp m'^2 \pm 31(m \mp m') \} \quad 3.43
 \end{aligned}$$

In the above expressions terms of order b_6b_4/H and $(b)^2/H$

were dropped. Also a small angle was assumed such that the term of order $(b_4)^2/H \sin^2 \theta$ were not included. $q = 1/8(3 + 5 \cos \theta)$ determines the angular dependence for angles $\theta \leq 5^\circ$. The allowed transitions of eq. 3.43 are displayed as the derivative of the microwave absorption versus the applied magnetic field. In the display of Fig. 3.2, the angle ϕ is zero. Figure 3.2 is the differentiated spectrum. Figures 3.3(a) through (c), show the transitions of Figure 3.2 as the angle θ is varied from zero to five degrees. It can be noticed that the line intensities are a function of angle, some lines being of zero intensity at zero degrees.

The transitions between the energy levels occur when the intensity, eq. 3.16, is other than zero.

$$I = g^2 \beta^2 H_1^2 |\langle M'm' | S_x | M_0 m \rangle|^2 \quad 3.44$$

The operator $S_x = \frac{1}{2}(S_+ + S_-)$ induces transition which follow the selection rules $\Delta M = \pm 1$. The selection rules are with respect to the unperturbed eigenfunctions of S^2 , S_z . If the wave functions of the energy levels were also eigenfunctions of S^2 , S_z ; the quantum numbers S and M would be said to be "good" quantum numbers. The wave functions are expressed as a linear combination of the

eigenfunctions of S^2 , S_z ; therefore, transitions between levels indexed M' and M of eq. 3.45 occur when M' and M do not differ by one. These transitions are usually weaker than those transitions between M , M' levels differing by one and are called "forbidden" transitions. In the Eu ion in fluorite crystals, "forbidden" transitions occur between levels indexed by different m as well, and are termed "forbidden hyperfine" transitions. As can be seen in Fig. 3.3, the forbidden lines can have greater intensity than allowed lines.

In the induced field method, the wave functions M , m are written in a representation where the product of wave function belonging to H_e and those belonging to H_n . The wave functions of H_n depend on the electronic state through the rotation matrix of eq. 3.35. Then eq. 3.45 becomes

$$I = q^2 \beta^2 H_1^2 |\langle \psi_e^{M'} \phi_m^{(M)} | S_x | \psi_e^M \phi_{m'}^{(M)} \rangle|^2$$

$$g^2 \beta^2 H_1^2 |\langle \psi_e^M | S_x | \psi_e^M \rangle|^2 |\langle \phi_m^M | \phi_{m'}^M \rangle|^2 \quad 3.45$$

Note that this expression consists of two parts, the probability of an electronic transition

$$w_n^{mm'} = |\langle \phi_m^M | \phi_{m'}^M \rangle|^2 \quad 3.46$$

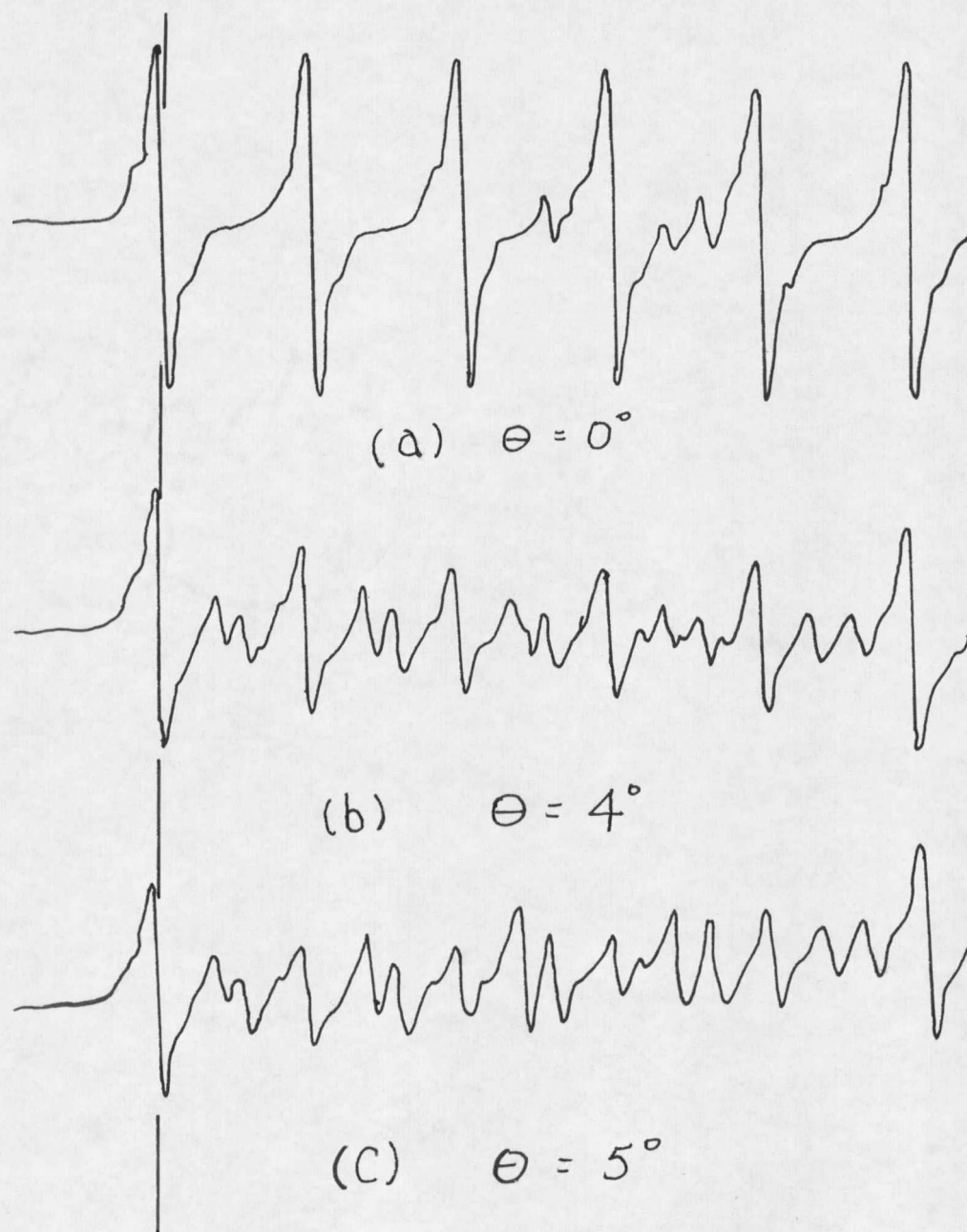


Figure 3.3 Hyperfine spectrum for $\Delta M = 1/2 \leftrightarrow -1/2$. Taken at room temperature, compare line width with Fig. 3.2. θ is angle between field and (100) axis.

Substituting from eqs. 3.42, 3.46 becomes

$$w_n^{mm'} = |\langle \phi_m^M | \sum_{m'} P_{mm'}^I(\mu) | \phi_{m'}^M \rangle|^2 \quad 3.47$$

In eq. 3.47 the superscript M's are now the same, the set $\{\phi_m^M\}$ is an orthonormal set thus

$$w_n^{mm'} = |P_{mm'}^I(\mu)|^2 \quad 3.48$$

The line intensities of eq. 3.45 can be found using $P_{mm'}^{5/2}(\mu)$ matrix elements of Table 3.2 (see Appendix A).

Table 3.2

Analytic Form of the Functions $|P_{mm'}^{5/2}(\mu)|^2$

(Bir and Sochava, 1964)

$ P_{5/2,5/2}^{5/2} $	$ P_{3/2,3/2}^{5/2} $	$ P_{1/2,1/2}^{5/2} $	$ P_{5/2,3/2}^{5/2} $
$(\frac{1+\mu}{2})^5$	$(\frac{1+\mu}{2})^3 (\frac{3-5\mu}{2})^2$	$(\frac{1+\mu}{2}) \cdot (\frac{5\mu^2-2\mu-1}{2})^2$	$5 \cdot (\frac{1-\mu}{2}) \cdot (\frac{1+\mu}{2})^4$
$P_{3/2,1/2}^{5/2}$		$P_{5/2,1/2}^{5/2}$	
$(\frac{1+\mu}{2})^2 \cdot (1-\mu) \cdot (\frac{1-5\mu}{2})^2$		$10 (\frac{1-\mu}{2})^2 \cdot (\frac{1+\mu}{2})^3$	

The argument of the $P_{mm'}^I(\mu)$'s, μ , is the cosine of the angle between the core hyperfine fields of state M and M' . The indices M and M' are those of the corresponding electronic part of the intensities of eq. 3.45. The experiment to be described in Chapter IV was performed by rotations of θ about a (100) crystal axis, thus by choice, the rotations take place in the $x-z$ plane.

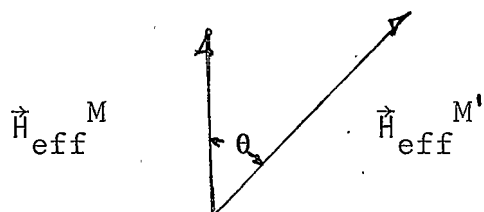


Figure 3.4

$$\mu = \cos \theta = \frac{H_{\text{eff}}^M \cdot H_{\text{eff}}^{M'}}{|H_{\text{eff}}^M| |H_{\text{eff}}^{M'}|} \quad 3.49$$

$$\mu = \frac{H_z^M H_z^{M'} + H_x^M H_x^{M'}}{\sqrt{H_z^M{}^2 + H_x^M{}^2} \sqrt{H_z^{M'}{}^2 + H_x^{M'}{}^2}} \quad 3.50$$

$$(H_z^2 + H_x^2)^{1/2} = H_z^{-1} [1 + (\frac{H_x}{H_z})^2]^{1/2} \quad 3.51$$

when H_x/H_z is small a Taylor's expansion of eq. 3.51 sub

stituted into eq. 3.50 results in

$$\mu = \frac{H_z^{M'} H_z^M}{|H_z^{M'} H_z^M|} \left\{ 1 - \frac{1}{2} \left[\frac{H_x^M}{H_z^M} - \frac{H_x^{M'}}{H_z^{M'}} \right] + \dots \right\} \quad 3.52$$

Substituting eq. 3.38 into 3.52 and using ψ_e^M to first order, only 0_4^1 is present in the perturbation calculation of H_x^M . In the calculation, a symmetrized S_x times 0_4^1 results in an 0_4^0 and 0_4^2 combination.

$$S_{\pm} Y_4^{\pm 1} = \sqrt{S(S+1) - M(M\pm 1)} Y_4^{2,0,-2}$$

Then eq. 3.52 becomes

$$\mu = \frac{MM'}{|MM'|} \left[1 - \frac{1}{2} \left(\frac{b_4 \sin 4\theta}{24g\beta H} \right)^2 \left(\frac{\langle M | 0_4^0 | M \rangle}{M} - \frac{\langle M' | 0_4^0 | M' \rangle}{M'} \right) \right] \quad 3.53$$

The values of the matrix elements of 0_4^0 are found in Low (1960, page 18). The approximation of eq. 3.53 is accurate for angles less than 10° . For angles greater than 10° , higher order calculations of eq. 3.50 could be made using ψ_e^M calculated to higher orders.

Eq. 3.53 is greater for the $\Delta M = 1/2 \leftrightarrow -1/2$ electronic calculation. The intensities of the lines in this group, therefore vary greatly as is seen from Fig. 3.3. Bir, Butikov, and Sochara (1965) measuring intensities of the $\Delta M = 1/2 \leftrightarrow -1/2$ spectrum were able to verify the predicted

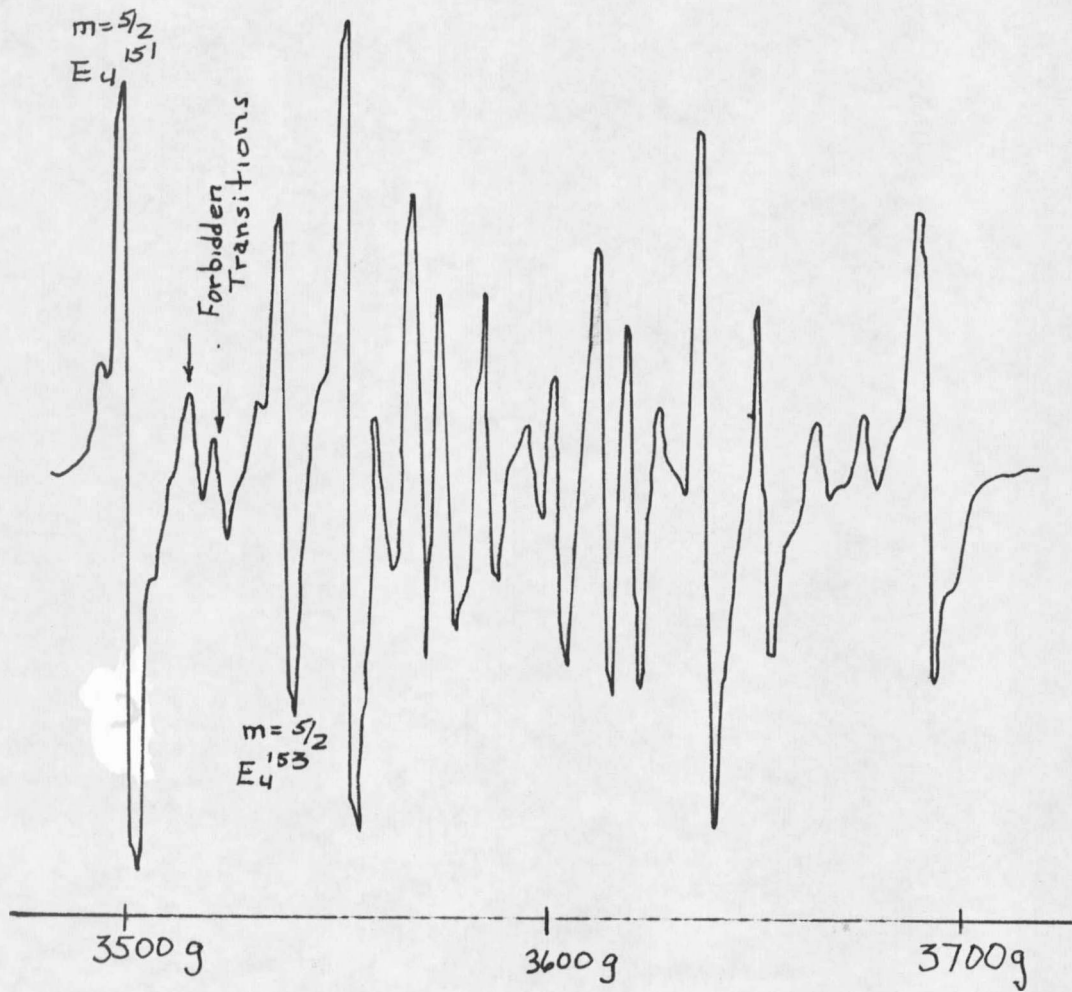


Figure 3.6 The $\Delta M = 1/2 \leftrightarrow -1/2$ hyperfine spectrum with both isotopes Eu^{151} and Eu^{153} in CaF_2 . The magnetic field is 3° to a (100) axis.

intensities of this theory for some lines of the spectrum. Namely the allowed, $\Delta m = \pm 5/2 \leftrightarrow \pm 5/2$ $\Delta m = \pm 3/2 \leftrightarrow \pm 3/2$ transitions and the forbidden $\Delta m = \pm 5/2 \leftrightarrow \pm 3/2$ and $\Delta m = \pm 5/2 \leftrightarrow \pm 1/2$ transitions. Application of the theory to other lines was not attempted because they used an europium sample containing both isotopes 151 and 153. Figure 3.6 shows the confusion resulting in this case since the two isotopes have different hyperfine coupling constants. Stice and Worsencroft (1970) were able to verify the theory for other lines in the $\Delta M = 1/2 \leftrightarrow -1/2$ spectrum by using the single isotope Eu^{151} . In that same work the weaker forbidden lines $\Delta m = \pm 1$ in $\Delta M = \pm 3/2 \leftrightarrow \pm 1/2$ spectrum were found and the theory applied to show good agreement. This was the first report of these lines as far as the author was able to ascertain. Figure 3.7 is a display of the $\Delta M = 3/2 \leftrightarrow 5/2$ spectrum which overlaps the $\Delta M = 5/2 \leftrightarrow 7/2$ spectrum. In Fig. 3.7 the same spectrum is displayed when an angle of $2 1/2^\circ$ was between the magnetic field and a (100) crystal axis. Figure 3.7(b) is a histogram of the position of the expected energy from the theory, the height is relative to the expected intensity and the width the measured line with at 78°K from the experiment.

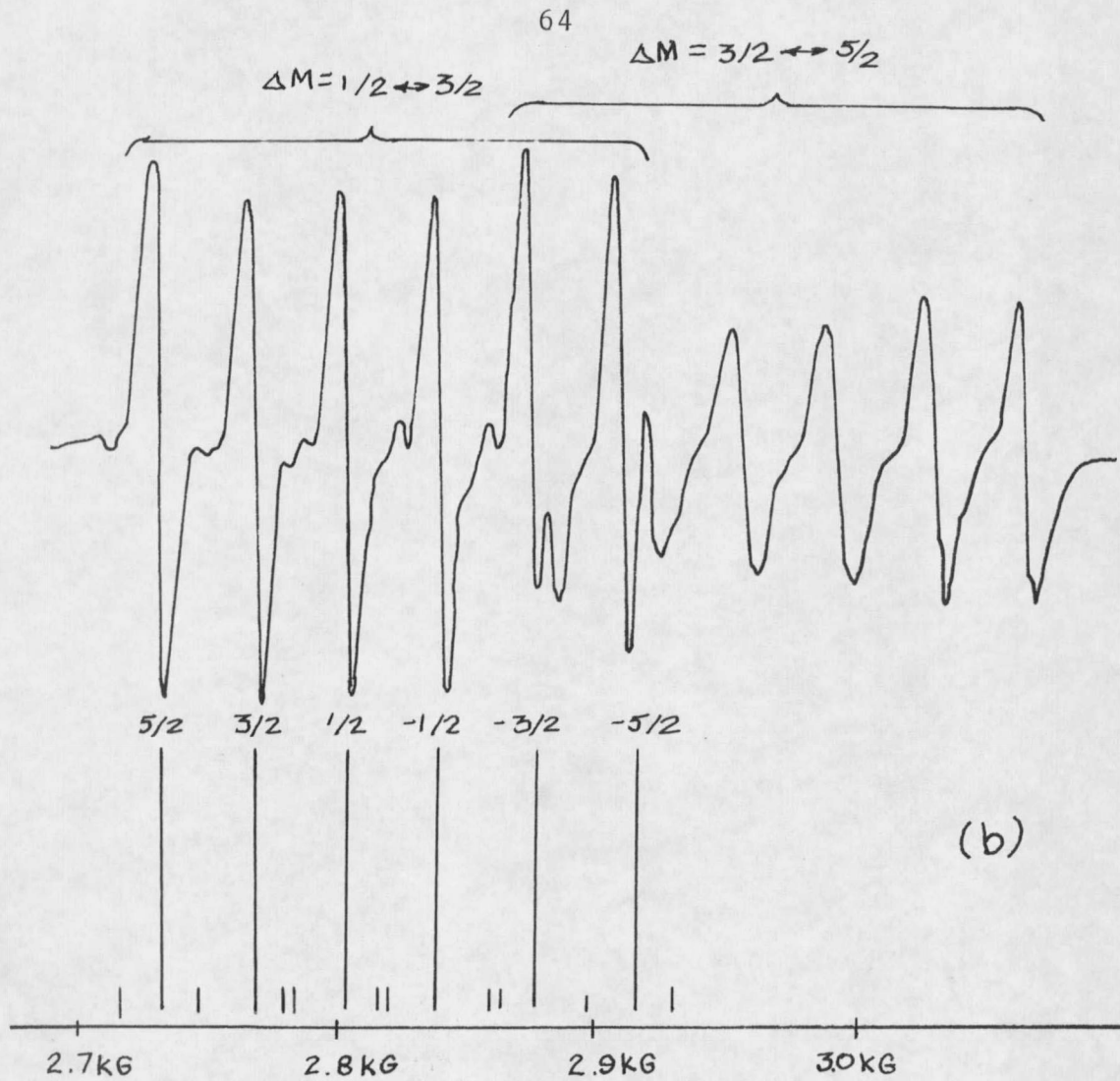


Figure 3.7 Forbidden hyperfine lines in the $\Delta M = 3/2 \leftrightarrow 1/2$ spectrum of Eu-CaF_2 . The doublet between $M = 1/2$, and $M = -1/2$ was later resolved but that between $M = -1/2$ and $M = 3/2$ was not.

Table 3.3

The line positions calculated for the hyperfine spectrum of Figure 3.7,

$H_{\text{center}} = 3547 - 726 = 2823$ gauss, the lines from

left to right of the $M = 1/2 \quad 3/2$ are:

$5/2, 3/2 = H_C - 108.3$	$1/2, 1/2 = H_C - 19.7$	$-5/2, -3/2 = H_C + 108$
$5/2, 5/2 = H_C - 91.4$	$1/2, -1/2 = H_C - 41.1$	$-3/2, -5/2 = H_C + 38.6$
$3/2, 5/2 = H_C - 38.7$	$-1/2, 1/2 = H_C + 41.4$	$-3/2, -3/2 = H_C + 54$
$3/2, 1/2 = H_C - 76.9$	$-1/2, -3/2 = H_C - 5.0$	$-5/2, -5/2 = H_C + 91$
$1/2, 3/2 = H_C - 1.3$	$-3/2, -1/2 = H_C + 75.3$	
$3/2, 3/2 = H_C - 55.5$	$-1/2, -1/2 = H_C + 15.6$	

CHAPTER IV

ORBIT-LATTICE INTERACTION

Necessary Approximations

Chapter II dealt with the interaction of the paramagnetic electrons and the crystal field. Chapter III then presented a theory which predicted the intensities of the E.P.R. transitions as function of spatial orientation. Both presentations assumed the crystal-lattice to be rigid. That is, the position of the lattice sites were assumed to be fixed in time. There is, of course, an internal energy which is associated with the vibrational-kinetic motion of the ions. Several macroscopic phenomena can be explained from the quantum treatment of these vibrations, called lattice vibrations. The local surroundings of the paramagnetic ions in fluorite crystals is altered in such a way as to "couple" the quantized vibrations or phonons to the paramagnetic electrons. Thus, temperature changes will shift the energy levels and subsequently alter the E.P.R. spectrum as to line position as well as the intensity of the hyperfine spectrum.

In this chapter appropriate corrections to the crystal field parameters will be proposed by an analysis of

of the orbit-lattice interaction. This interaction can be imagined to be an interaction between the quantized lattice vibrations and the paramagnetic electrons.

The potential energy term or binding energy of a periodic crystal varies as the ions in the crystal are displaced from equilibrium by a displacement $\vec{u}_{s\ell}$ of the s th ion in the ℓ th unit cell. The potential expanded in a Taylor's series is

$$\begin{aligned}
 V = V_0 + \sum_{s\ell j} u_{s\ell}^j \left(\frac{\partial V}{\partial u_{s\ell}^j} \right)_0 + \sum_{ss', \ell\ell', jj'} u_{s\ell}^j \\
 \times u_{s'\ell'}^{j'} \left(\frac{\partial^2 V}{\partial u_{s\ell}^j \partial u_{s'\ell'}^{j'}} \right)_0 \\
 + \sum_{ss's'', \ell\ell'\ell'', jj'j''} u_{s\ell}^j u_{s'\ell'}^{j'} u_{s''\ell''}^{j''} \\
 \left(\frac{\partial^3 V}{\partial u_{s\ell}^j \partial u_{s'\ell'}^{j'} \partial u_{s''\ell''}^{j''}} \right)_0 + \dots \quad 4.1
 \end{aligned}$$

where $u_{s\ell}^j$ refers to the j th cartesian component of $u_{s\ell}$. The cubic term in the binding energy expansion is the anharmonic term and it accounts for the first order correction to lattice expansion which would be zero if only harmonic corrections were considered. The effect of

anharmonic forces as explained by Ziman (1965) follows:

"As the temperature rises the amplitude of the lattice vibrations increases, so that the average R.M.S. values of the displacement $u_{s\alpha}$ etc., increase. The anharmonic terms contribute to the free energy of the crystal, which is now no longer necessarily a minimum for vibrations around the assumed 'equilibrium' configuration in which each $u_{s\alpha}$ vanishes. The whole crystal then expands (or contracts) until it finds the volume where the total free energy is a minimum."

In analyzing the temperature dependence, corrections for lattice expansion will be made as if it were an independent effect from the harmonic term. This assumption, that the effects can be separated, is then based on the assumption that a Taylor's series expansion is valid.

In Chapter V corrections for the anharmonic term will be made from measurements of the dependence of crystal-field parameters on hydrostatic pressure. Then the crystal field will be expanded as a Taylor's series in terms of the ion displacements. As a further simplification it is assumed that only nearest neighbor ions will contribute to a crystal field, thus upon replacing the displacement variables with normal mode variables only the 27 normal modes of the XY_8 functional cell will be considered. The normal modes will then be written in terms of phonons by quantizing the harmonic oscillators and a simple Debye model will allow

averaging which will predict a temperature dependence.

To effect these corrections a model based on vibrations of small amplitude is adopted. The binding energy of the crystal, which is assumed to be a function of the positions of the ions, is expanded in a Taylor's series of displacements from equilibrium of the ions. The equilibrium state is that where no unbalanced force would be acting on the ions. The expression to third order terms is eq. 4.1. The zero order term is constant and can be neglected as long as the crystal remains intact. The first order term is zero from the definition of equilibrium. The quadratic order term is called the harmonic term and approximates the deviation from a rigid lattice by considering a restoring force which varies linearly with displacement. The harmonic motion of the ions will affect the crystal-field seen by the paramagnetic ions. The crystal-field should not be confused with the binding energy of the crystal. The crystal-field is measured at the electron of a paramagnetic ion from a coordinate system fixed to the nucleus of that ion and is given in a simplified system which only considers the effect from the nearest neighbor fluorine ions.

Again, as in Chapter II, the classical solution of the

electric potential energy of the paramagnetic f electrons of Eu interacting with the eight ligand fluorine ions which are the nearest neighbors is expressed in terms of spherical harmonics

$$V_c = \sum_e \sum_{\ell=0}^{\infty} \sum_{m=-\ell}^{\ell} r_e^{-\ell} V_{\ell}^m Y_{\ell}^{-m}(\theta_e, \phi_e) \quad 4.2$$

In eq. 4.2 \sum_e means the summation over all f electrons each being positioned at coordinates (r_e, θ_e, ϕ_e) . Further simplification is obtained by assuming point charges for the fluorine ions. This assumption neglects covalency and overlap which, while they are not negligible, are at least a lesser effect for deep-seated f electrons than would appear in transition metal ions (Simanek and Huang, 1966). Assuming point charges in eq. 4.2 the coefficients

$$V_{\ell}^m = \sum_{i=1}^8 \frac{-e'e}{R_i^{\ell+1}} \frac{Y_{\ell}^m(\theta_i, \phi_i)}{2\ell+1} \quad 4.3$$

where the i th fluorine ion is located at position (R_i, θ_i, ϕ_i) and has an effective charge e' . This potential energy results from a solution to the point charge Laplace equation solved in terms of Legendre polynomials subsequently expanded to the solution of eq. 4.2 and 4.3 by the addition theorem for spherical harmonics (Arfken, 1966).

The position of the fluorine ions (R_i, θ_i, ϕ_i) of eq. 4.3 is not constant. Because of lattice vibration, which are assumed to be much smaller in magnitude than R_i , V_c of eq. 4.2 can be expressed as a Taylor's series in terms of the cartesian coordinates of the ionic displacements α_j .

$$V_c = \sum_i \left[\sum_{\ell} \sum_{m=-\ell}^{\ell} \left\{ V_{\ell}^m \Big|_0 + \sum_{j,i} \left(\frac{\partial V_{\ell}^m}{\partial \alpha_j^i} \right) \Big|_0 \alpha_j^i + \dots \right\} \right. \\ \left. \times r_e^{\ell} Y_{\ell}^m(\theta_e, \phi_e) \right] \quad 4.4$$

In eq. 4.4 α_j^i refers to the α_j th component [$\alpha_j = (x, y, z)$ as $j = (1, 2, 3)$] of the displacement of the i ion. In the XY_8 functional cell there are 27 degrees of freedom; that is, the motion of the complex can be described with 27 linearly independent variables. The choice of the cartesian (x, y, z) components of all nine ions could be exchanged for "normal" coordinates of like number 27. The subscript 0 of eq. 4.4 refers to the value of these functions at zero displacement or at R_{i0} , the equilibrium position. The first term of eq. 4.4 is then the rigid lattice crystal field presented in Chapter II. The term linear in α_j^i is called the orbit-lattice interaction following Van Vleck (1939).

The orbit-lattice interaction

$$V_{OL} = \sum_e \sum_{m \neq 0, \ell} \sum_{j, i} \left. \frac{\partial Y_{\ell}^m}{\partial \alpha_j} \right|_0 \alpha_j^i r e^{\ell} Y_{\ell}^m (\theta_e \phi_e) \quad 4.5$$

is now expanded in terms of the normal modes of XY_8 using the chain rule of differentiation,

$$\frac{\partial Y_{\ell}^m}{\partial \alpha_j^i} = \sum_k \frac{\partial Y_{\ell}^m}{\partial q_k} \frac{\partial q_k}{\partial \alpha_j^i}$$

The q 's are the normal modes coordinates and V_{ℓ}^m from the point charge model is given by eq. 4.3.

The ground state of the Eu ion is an $^8S_{7/2}$. As pointed out in Chapter II a Stark effect of an electric field and S state system does not exist. It is through admixing of higher order states into the ground state that a crystal field splitting results. Similarly, the orbit-lattice interaction will add to the splitting by admixing higher order states into the ground state of several 4f electrons. Because the excited states of Eu are separated by large energies the perturbation of the orbit-lattice interaction will be calculated considering only the coupling of 6s orbitals into the 4f orbitals of the ground state.

The type of matrix elements which will be used in the perturbation of the rigid-lattice crystal-field by the

orbit-lattice interaction are

$$\langle \Psi_{(4f)6, 6s} | V_{OL} | \Psi_{(4f)7} \rangle, \quad 4.6$$

The ground state wave function $\Psi_{(4f)7}$ is a product wave function

$$| \Psi_{(4f)7} \rangle = | (4f)_3^+ (4f)_2^+ (4f)_1^+ (4f)_0^+ (4f)_{-1}^+ (4f)_{-2}^+ \rangle \\ \times | (4f)_{-3}^+ \rangle \quad 4.7$$

and the excited state

$$| \Psi_{(4f)6, 6s} \rangle = P_6^7 | (4f)_i^+ (4f)_j^+ (4f)_k^+ (4f)_l^+ (4f)_m^+ \rangle \\ \times | (4f)_n^+ 6s^+ \rangle \quad 4.8$$

The symbol P_6^7 refers to a normalized sum of the wave functions made by a combination of (3,2,1,0,±1,-2,-3) taken six at a time for (i,j,k,l,m,n). The angular part of the atomic wave functions are spherical harmonics of order three for the 4f orbitals. The + sign refers to the spin being up. All orbitals are + spin in keeping with Hund's rules. Resulting non-zero wave functions will be of the type

$$\langle (4f)_m^+ | V_{OL} | 6s^+ \rangle, \quad 4.9$$

From eq. 4.5 V_{OL} is seen to be an infinite series of all

spherical harmonics. Of these only those spherical harmonics of order three ($l = 3$) of eq. 4.5 will result in non-zero terms in eq. 4.9.

Symmetry Reductions

From eq. 4.5 only the terms where $l = 3$ need to be retained. Also in eq. 4.5 the variables α_i^j can be changed to the normal coordinates of XY_8 which will allow great simplification in the calculations, by use of group theory. In eq. 4.5 it is desirable to use those particular combinations of Y_3^m which form the basis of the irreducible representation of the O_h group. These functions transform among themselves without being reduced to other combinations of the O_h group (Tinkham, 1964 Chapter III). As is shown in Appendix A the character of Y_3^m under O_h under O_h is reducible as

$$\Gamma(Y_3)_{O_h} \rightarrow \Gamma_{2u} + \Gamma_{4u} + \Gamma_{5u} \quad 4.10$$

See Table 4.1. Since Y_3 is reducible only in terms of odd inversion symmetry representations the one dimensional Γ_{2u} and both three dimensional Γ_{4u} and Γ_{5u} , then only the base functions of these irreducible representations can be expressed in terms of order three spherical harmonics.

(Griffith, 1961 pg. 166). More simply stated, since by eq. 4.10 Y_3 is reducible in terms of the basis functions given, then it is possible to find an inverse function where the basis functions Γ_{2u} , Γ_{4u} and Γ_{5u} are expressible in terms of Y_3^m 's.

From Table A.19 of Griffith, (1961) the basis functions for the irreducible representations Γ_{2u} , Γ_{4u} , and Γ_{5u} in terms of the Y_3^m are

$$C(\Gamma_{2u}^3, A_2) = (4\pi/14)^{1/2} (Y_3^2 - Y_3^{-2}),$$

$$C(\Gamma_{4u}^3, 1) = -1/2(4\pi/14)^{1/2} [(5)^{1/2} Y_3^{-3} + (3)^{1/2} Y_3^1],$$

$$C(\Gamma_{4u}^3, 0) = (4\pi/7)^{1/2} Y_3^0,$$

$$C(\Gamma_{4u}^3, -1) = -1/2(4\pi/14)^{1/2} [5^{1/2} Y_3^3 + (3)^{1/2} Y_3^{-1}],$$

$$C(\Gamma_{5u}^3, 1) = -1/2(4\pi/14)^{1/2} [3^{1/2} Y_3^3 - 5^{1/2} Y_3^{-1}],$$

$$C(\Gamma_{5u}^3, 0) = (4\pi/14)^{1/2} (Y_3^2 + Y_3^{-2}),$$

and

$$C(\Gamma_{5u}^3, -1) = -1/2(4\pi/14)^{1/2} [3^{1/2} Y_3^{-3} - 5^{1/2} Y_3^1]. \quad 4.11$$

In eq. 4.5 for V_{0L} , the Y_{ρ}^m as above are arranged in linear combinations of 0_h and can be expressed in terms of the Y_3^m . The particular combination of the displacement

Table 4,1

0h	E	8C ₃	3C ₂	6C ₂	6C ₄	σ _h	8S ₃	3S ₂	6S ₂	6S ₄
Γ _{1g}	1	1	1	1	1	1	1	1	1	1
Γ _{2g}	1	1	1	-1	-1	1	1	1	-1	-1
Γ _{3g}	2	-1	2	0	0	2	-1	2	0	0
Γ _{4g}	3	0	-1	-1	1	3	0	-1	-1	1
Γ _{5g}	3	0	-1	1	-1	3	0	-1	1	-1
Γ _{1u}	1	1	1	-1	-1	-1	-1	-1	-1	-1
Γ _{2u}	1	1	1	-1	-1	-1	-1	-1	1	1
Γ _{3u}	2	-1	2	0	0	-2	1	-2	0	0
Γ _{4u}	3	0	-1	-1	1	-3	0	1	1	-1
Γ _{5u}	3	0	-1	1	-1	-3	0	1	-1	1
Γ(XY ₈)	27	0	-1	-1	1	-3	0	1	3	-1
Γ(Y ₃)	7	1	-1	-1	-1	7	-1	1	1	1

$$\begin{aligned}
 \checkmark \quad (XY_8): \quad & \Gamma_{1g} + \Gamma_{2g} + \Gamma_{3g} + 2\Gamma_{4g} + \Gamma_{5g} + \Gamma_{1u} + \Gamma_{2u} + \Gamma_{3u} \\
 & + 3\Gamma_{4u} + \Gamma_{5u}
 \end{aligned}$$

α_i^j multiplying these bases functions must have the same symmetries as the bases functions themselves since the potential V_{OL} has O_h symmetry. These combinations of α_i^j which transform as the irreducible representations of O_h are simply the normal modes of the XY_8 molecule. The XY_8 molecule then has a unitary transformation matrix for which each operation of the group transforms the 27 components of the nine ion displacements among themselves.

The character of these 27 x 27 matrices can be obtained as follows: The identity leaves all 27 components unchanged; or a 27 x 27 unit matrix. The trace is 27. An inversion leaves only the center ion in place, thus the matrix must contain off diagonal elements to transform the three cartesian displacements of one ion to other ionic positions. The central ion is not transformed to a new position but the components of the axial type vector displacement of this central ion transforms as Γ_{4u} of Table 4.1. Γ_{4u} is the basis of an axial character of XY_8 on inversion σ_h is then inversion for a single Γ_{4u} basis, that is -3. The character of XY_8 under any class of symmetry operations of O_h is then the product of the number of ions not moved from their original place by the operation times the character of the axial vector Γ_{4u} for

that operation. Table 4.1 lists the character representation of (XY_8) . This representation is reducible as (see Appendix A)

$$\Gamma(XY_8) \rightarrow \Gamma_{1g} + \Gamma_{2g} + \Gamma_{3g} + \Gamma_{4g} + 2\Gamma_{5g} + \Gamma_{2u} \\ + \Gamma_{3u} + 3\Gamma_{4u} + \Gamma_{5u} \quad 4.12$$

Landau and Lifshitz (1958, Chapter XII) show these to be the 27 normal modes. Γ_1 and Γ_2 are one dimensional. One of the three Γ_{4u} 's represents a translation of the whole molecule while one of the polar Γ_{5g} 's is a rotation of the molecule. The other 21 representations are the normal modes of vibration. Since only those modes which transform as order three spherical harmonics contribute to V_{OL} , the antisymmetric Γ_{2u} , Γ_{4u} and Γ_{5u} normal modes are the only ones that need be considered. Again this results from expressing V_{OL} in terms of those basis functions of O_h expressible in terms of Y_3^m , the normal modes multiplying them must have the same symmetry since V_{OL} itself must have O_h symmetry.

Equation 4.5 written using the basis functions of eq. 4.11, each multiplying the q normal mode of like symmetry, becomes

$$\begin{aligned}
V_{0L} = & V(\Gamma_{2u}, 3) C(\Gamma_{2u}^3, A_2) q(\Gamma_{2u}, A_2) \\
& + \sum_{i=\pm 1, 0} \sum_{\phi=a, b} V(\phi\Gamma_{4u}, 3) C(\Gamma_{4u}^3, i) q(\phi\Gamma_{4u}, i) \\
& + \sum_{i=\pm 1, 0} V(\Gamma_{5u}, 3) C(\Gamma_{5u}^3, i) q(\Gamma_{5u}, i). \quad 4.13
\end{aligned}$$

The coupling coefficients $V(\Gamma_{iu}, 3)$ determined for a point charge model are (Huang and Inone, 1964 and Menne, Lee, and Ames, 1968)

$$\begin{aligned}
V(\Gamma_{2u}, 3) &= \frac{8\sqrt{10}}{3} ee' (r^3/R^5), \\
V(a\Gamma_{4u}, 3) &= \frac{(20 ee')}{9} (r^3/R^5), \\
V(b\Gamma_{4u}, 3) &= \frac{28\sqrt{2} ee'}{27} (r^3/R^5), \text{ and} \\
V(\Gamma_{5u}, 3) &= \frac{4\sqrt{15}}{3} ee' (r^3/R^5). \quad 4.14
\end{aligned}$$

The a and b designation refer to the two different three dimensional Γ_{4u} representations.

If d electrons, as in transition metal ions, were present in the crystal only gerade (even) normal modes would be required to write V_{0L} since the bases functions would then be expressed in terms of Y_2^m .

In order to express the normal modes of XY_8 as Debye waves to effect a quantization of the vibrational spectrum the normal modes q_k must be expressed in terms of the displacement's α_i^j . This can be done by equating coefficients

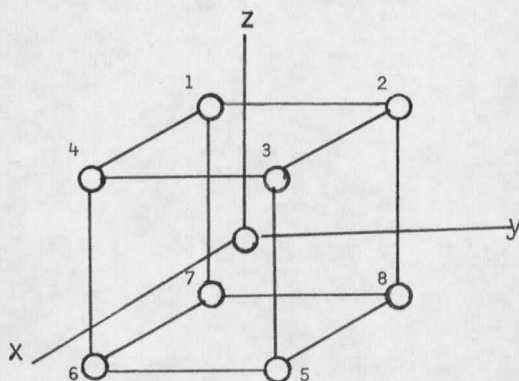


Figure 4.1

between eq. 4.5 and 4.14 or by use of the formula (Huang and Inone, 1964) taken from Heine, 1960)

$$q(\lambda) = \sum_R \Gamma_{\lambda}^{ii}(R) R\alpha$$

where the R 's are the point group operations of O_h , $\Gamma_{\lambda}^{ij}(R)$ is the matrix element of the λ th representation of the matrix which transforms the bases of eq. 4.11 under the operation R . These are given in Table A.16 of Griffith, (1961). α is any component of displacement of a fluorine ion and the Eu ion. A physical model of Fig. 4.1 is very

helpful in finding these normal modes. The normal modes of interest are (Menne, Ames, and Lee, 1968).

$$q(\Gamma_{2u}, a) = i/\sqrt{24} [Q_x^1 + Q_y^1 - Q_z^1 - Q_x^2 + Q_y^2 + Q_z^2 - Q_x^3 - Q_y^3 - Q_z^3 + Q_x^4 + Q_y^4 + Q_z^4],$$

$$q(a\Gamma_{4u}, 1) = \sqrt{2}/8 [(Q_y^1 - Q_z^1 - Q_y^2 + Q_z^2 + Q_y^3 + Q_z^3 - Q_y^4 + Q_z^4) + i(Q_x^1 - Q_z^1 - Q_x^2 + Q_z^2 + Q_x^3 + Q_z^3 - Q_x^4 - Q_z^4)],$$

$$q(a\Gamma_{4u}, -1) = q^*(a\Gamma_{4u}, 1), \text{ (the complex nature results from using a standard representation, see Griffith, 1961 page 36.)}$$

$$q(a\Gamma_{4u}, 0) = \frac{1}{4} [Q_x^1 + Q_y^1 + Q_x^2 - Q_y^2 - Q_x^3 - Q_y^3 - Q_x^4 + Q_y^4],$$

$$q(b\Gamma_{4u}, 1) = \frac{1}{12} [(Q_x^1 + Q_x^2 + Q_x^3 + Q_x^4 - 8X_n) + i(Q_y^1 + Q_y^2 + Q_y^3 + Q_y^4 - 8Y_n)],$$

$$q(b\Gamma_{4u}, -1) = q^*(b\Gamma_{4u}, 1),$$

$$q(b\Gamma_{4u}, 0) = \frac{1}{6\sqrt{2}} [Q_z^1 + Q_z^2 + Q_z^3 + Q_z^4 - Z_n],$$

$$\begin{aligned}
 q(\Gamma_{5u}, -1) &= q^*(\Gamma_{5u}, 1), \\
 + q(\Gamma_{5u}, 1) &= \frac{1}{\sqrt{2}^4} [(Q_y^1 + Q_z^1)(Q_y^2 + Q_z^2)(Q_y^3 + Q_z^3)(Q_y^4 + Q_z^4) \\
 &\quad + i(Q_x^1 + Q_z^1)(Q_x^2 + Q_z^2)(Q_x^3 + Q_z^3)(Q_x^4 + Q_z^4)],
 \end{aligned}$$

and

$$q(\Gamma_{5u}, 0) = \frac{1}{4} (Q_x^1 + Q_y^1 + Q_x^2 + Q_y^2 + Q_x^3 + Q_y^3 + Q_x^4 + Q_y^4). \quad 4.15$$

In eq. 4.15 the displacements of opposite ions have been coupled to a single variable which reflect the antisymmetric nature of the normal modes considered,

$$Q_\alpha^j = \alpha_\alpha^j + \alpha^{j+4} \quad 4.16$$

where the j th ion is given as in Fig. 4.1. X_n , Y_n , and Z_n are the appropriate displacements of the central ion.

Quantization of The Lattice Vibrations

In order to obtain the temperature dependence through an orbit-lattice interaction of the crystal-field coupling, the quantum nature of coupled harmonic oscillators should be applied. As shown in Appendix C the α th component of the displacement of the j th ion in the N-representation is the operator

$$\alpha^j = \sum_{\mathbf{k}, \sigma} (\hbar/2\omega_{\mathbf{k}, \sigma}^M)^{1/2} \phi^\sigma \left[a_{\mathbf{k}}^\dagger \exp(i\mathbf{k} \cdot \mathbf{r}_j) + a_{\mathbf{k}} \exp(i\mathbf{k} \cdot \mathbf{r}_j) \right] \quad 4.17$$

M is the mass of the crystal. The σ 's are the three acoustic modes of sound in the crystal; two transverse and one longitudinal. \vec{k} is the wave vector of phonon state k^* . \vec{r}_j is the position vector of ion j . $\Phi_{\alpha k}^{\sigma}$ is the direction cosine between polarization vector $\vec{\sigma}$ and the α direction in the crystal, $\alpha \rightarrow (x, y, z)$. Finally a_k and a_k^\dagger are annihilated and creation operators for occupation number space of the phonons of wave vector \vec{k} .

The position vector \vec{r}_i of eq. 4.17 can be written as

$$\vec{r}_i = \vec{r}_j^0 + \vec{R}_i \quad 4.18$$

where \vec{r}_j^0 is position of the j th paramagnetic ion and \vec{R}_i^0 is the position of the i th ligand ion from the center of the XY_8 configuration. The long wave length approximation is made by assuming $\vec{k} \cdot \vec{R}_j = k(\lambda_{xk} X_j^0 + \lambda_{yk} Y_j^0 + \lambda_{zk} Z_j^0) \ll 1$ where $\lambda_{\alpha k}$ are direction cosines between the α axis and \vec{k} . Menne (1969) has been able to express eq. 4.17 exactly and found little difference in assuming a long wave length approximation. With the long wave-length approximation

* In the Debye approximation the dispersion relation is such that the group velocity equals the phase velocity,
 $V_{\sigma} = \omega_{k\sigma}$

substituted into 4.17

$$e^{i\vec{k}\cdot\vec{x}_i} = e^{i\vec{k}\cdot\vec{x}_j^0} [1 + i\vec{k}\cdot\vec{R}_i^0 + 1/2(\vec{k}\cdot\vec{R}_i^0)^2 + \dots]$$

expanded to second order, and

$$e^{i\vec{k}\cdot\vec{x}_i} = e^{i\vec{k}\cdot\vec{x}_j^0} [1 + i\vec{k}\cdot\vec{R}_i^0 + 1/2(\vec{k}\cdot\vec{R}_i^0)^2 + \dots], \quad 4.18$$

The normal modes of eq. 4.15 are linear combinations of the antisymmetric Q_α^j of eq. 4.16. The terms linear in $i\vec{k}\cdot\vec{R}_i^0$ of eq. 4.18 will add to zero when substituted into the normal modes of eq. 4.15. Also since the normal modes have a net displacement of zero the constant terms will add to zero. Then

$$\begin{aligned} \alpha^i = & \sum_{k,\sigma} \frac{U_{k,\sigma} \phi_{\sigma k}^\alpha}{3} \{ (g_x^i \lambda_{xk} + g_y^i \lambda_{yk} + g_z^i \lambda_{zk})^2 \\ & + (g_x^{i+4} \lambda_{xk} + g_y^{i+4} \lambda_{yk} + g_z^{i+4} \lambda_{zk})^2 \}, \end{aligned}$$

where

$$U_{k,\sigma} = (\hbar/2\omega_{k\sigma} M) 1/2 k^2 R^2 (a_k e^{i\vec{k}\cdot\vec{x}_j^0} + a_k^\dagger e^{-i\vec{k}\cdot\vec{x}_j^0}). \quad 4.19$$

The coordinate location of the fluorine ions is $\pm(1/\sqrt{3})R$ and g's are defined

$$\begin{aligned} g_x^i &= \begin{cases} 1 & \text{if } i = 3, 4 \\ -1 & \text{if } i = 1, 2 \end{cases} \\ g_y^i &= \begin{cases} 1 & \text{if } i = 2, 3 \\ -1 & \text{if } i = 1, 4 \end{cases} \\ g_z^i &= 1 \text{ if } i = 1, 2, 3, 4 \end{aligned} \quad g^{i+4} = g^i, \quad 4.20$$

Since

$$[g_x^{i+4} \lambda_{xk} + g_y^{i+4} \lambda_{yk} + g_z^{i+4} \lambda_{zk}]^2 = [g_x^i \lambda_{xk} + g_y^i \lambda_{yk} + g_z^i \lambda_{zk}]^2,$$

$$Q_i^\alpha = \sum_{k,\sigma} U_{k\sigma} \Phi_{k\sigma}^{i+4} \frac{2i}{3} (g_x^i \lambda_{xk} + g_y^i \lambda_{yk} + g_z^i \lambda_{zk})^2.$$

Then the normal modes of eq. 4.15 are written in operator form using the small wave-length approximations, as

$$\begin{aligned} q(\Gamma_{2u}, A_2) = & \sum_{k,\sigma} U_{k\sigma} \frac{2i}{3\sqrt{24}} [\Phi_{xk}^\sigma (-\lambda_{xk} - \lambda_{yk} + \lambda_{zk})^{2+\Phi^\sigma} \\ & \times (-\lambda_{xk} - \lambda_{yk} + \lambda_{zk})^2 \\ & - \Phi_{zk}^\sigma (-\lambda_{xk} - \lambda_{yk} + \lambda_{zk})^2 - \Phi_{xk}^\sigma (-\lambda_{xk} - \lambda_{yk} - \lambda_{zk})^2 \\ & + \Phi_{yk}^\sigma (-\lambda_{xk} + \lambda_{yk} + \lambda_{zk})^{2+\Phi^\sigma} + \Phi_{zk}^\sigma (-\lambda_{xk} + \lambda_{yk} + \lambda_{zk})^2 \\ & - \Phi_{xk}^\sigma (\lambda_{xk} + \lambda_{yk} + \lambda_{zk})^2 - \Phi_{yk}^\sigma (\lambda_{xk} + \lambda_{zk} + \lambda_{yk})^2 \\ & - \Phi_{zk}^\sigma (\lambda_{xk} + \lambda_{yk} + \lambda_{zk})^{2+\Phi^\sigma} + \Phi_{xk}^\sigma (\lambda_{xk} - \lambda_{yk} - \lambda_{zk})^2 \\ & - \Phi_{yk}^\sigma (\lambda_{xk} - \lambda_{yk} + \lambda_{zk})^{2+\Phi^\sigma} + \Phi_{zk}^\sigma (\lambda_{xk} - \lambda_{yk} + \lambda_{zk})^2] \quad 4.21 \end{aligned}$$

which reduces to

$$\begin{aligned} q_1 = q(\Gamma_{2u}, A_2) = & \sum_{k,\sigma} \frac{8i}{3\sqrt{6}} U_{k\sigma} [\Phi_{xk}^\sigma \lambda_{xk} \lambda_{yk} \lambda_{zk} + \Phi_{yk}^\sigma \lambda_{xk} \lambda_{zk} \\ & + \Phi_{zk}^\sigma \lambda_{xk} \lambda_{yk}], \end{aligned}$$

similarly the other normal mode becomes

$$q_2 = q(a\Gamma_{4u}, 1) = \frac{4}{3\sqrt{2}} \sum_{k,\sigma} U_{k,\sigma} [\Phi_{yk}^{\sigma} \lambda_{xk}^{\lambda} \lambda_{yk}^{\lambda} + i\Phi_{xk}^{\sigma} \lambda_{xk}^{\lambda} \lambda_{yk}^{\lambda}] = q_4^*$$

$$q_3 = q(a\Gamma_{4u}, 0) = \frac{4}{3} \sum_{k,\sigma} U_{k,\sigma} [\Phi_{xk}^{\sigma} \lambda_{xk}^{\lambda} \lambda_{zk}^{\lambda} + \Phi_{yk}^{\sigma} \lambda_{yk}^{\lambda} \lambda_{zk}^{\lambda}],$$

$$q_5 = q(b\Gamma_{4u}, 1) = \frac{2}{3} \sum_{k,\sigma} U_{k,\sigma} [\Phi_{xk}^{\sigma} + i\Phi_{yk}^{\sigma}] [\lambda_{xk}^2 + \lambda_{yk}^2 + \lambda_{zk}^2] = q_7^*$$

$$q_6 = q(b\Gamma_{4u}, 0) = \frac{2\sqrt{2}}{9} \sum_{k,\sigma} U_{k,\sigma} \Phi_{zk}^{\sigma} (\lambda_{xk}^2 + \lambda_{yk}^2 + \lambda_{zk}^2),$$

$$q_8 = q(\Gamma_{5u}, 1) = \frac{4}{3\sqrt{2}} \sum_{k,\sigma} U_{k,\sigma} [-\Phi_{yk}^{\sigma} \lambda_{xk}^{\lambda} \lambda_{yk}^{\lambda} + i\Phi_{xk}^{\sigma} \lambda_{xk}^{\lambda} \lambda_{yk}^{\lambda} + \Phi_{zk}^{\sigma} (\lambda_{xk}^{\lambda} \lambda_{zk}^{\lambda} - i\lambda_{yk}^{\lambda} \lambda_{zk}^{\lambda})] = q_{10}^*$$

and

$$q_9 = q(\Gamma_{5u}, 0) = \frac{4}{3} \sum_{k,\sigma} U_{k,\sigma} [\Phi_{xk}^{\sigma} \lambda_{xk}^{\lambda} \lambda_{zk}^{\lambda} - \Phi_{yk}^{\sigma} \lambda_{yk}^{\lambda} \lambda_{zk}^{\lambda}] \quad 4.22$$

Crystal-field Energy Shift Due to Orbit-lattice Interaction

The energy shift of the ground state by the orbit-lattice interaction is a second order perturbation calculation thus,

$$\Delta E_{OL} = \frac{\sum_i |\langle \Psi^* | V_{OL} | \Psi \rangle|^2}{(E_i - E^*)}; \quad 4.23$$

where from eq. 4.7

$$|\Psi\rangle = |(4f)_{-3}^+ (4f)_{-2}^+ (4f)_{-1}^+ (4f)_0^+ (4f)_1^+ (4f)_2^+ (4f)_3^+ \rangle .$$

The $(4f)_m$ are the wave functions of the 4f electrons. The plus or minus sign refers to the spin. Then as defined in eq. 4.8,

$$|\Psi^*\rangle = |(6s)^+ 6(4f)_m^+ \rangle \quad -3 \leq m \leq 3 . \quad 4.24$$

In eq. 4.23 (6s) refers to an electron in a higher-unfilled level. In the calculation only the 6s electronic excited state will be mixed into the ground state by V_{0L} . This assumes other excited states being too far removed in energy above the ground state to contribute significantly. Also atomic ground state and excited state functions will be used since the energy levels of Eu^{++} in a crystal environment have not been calculated. Then

$$\Delta E = \sum_m \frac{|\langle (6s) 6(4f)_m | V_{0L} | 7(4f)_m \rangle|^2}{E_{4f} - E_{6s}} \quad 4.25$$

where V_{0L} is given by eq. 4.14. Substituting V_{0L} into eq. 4.25 the energy shift is calculated by evaluating the matrix elements. Let

$$D = \frac{ee^2}{R^5} |\langle R_{6s} | r^3 | R_{4f} \rangle|^2 \frac{1}{E_{4f} - E_{6s}} \quad 4.26$$

then

$$\begin{aligned}
 \Delta E = & D \sum_m \frac{1}{14} \left| \frac{8\sqrt{10}}{3} [(Y_3^2, Y_3^m) + (Y_3^{-2}, Y_3^m)] q_1 \right. \\
 & + \frac{4\sqrt{15}}{3} [(Y_3^2, Y_3^m) + (Y_3^{-2}, Y_3^m)] q_9 \left. \right|^2 \\
 & + \frac{1}{4} \left| -\frac{20}{9} [\sqrt{5} (Y_3^{-3}, Y_3^m) + \sqrt{3} (Y_3^{-1}, Y_3^m)] q_2 \right. \\
 & + \frac{4\sqrt{15}}{3} [\sqrt{3} (Y_3^{-3}, Y_3^m) - \sqrt{5} (Y_3^{-1}, Y_3^m)] q_{10} \\
 & + \frac{28\sqrt{2}}{27} [\sqrt{5} (Y_3^{-3}, Y_3^m) + \sqrt{3} (Y_3^{-1}, Y_3^m)] q_5 \left. \right|^2 \\
 & + \frac{1}{4} \left| -\frac{20}{9} [\sqrt{5} (Y_3^3, Y_3^m) + \sqrt{3} (Y_3^1, Y_3^m)] q_4 \right. \\
 & \quad \left. [\sqrt{3} (Y_3^3, Y_3^m) - \sqrt{5} (Y_3^1, Y_3^m)] q_8 - \frac{28\sqrt{2}}{27} [\sqrt{5} (Y_3^3, Y_3^m) \right. \\
 & \quad \left. + \sqrt{3} (Y_3^1, Y_3^m)] q_7 \right|^2 + 2 \left| \frac{20}{9} (Y_3^0, Y_3^m) q_3 + \frac{28\sqrt{2}}{27} (Y_3^0, Y_3^m) q_6 \right|^2
 \end{aligned}
 \tag{4.27}$$

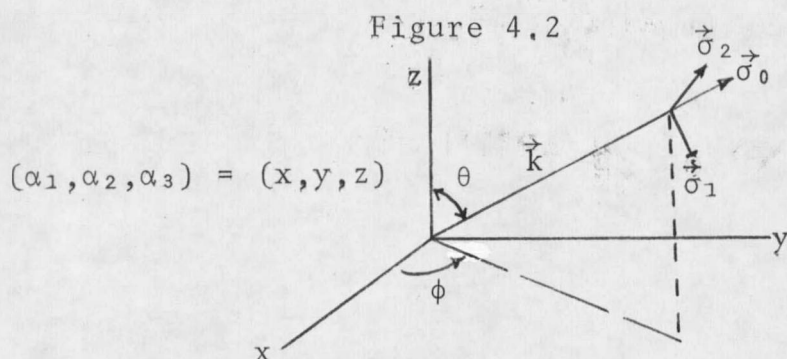
The notation (Y_3^m, Y_3^n) refers to scalar products of spherical functions. Using the orthogonal properties of the Y_3^m 's;

$$\begin{aligned}
 \Delta E = & \frac{2D}{7(81)} [5 |5q_2 + 9q_{10} + \frac{7\sqrt{2}}{3} q_5|^2 + 4(45) |2\sqrt{2}q_1 - 3q_9|^2 \\
 & + 3 |5q_4 - 15q_8 + \frac{7\sqrt{2}}{3} q_7|^2 + 8 |5q_3 + \frac{7\sqrt{2}}{3} q_8|^2 \\
 & + 3 |5q_2 - 15q_{10} + \frac{7\sqrt{2}}{3} q_5|^2 + 5 |5q_4 + 9q_8 + \frac{7\sqrt{2}}{3} 9q_7|^2 \\
 & + 4(45) |2\sqrt{2} q_1 - \sqrt{3} q_9|^2]
 \end{aligned}
 \tag{4.28}$$

Since q_1 is imaginary and q_9 real,

$$|2\sqrt{2} q_1 - \sqrt{3} q_9| = |2\sqrt{2} q_1 + \sqrt{3} q_9|.$$

To evaluate 4.28, Van Vleck-type directional averages over the Debye wave present in the crystal are performed (Van Vleck, 1939).



In Fig. 4.2 $\lambda_{\alpha k} = \cos(\vec{\alpha}, \vec{k})$ and $\phi_{\alpha k}^{\vec{\sigma}} = \cos(\vec{\alpha}, \vec{\sigma}_k)$. Each vector \vec{k} has three polarizations, one longitudinal, σ_0 , in the \vec{k} direction; and two transverse, σ_1 , and σ_2 . The three are mutually orthogonal, thus there is no loss of generality by choosing $\vec{\sigma}$, in direction of increasing θ . Then

$$\lambda_{xk} = \sin \theta \cos \phi; \lambda_{yk} = \sin \theta \sin \phi,$$

and $\lambda_{zk} = \cos \theta$

also

also

$$\Phi_{xk}^{\sigma_1} = \cos \theta \cos \phi; \quad \Phi_{yk}^{\sigma_1} = \cos \theta \sin \phi \quad 4.29$$

and

$$\Phi_{zk}^{\sigma_1} = \sin \theta .$$

The products of the $\Phi_{\alpha k}$'s and $\lambda_{\alpha k}$'s which occur in eq. 4.28 are averaged over all possible directions of \vec{k} . This average is taken as follows: as an example in $\langle (\Phi_{\alpha k}^{\sigma_0})^2 (\lambda_{\alpha k})^4 \rangle_{av}$ let $\alpha = z$, all directions are equivalent in the average over all space thus

$$\begin{aligned} \langle (\Phi_{\alpha k}^{\sigma_0})^2 (\lambda_{\alpha k})^4 \rangle_{av} &= \frac{1}{4\pi} \int_{\alpha}^{\pi} \int_{\alpha}^{2\pi} \cos^2 \theta \cos^4 \theta \sin \theta \, d\theta \, d\phi \\ &= \frac{1}{2} \int_0^{\pi} \cos^6 \theta \sin \theta \, d\theta = \frac{1}{7} \end{aligned}$$

and for the transverse mode

$$\begin{aligned} \langle (\Phi_{\alpha k}^{\sigma_1})^2 (\lambda_{\alpha k})^4 \rangle_{av} &= \frac{1}{4\pi} \int_0^{\pi} \int_0^{2\pi} (-\sin \theta)^2 \cos^4 \theta \sin \theta \, d\theta \, d\phi \\ &= \frac{1}{2} \int_0^{\pi} (\cos^4 \theta + \cos^6 \theta) \sin \theta \, d\theta = 2/35 . \end{aligned}$$

However, in averaging over all possible \vec{k} both σ_1 and σ_2 spanned all space. Thus for each transverse mode

$$\langle (\Phi_{\alpha k}^{\sigma_1})^2 (\lambda_{\alpha k})^4 \rangle_{av} = 1/35$$

The other averages in eq. 4.28 are easily obtained in the same manner. Thus for σ_a :

$$\langle \Phi_{\alpha k}^2 \lambda_{\alpha k}^2 \rangle_{av} = 1/35 \quad 4.30$$

$$\langle \Phi_{\alpha k}^2 \lambda_{\beta k}^2 \lambda_{\gamma k}^2 \rangle_{av} = \langle \Phi_{\alpha k} \Phi_{\beta k} \lambda_{\alpha k} \lambda_{\beta k} \lambda_{\gamma k} \rangle_{av} = 1/105$$

$$\langle \Phi_{\alpha k}^2 \lambda_{\alpha k}^2 \lambda_{\beta k}^2 \rangle_{av} = \langle \Phi_{\alpha k} \Phi_{\beta k} \lambda_{\alpha k}^3 \lambda_{\beta k} \rangle_{av} = \langle \Phi_{\alpha k}^3 \lambda_{\beta k} \rangle_{av} = \frac{1}{35}$$

For the transverse modes $\vec{\sigma}$

$$\langle \Phi_{\alpha k}^2 \lambda_{\alpha k}^2 \rangle_{av} = \langle \Phi_{\alpha k}^2 \lambda_{\beta k}^2 \lambda_{\gamma k}^2 \rangle_{av} = 1/35,$$

$$\langle \Phi_{\alpha k} \Phi_{\beta k} \lambda_{\alpha k} \lambda_{\beta k} \lambda_{\gamma k}^2 \rangle_{av} = 1/210$$

$$\langle \Phi_{\alpha k}^2 \lambda_{\alpha k}^2 \lambda_{\beta k}^2 \rangle_{av} = 2/105$$

$$\langle \Phi_{\alpha k} \Phi_{\beta k} \lambda_{\alpha k}^3 \lambda_{\beta k} \rangle_{av} = -1/70$$

and

$$\langle \Phi_{\alpha k}^2 \lambda_{\beta k}^4 \rangle_{av} = 3/35. \quad 4.31$$

The normal modes q_i of eq. 4.22 are each multiplied by

$$U_{k\sigma} = k^2 R^2 \left(\frac{\hbar}{2w_{k\sigma} M} \right)^{1/2} [a_k \exp(i\vec{k} \cdot \vec{r}_j^0) + c.c.]$$

then

$$|U_{k\sigma}|^2 = \frac{k^4 R^4 \hbar}{2\omega_{k\sigma} M} [a_k^2 \exp(2i\vec{k} \cdot \vec{\ell}_j) + a_k a_k^\dagger + a_k^\dagger a_k + a_k^{\dagger 2} \exp(-2i\vec{k} \cdot \vec{\ell}_j)] \quad 4.32$$

The wave functions used in computing the matrix elements of V_{0L} are now the particular Born-Oppenheimer states (Bak, page 6, 1964)

$$|\psi_s\rangle \cdot |n_k\rangle = \psi_k^{ms} \quad 4.33$$

and the matrix elements of the combination of normal modes involving the occupation number space of phonons are

$$|\langle n_k | U_{k\sigma} | n_k \rangle|^2 \quad 4.34$$

Thus eq. 4.32 becomes

$$|U_{k\sigma}|_{\text{av}}^2 = \frac{k^4 R^4 \hbar}{2\omega_{k\sigma} M} 2(n_k + \frac{1}{2}) \quad 4.35$$

When eq. 4.35 is averaged over all k , the terms involving $\exp(2i\vec{k} \cdot \vec{\ell}_j)$ and $\exp(-2i\vec{k} \cdot \vec{\ell}_j)$ average to zero. The average number of phonons in state k is the Bose-Einstein function for Bosons

$$\langle n_k \rangle_{\text{av}} = \frac{1}{\exp(\hbar\omega/KT) - 1} \quad 4.36$$

$$|U_{k\sigma}|^2 = \frac{k^4 R^4 \hbar}{\omega_{k\sigma} M} \{ [\exp(\hbar\omega/kT) - 1]^{-1} + 1/2 \}, \quad 4.37$$

K is the Boltzmann constant. The relation between the frequency $\omega_{k\sigma}$ and the wave number k is obtained by using Debye approximation, i.e.,

$$\frac{\omega_{k\sigma}}{k} = V_{g\sigma} \quad 4.38$$

$V_{g\sigma}$ is the group velocity of the σ mode of phonons in the crystal. Equation 4.37 then becomes, neglecting ground state corrections*,

$$|U_{k\sigma}|^2 = \frac{\omega^3 R^4 \hbar}{V_0^4 M} [\exp(\hbar\omega/kT) - 1]^{-1} \quad 4.39$$

The density of k states is assumed dense and

$$\sum_k \rightarrow \frac{V}{(2\pi)^3} \int k^2 dk d\Omega$$

where V is the volume of the crystal. From eq. 4.38

$$k^2 dk = \frac{\omega^2 d\omega}{V_{g\sigma}^3}$$

* The energy of a harmonic oscillator is $E_n = (n+1/2)\hbar\omega$. The ground state energy is then $E_0 = 1/2\hbar\omega$ for each oscillator.

then

$$\sum_k |U_{k\sigma}|^2 = \frac{R^4 \hbar}{2V \rho \pi^2} \int_0^{\omega_{\max}} \frac{\omega^5 d\omega}{\exp(\hbar\omega/KT) - 1} \quad 4.40$$

where ρ is the crystal density $\rho = M/V$. In eq. 4.39 let

$$x_\sigma = \hbar \omega_\sigma / KT$$

then

$$\omega_\sigma = \frac{KT}{\hbar} x_\sigma$$

and

$$d\omega_\sigma = \frac{KT}{\hbar} dx_\sigma$$

then

$$\sum_k |U_{k\sigma}|^2 \rightarrow \frac{R^4 \hbar}{2V_{g\sigma} \rho \pi^2} \left(\frac{KT}{\hbar}\right)^6 \int_0^\theta \frac{x_\sigma^5 dx_\sigma}{e^{x_\sigma} - 1} \quad 4.40(a)$$

$$\theta = \frac{\hbar}{K} \omega_{\max}$$

ω_{\max} is the cut off frequency of the crystal for the mode. It is determined by the finite number of lattice sites in a real crystal.

The Debye model averages over the wave vector 4.30 are substituted into 4.27. The summation over the modes σ . Then from eq. 4.40, 4.27 becomes

$$E = b_4 = \frac{(ee^2)^2 \left| \langle R_{4f} \rangle \langle R_{6s} \rangle \right|^2 (64)(53)}{|E_{4f} - E_{6s}|} \quad (81) (49)$$

$$x = \frac{R^4}{\rho\pi^2} \left(\frac{2}{3\gamma} + \frac{1}{\gamma} \right) \left(\frac{K}{h} \right)^6 T^6$$

$$\int_0^{\theta/T} \frac{x^5 dx}{e^x - 1}$$

In Chapter III the intensities of the hyperfine lines depend on b_4 through the terms of eq. 3.53. It is given for small angles between a (100) crystal axis and the external magnetic field to be

$$I_{1/2, -1/2} = 1 - \left(\frac{b_4 \sin 4\theta}{g\beta H_0} \right)^2 \quad 4050 \quad 4.41$$

Substituting for b_4 , $b_4^{RL} - b_4^{OL}$. b_4^{RL} being the rigid lattice term and b_4^{OL} being the energy shift of orbit-lattice then

$$I_{1/2, -1/2} = 1 - \left(\frac{b_4^{RL} \sin 4\theta}{g\beta H_0} \right)^2 \quad 4050$$

$$+ \frac{2b_4^{OL}}{b_4^{RL}} \left(\frac{b_4^{RL} \sin 4\theta}{g\beta H_0} \right)^2 \quad 4050 \quad 4.42$$

The effect of b_4^{OL} appears to decrease the angle between the core hyperfine fields the nucleus see as b_4^{OL} increases. The relative intensities between the $\Delta m = \pm 5/2 \leftrightarrow \pm 5/2$ lines and the $\pm 5/2 \leftrightarrow \pm 3/2$ lines of $\Delta M = 1/2 \leftrightarrow -1/2$ transitions is predicted from eq. 3.48 to be

$$\frac{I_f/I_a = \frac{|P^{5/2}_{3/2, 5/2}|^2}{|P^{5/2}_{5/2, 5/2}|^2} = \frac{5(1-\mu)}{1+\mu} \quad 4.43$$

I_f designates the intensity of a forbidden transition and I_a the intensity of an allowed transition. Then

$$I_f/I_a \approx (I_f/I_a)^{RL} [1 - Cf(t)] \quad 4.44$$

where

$$Cf(t) = \frac{2}{b_4^{RL}} (ee'/R^3)^2 \frac{|\langle R_{4f} | r^3 | R_{6s} \rangle|^2}{|E_{4f} - E_{6s}|} \quad \begin{matrix} (64) (53) \\ (81) (49) \end{matrix}$$

$$x \left(\frac{\hbar}{3V_l^7} + \frac{1}{V_t^7} \right) \left(\frac{TK}{\hbar} \right)^6 \int_a^{\theta/T} x^5 (e^x - 1)^{-1} dx \quad 4.45$$

and

$$f(t) = T^6 \int_a^{\theta/T} x^5 (e^x - 1) dx \quad 4.46$$

For CaF_2 , the parameters are $\rho = 3.8 \text{ g/cm}^3$, $R = 2.27 \text{ \AA}$,
 $v_t = 3.34 \times 10^5 \text{ cm/sec}$, $v_l = 7.36 \times 10^6 \text{ cm/sec}$
 and the values of $\langle r^3 \rangle$ and E are.

$$E_{6s} - E_{4f} = 0.7 R_4$$

$$\langle R_{4f} | r^3 | R_{6s} \rangle = 4.2 \times 10^{-25} \text{ cm}^3$$

(See Ho and Ruoff, 1967; Menne, Ames, and Lee, 1968 and
 Herman and Skillman, 1963).

CHAPTER V

EXPERIMENTAL RESULTS

The Correction Due to Lattice Expansion

The anharmonic contribution to the free energy of the crystal cause the crystal to expand or contract with temperature until it finds a volume where the total free energy is a minimum (Ziman, 1965). The effect of expansion is to move the ligand ions further from the paramagnetic ion, thus weakening the crystal field. Attempts to predict the anharmonic effects via third order corrections to the binding energy of the crystal are beginning to come forth (Sharma, 1970). The theory has not, to the author's knowledge, been extended to predict corrections of crystal field parameters. However, the crystal field parameters have been measured at various hydrostatic pressures and from bulk modulus data their dependence on nearest-neighbor distances has been determined (Hurren, et. al., 1969).  Hurren's work predicts the following dependences:

$$b_4 = KR^{-8.79} \quad 5.1$$

and

$$b_6 = K'R^{-13.6}$$

R is the nearest neighbor distance.

T. Rewaj (1968) measured b_4 as a function of temperature. In this work he included the low temperature measurements of K. Horai (1964). Rewaj assumed the variation of b_4 resulted totally from lattice expansion. These results led him to predict that b_4 would depend on the nearest neighbor distance as

$$b_4 = KR^{-16.3}$$

for CaF_2 ,

$$b_4 = KR^{-21.2} \quad \text{and} \quad KR^{-23.8} \quad 5.2$$

for SrF_2 and BaF_2 respectively, Rewaj's results indicate other temperature dependent mechanisms than lattice expansion are effecting b_4 , when they are compared with the pressure dependent data of Hurren.

This thesis proposes that an orbit-lattice interaction of the type developed in Chapter IV is responsible for the additional temperature dependence of b_4 . To examine this proposal, the intensities of the hyperfine spectrum lines were compared to the intensities predicted by the theory outlined in Chapter III. Specifically, the ratio of the intensities of the $\Delta m = \pm 3/2 \leftrightarrow \pm 5/2$ to the $\Delta m \pm 5/2 \leftrightarrow \pm 5/2$ lines of the $M = 1/2 \leftrightarrow -1/2$ spectrum were examined for

small angles between a (100) crystal axis and the external magnetic field. This ratio is dependent on b_4^2 . The dependence is outlined in Chapter III.

Phonon Contribution

To correct for the lattice expansion dependence, the pressure data of Hurren, et. al. (1969) were used with the thermal expansivity data, Fig. 5.2. Finally, b_4 as a function of temperature was plotted in Fig. 5.3. The relative intensities from Table 3.2 for $\Delta m = \pm 5/2 \leftrightarrow \pm 3/2$ to $\Delta m = \pm 5/2 \leftrightarrow \pm 5/2$ are with eq. 3.48

$$I_f/I_a = 5(1 - P)/(1 + P)$$

where from eq. 3.53

$$P = 1 - \left(\frac{b_4}{g\beta H_0} \sin 4\theta \right)^2 4050.$$

Then (I_f/I_a) 's were found for each $b_4(T)$. $b_4(T)$ are the predicted b_4 from Fig. 5.3. The experimentally measured I_f/I_a were then corrected by subtracting off the thermal expansion correction and these data plotted in Fig. 5.4. The theoretical curve plotted in Fig. 5.4 is the function

$$I_f/I_a = (I_f/I_a)^{RD} [1 - CF(T)] \quad 5.3$$

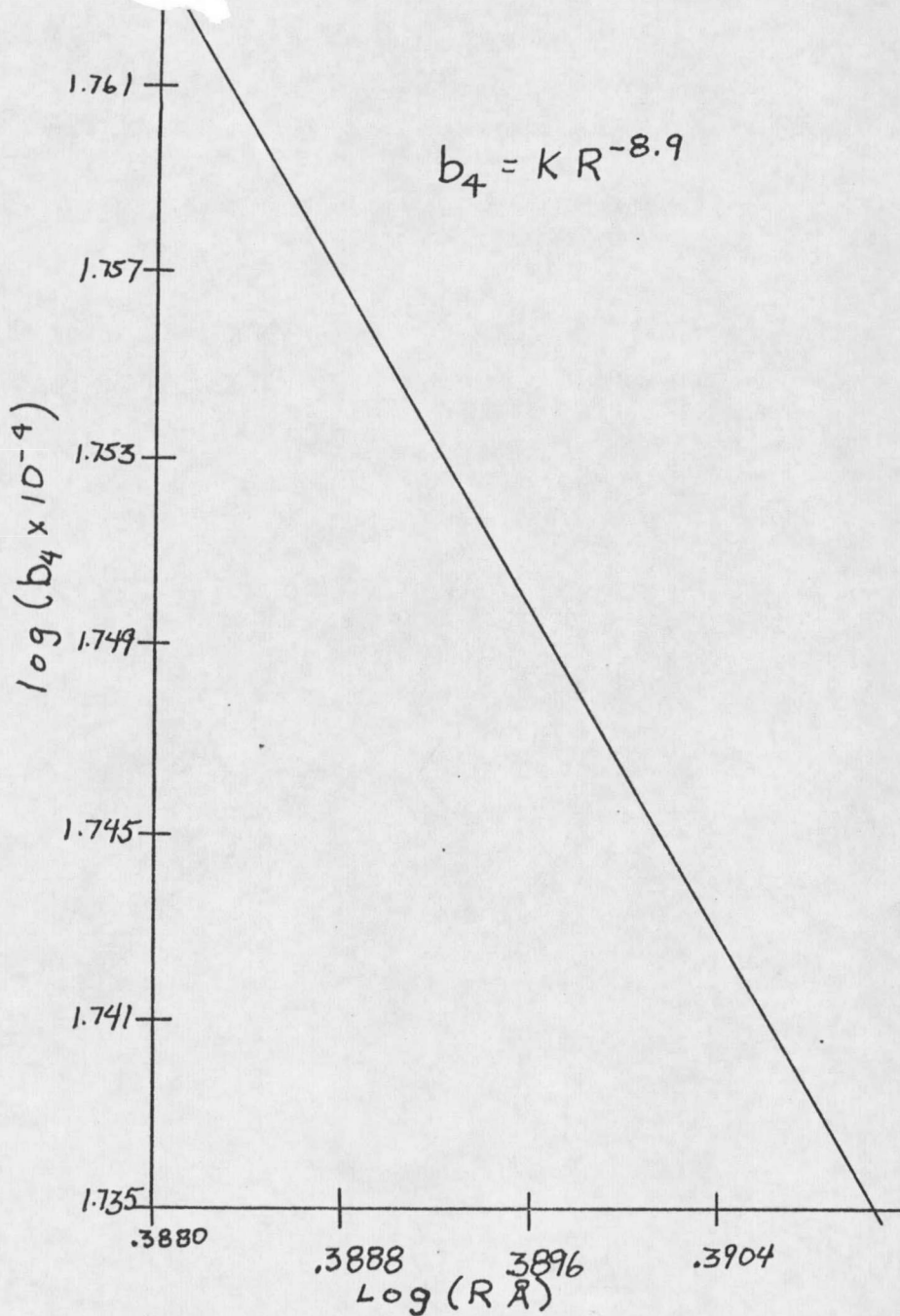


Figure 5.1 b_4 versus nearest neighbor distance from pressure data of Hurren et. al., (1969).

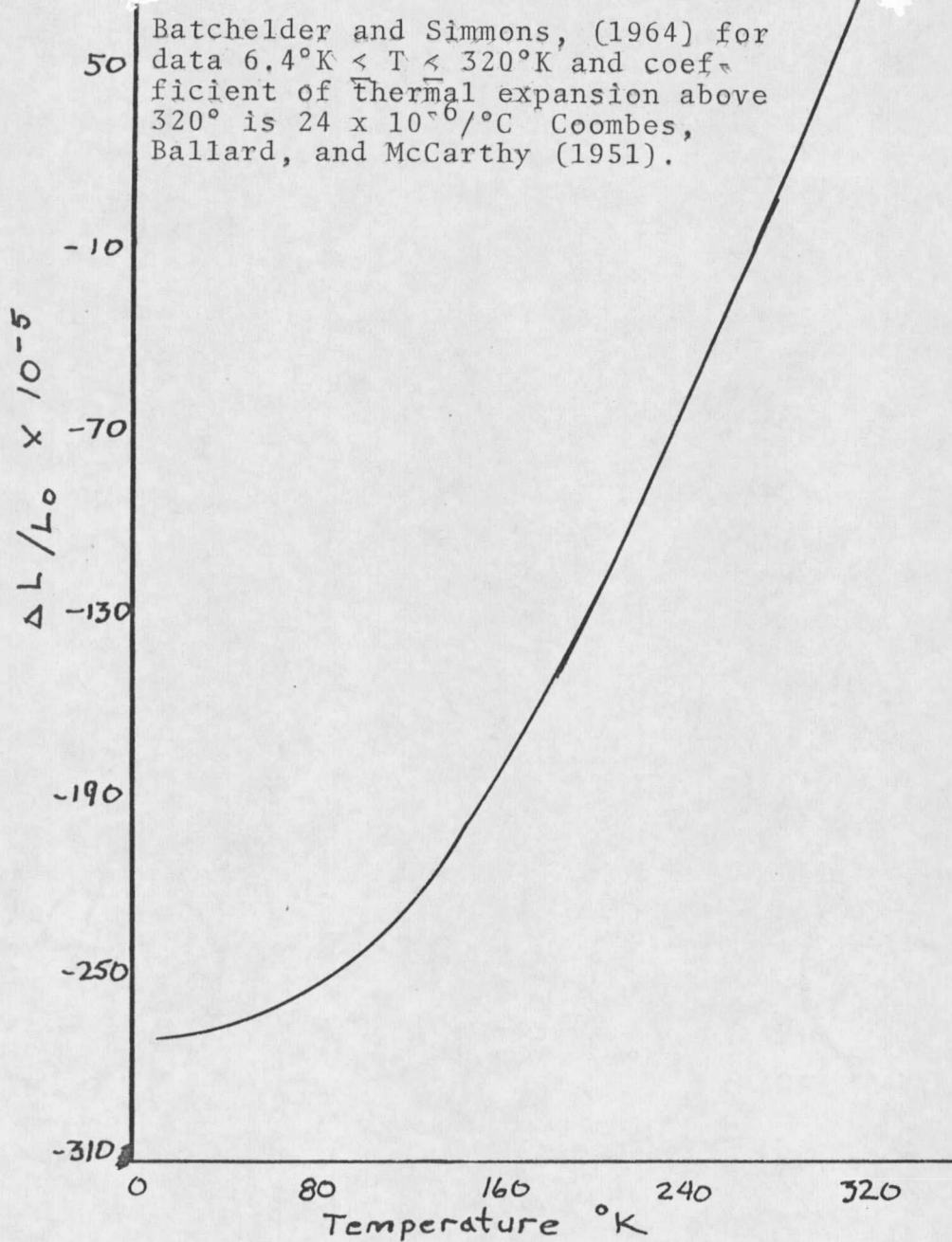


Figure 5.2 Thermoexpansivity of CaF_2 .

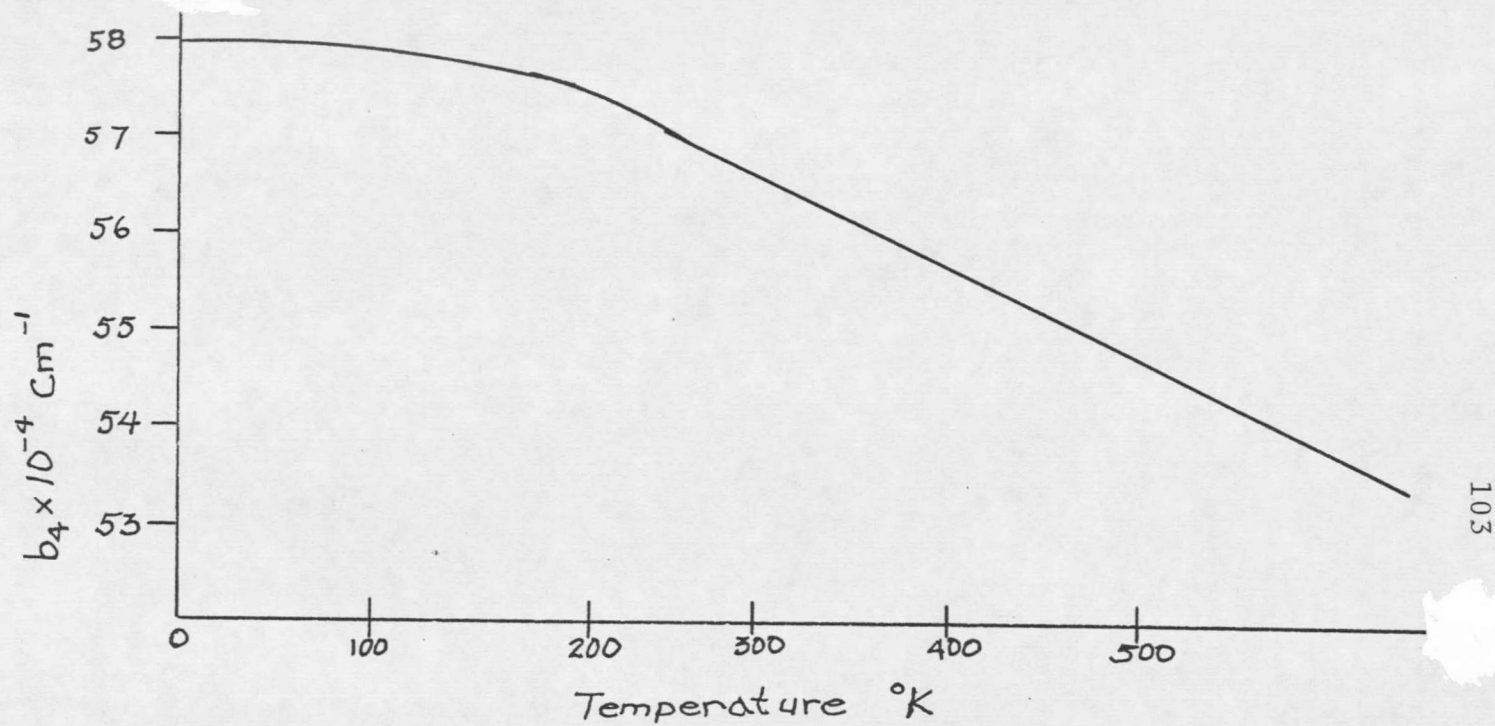


Figure 5.3 b_4 versus temperature due to lattice expansion. Actual variation of b_4 from all effects can be found in Rewaj (1968) and Horai (1964).

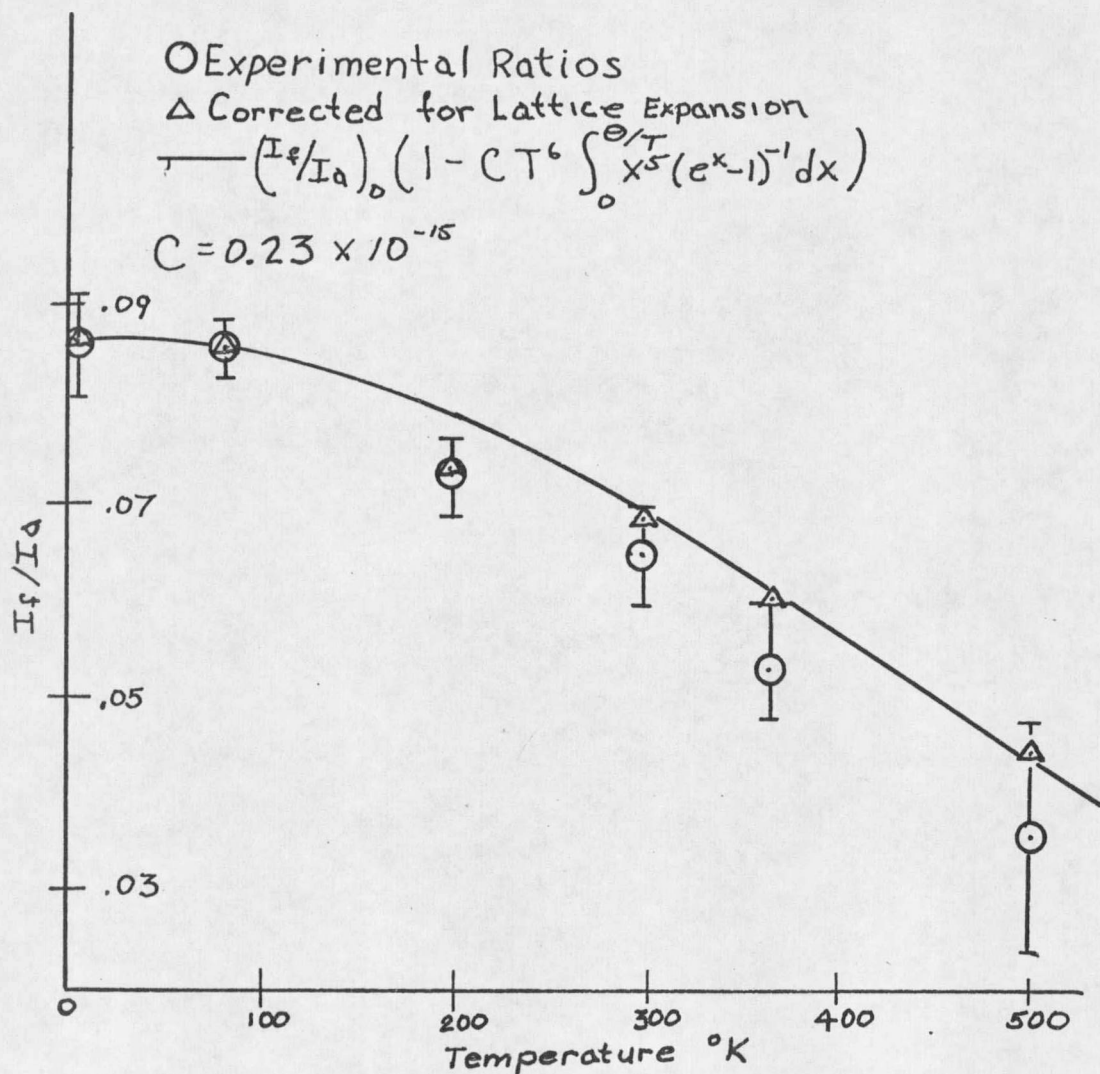


Figure 5.4(a) Ratio of forbidden to allowed intensities of hyperfine spectrum as they vary because of orbit-lattice interaction. Angle between (100) axis and field 2.3° .

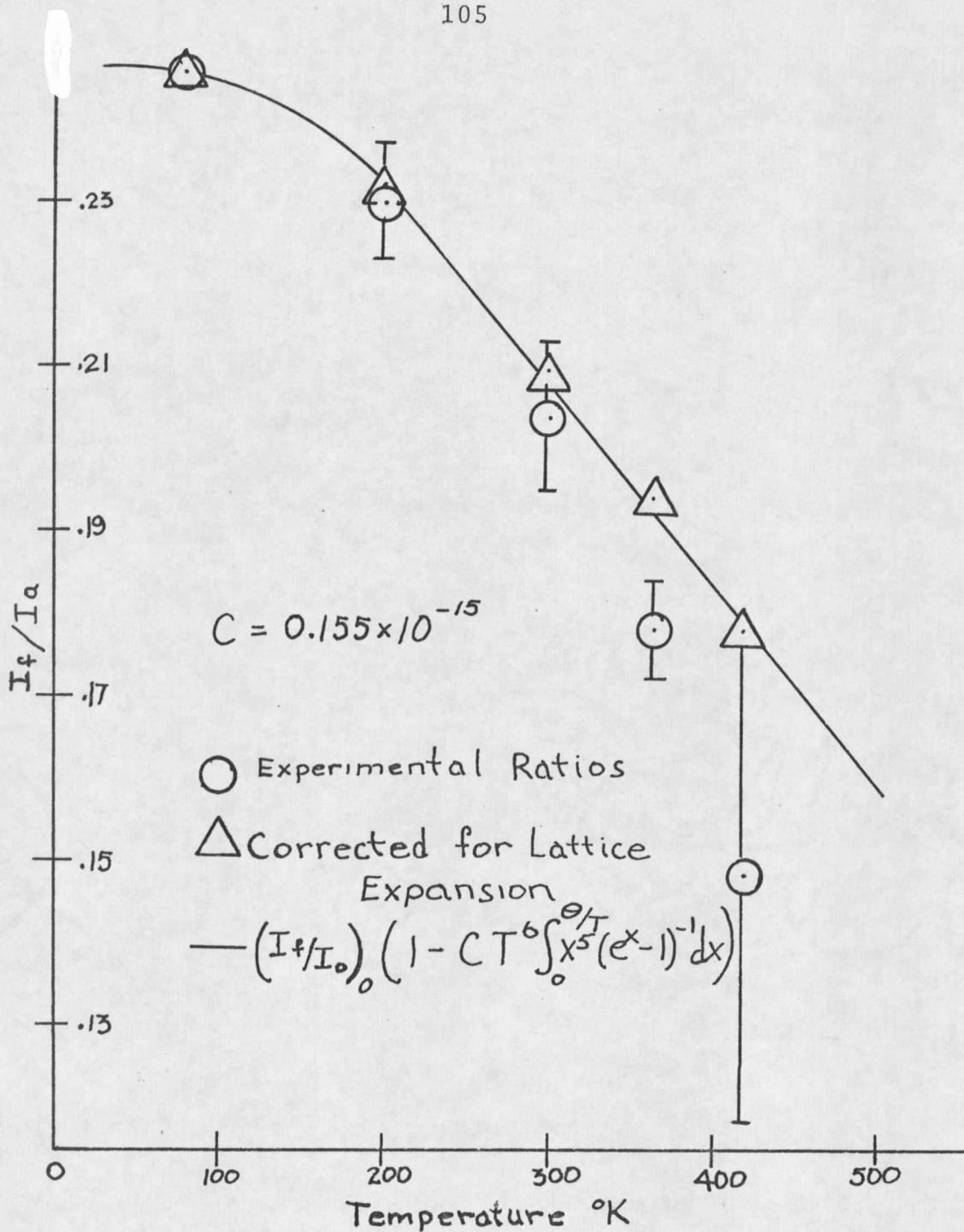


Figure 5.4 (b) Ratio of forbidden to allowed intensities as in Fig. 5.4 (a) when angle is 3.9° .

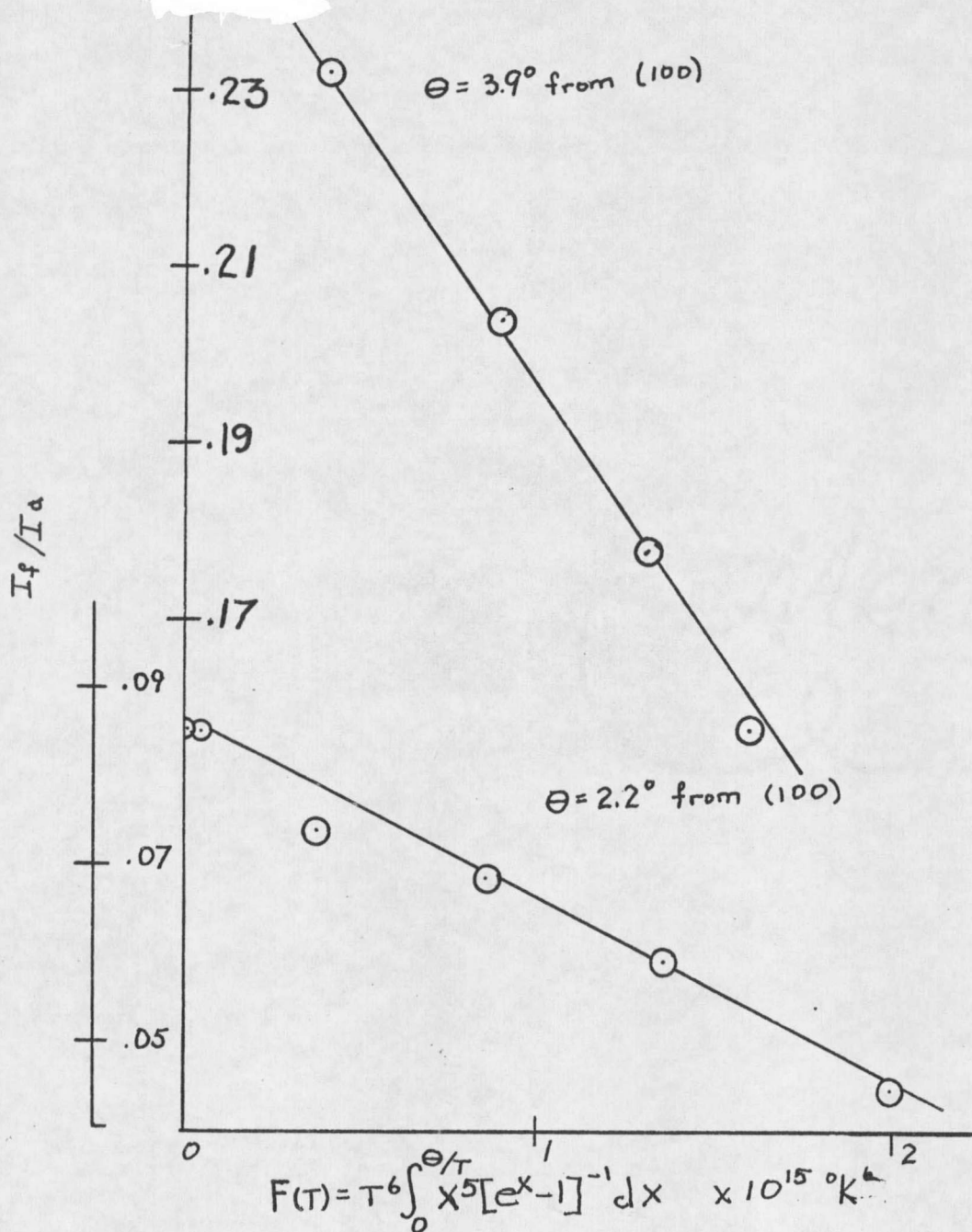


Figure 5.5 Forbidden to allowed intensity ratio depend linearly on $F(\tau)$.

Table 5.1

θ = Angle between (100) axis and Magnetic Field

Temperature $^{\circ}\text{K}$	b_4 expansion $\times 10^{-4} \text{ cm}^{-1}$	I_f/I_a experimental	I_f/I_a corrected
4.2	57.9	0.087 ± 0.01	0.087
78	57.9	0.087 ± 0.003	0.087
198	57.5	0.073 ± 0.005	0.074
298	56.6	0.065 ± 0.005	0.069
363	55.9	0.054 ± 0.008	0.060
498	54.7	0.036 ± 0.012	0.045
$\theta = 3.9^{\circ} \text{ K}$			
78	57.9	0.246 ± 0.001	0.246
198	57.5	0.230 ± 0.007	0.232
291	56.6	0.204 ± 0.009	0.217
363	55.9	0.178 ± 0.006	0.184
418	55.0	0.148 ± 0.03	0.174

where

$$F(T) = T^6 \int_0^{\frac{\theta}{T}} x^5 (e^x - 1)^{-1} dx$$

The values for $F(T)$ were computed on a Hewlett-Packard Model 9100 A calculator. The Debye temperature was taken as 500°K . Huffman and Norwood (1960) found

$$H = (5136 \pm 2.5)^\circ\text{K} \quad (\text{elastic constants})$$

and

$$H = 508 \pm 5)^\circ\text{K} \quad (\text{specific heat}).$$

In Chapter IV the orbit-lattice interaction predicts the result of eq. 5.3, with

$$C = \frac{2}{b_4} \frac{ee'}{R^3} \left(\frac{ee'}{R^3} \right)^2 \frac{|\langle R_{4f} | r^3 | R_{6s} \rangle|^2}{E_{4f} - E_{6s}} \quad 4.45$$

$$\times \frac{(64)(53)}{(81)(49)} \frac{\hbar}{\rho\pi^2} \left(\frac{2}{3V} + \frac{1}{V_T} \right) \left(\frac{k_B}{\hbar} \right)$$

The calculation assumes point charge interaction between 4f electrons and the fluorine ions which are modulated by lattice vibrations. As was pointed out in Chapter II, a crystal field interaction for S-state ions results from perturbations to the ground state. Therefore, a crystal field splitting results where

$$\frac{K e e' \langle r^4 \rangle}{R^5} \quad 5.4$$

is replaced by B_4 and a spin Hamiltonian is used. For this reason the orbit-lattice interaction was also expected to be less than that predicted in eq. 5.3. When

$$\frac{b_4 R^2}{\langle r^4 \rangle} = \frac{e e'}{R^3} \quad 5.5$$

is substituted into eq. 4.45

$$C = \frac{2b_4 R^4 |\langle R_{4f} | r^3 | R_{6s} \rangle|^2}{|\langle r^4 \rangle|^2 (E_{4f} - E_{6s})} \times \frac{(64)(53)}{(81)(49)} \quad 5.6$$

$$\times \frac{\hbar}{e\pi^2} \left(\frac{1}{V_T} \right) \left(\frac{K}{\hbar} \right)^6$$

In eq. 5.6 $2/3V_L$ is left off since it is very small compared to $1/V_T$. This satisfies ones intuition which suggest only the transverse modes should contribute significantly to V_{OL} . In this case, however, a lower Debye temperature should have been used. The cut off frequency for the transverse modes was not available to allow the calculation for a lower Debye temperature. The data plotted in Fig. 5.4 and 5.5 indicate a lower Debye temperature could have been used. In eq. 5.6

$$\langle r^4 \rangle = \langle R_{4f} | r^4 | R_{4f} \rangle \quad 5.7$$

The value of $\langle r^4 \rangle$ was also calculated on the Hewlett-Packard 9100A calculator from 4f wave function of Eu given by Herman and Skillman, (1963).

$$\langle r^4 \rangle = 0.1744 \text{ (\AA)}^4 \quad 5.8$$

Using the data listed at the end of Chapter IV with these results then

$$C_{\text{theory}} = 0.13944 \times 10^{-5} (\text{°K})^{-6} \quad 5.9$$

From the data of Fig. 5.5

$$C_{\text{exp}} = 0.155 \times 10^{-5} (\text{°K})^{-6} \text{ at } \theta = 3.9^\circ$$

and

$$C_{\text{exp}} = 0.23 \times 10^{-5} (\text{°K})^{-6} \text{ at } \theta = 2.3^\circ$$

The intensity measurements were hampered by changing line widths. The line width at 4.2°K was 2 gauss for the allowed line and was 4 gauss at 498°K. The intensities are proportional to the area under the absorption curve. Since the derivative of the absorption curve was taken

$$I = \int_{-\infty}^{\infty} x \left(\frac{dE}{dx} \right) dx = \int_{-\infty}^{\infty} E dx. \quad (E_{\infty} \rightarrow 0) \quad 5.10$$

The integrals are the Cauchy principle value integrals and were evaluated using a 10 grid numerical integration. Since the ratios of intensities were measured at fixed temperatures the line width ratio were assumed constant. This assumption proved fairly accurate, however, line widths are difficult to measure to better than 0.1 gauss. If the line widths ratios do not vary, the intensity can be approximated by measuring the height between inflection points or the total height of the derivative trace.

The cavity resonance frequency changes with temperature, because of expansion. Then parameter measurements involving $g\beta H$ were made at each temperature since $g\beta H_1 = h\nu$ is different at each temperature point.

A possibility of saturating the strong absorption lines exists at low temperature where the relaxation times are long. The microwave power was reduced at low temperatures to eliminate saturation. The signal to noise ratio is greatly improved at low temperatures but the lower power setting account for the large error bars in Fig. 5.4.

The agreement is better than should be expected. If an exact calculation of the crystal field interaction from a single 4f electron is used to determine the constant K in eq. 5.4, the theoretical value of C, eq. 5.9 would be

1/25th the value given. Usually orbit-lattice interactions are an order of magnitude lower than predicted, [Simanek and Orbach (1966), Menne, Ames, and Lee (1968), and Shrivastava and Drumheller (1969)]. This would seem to justify the substitution in eq. 5.4 where K is determined from a single 4f electron calculation. The use of the Debye model for phonons is of course an obvious area for improvement. The better results are obtained in the high temperature portion of the data, however, where the Debye model is least reliable. In the high temperature region

$$F(T) \propto T, \quad 5.10$$

while in the low temperature region

$$F(T) \propto T^6. \quad 5.11$$

The $\theta = 4^\circ$ data show the better results indicating perhaps a consistent tilting of the crystal at low temperatures, for the $2\ 1/2^\circ$ data because of contractions of the crystal mounting. The experiment was much more effected by angular variation than temperature variation, thus the data at any particular orientation was completed for all temperatures before a new orientation was attempted. The results of $\theta = 4^\circ$ were calculated at $\theta = 3.9^\circ$ to

obtain an agreement of the 4°K points. The angle could not be measured to better than 0.2° , thus these results are consistent.

Menne (1969) presented an improved theory for the orbit-lattice interaction where an exact result replaced the long wave length approximation of Chapter IV. Also the optical modes of the phonon spectrum were considered. These improvements reduce to the long wave-length result obtained earlier (Menne, Ames, and Lee, 1968). Simanek and Huang, (1966) improved the results of Simanek and Orbach, (1966) by including covalency effects. These improvements are more important for transition metal ion than for rare earth ions since the 4f electrons are deep-seated and covalency with the fluorine ion wave function is less. Using $-e$ for e' , the point charge of the fluorine may also be erroneous. Since the crystal field is effected by more than nearest-neighbor effects, a charge Me might be used where M is a Madelung constant for CaF_2 . This effect was accounted for by replacing ee'/R^5 by B_4 .

Results of this experiment confirmed that the temperature dependence of the intensities of the hyperfine interaction is associated with an orbit-lattice interaction and do not result only from lattice expansion. This

result increases the understanding of crystal fields and the dependence of even deeply seated core electrons on the periodic structure of the crystal.

APPENDIX A

Notes on Representations

A representation of a finite group is a mapping $g \rightarrow T_g$, such that each element of the group corresponds to a linear transformation of a finite-dimensional space R . The representation is irreducible if R has no invariant subspaces, other than the null subspace, with respect to the transformation T_g . A subspace R_1 of R is invariant with respect to the representation T_g if all operation T_g transform the components of R_1 only within the closed space of R_1 (Gel'fand, Minlos, and Shapiro, 1963).

The representation of the group O_h , see Chapter II, is chosen as the unitary matrices which transform the irreducible base functions of O_h . Tinkham (1964), in his Chapter three presents proofs and methods by which any representation can be reduced to a linear compositions of irreducible representations. Only physical quantities having the same irreducible representations can have non-zero effects on a system, if they do not have the same symmetry for certain irreducible basis function a combination of the quantities cannot have like symmetries. For instance the product of a normal mode of the XY_8 molecule of Chapter IV with the basis function which are expressible

in terms of spherical harmonics of order three must have the same symmetry as the potential energy function they represent if the potential function is to be invariant under the operation of the group O_h . It is inferred from the nature of electric field that the potential function must have O_h symmetry.

Reduction of Spherical Harmonics

In the character table for the O_h group, the gerade (g) representation refer to those bases which are "even" with respect to inversion and the ungerade (u) representations have odd parity. Since spherical harmonics Y_{ℓ}^m are also g or u, the reduction need only be accomplished with O rather than O_h . Then the odd Y_{ℓ}^m will reduce in terms of the u bases Γ_u and the even Y_{ℓ}^m in terms of the Γ_g bases.

A rotation of θ about any symmetry axis in the same class is equivalent through a unitary transformation to all θ rotations in the same class. The character of the class is given by the trace of the transformation matrix since

$$\text{Tr}(\Gamma_g) = \text{Tr}(u\Gamma_g u^+). \quad \text{A.1}$$

A rotation about the z axis transforms Y_{ℓ}^m as

$$C_z(\alpha) Y_\ell^m(\theta, \phi) = Y_\ell^m(\theta, \phi + \alpha) \quad \text{A.2}$$

Where $C_z(\alpha)$ is a rotation matrix of the rotation α about the z axis.

$$Y_\ell^m(\theta, \phi + \alpha) = e^{im\alpha} Y_\ell^m(\theta, \phi), \quad \text{A.3}$$

The $2\ell + 1$ dimensional square matrix which transforms the subspace

$$R = (Y_\ell^{-\ell}, Y_\ell^{-\ell+1}, \dots, Y_\ell^{\ell-1}, Y_\ell^\ell) \quad \text{A.4}$$

by the equation

$$\phi_\ell^n = \sum_{m=-\ell}^{\ell} T_{um}^\ell Y_\ell^m \quad \text{A.5}$$

has be eq. A.3 diagonal elements as

$$\begin{array}{c} e^{-i\ell\alpha} \text{-----} \\ | \\ e^{i\alpha(-\ell+1)} \text{-----} \\ | \\ e^{i\alpha} \end{array} \quad \text{A.6}$$

The trace of eq. A.6 is

$$\text{tr} [T_g(\alpha)] = \sum_{m=-\ell}^{\ell} e^{im\alpha} \quad \text{A.7}$$

Equation A.7 reduces to

$$\sum_{-\ell}^{\ell} e^{im\alpha} = \frac{\sin(\alpha+1/2)}{\sin \alpha/2} \quad \text{A.8}$$

By eq. A.8 it is possible to deduce the character for the operation α for Y_{ℓ}^m of order ℓ . Table 4.1 of Chapter IV shows these characters for Y_3^m .

The number of times a^{α} an irreducible representation occurs in a reducible representation is given as

$$a^{\alpha} = \frac{1}{h} \sum_c \ell_c \chi^{\alpha}(c) \chi(c) \quad \text{A.9}$$

where χ^{α} are the characters of the irreducible representation of class c , $\chi(c)$ the character of the reducible representation of class c , ℓ_c the number of operations in class c and h is obtained from

$$\sum_c \ell_c \chi^{\alpha}(c) \chi^{\beta}(c) = h \delta_{\alpha\beta} \quad \text{A.10}$$

As an example, to ascertain the number of times Γ_{2u} occurs in the reduction of Y_3^m under O_h symmetry, the character of Γ_2 are:

$$\chi^{\Gamma_2}(E) = 1, \ell_E = 1; \chi^{\Gamma_2}(2\pi/3) = 1,$$

$$\chi_{2\pi/3}^{\Gamma_2} = 8; \chi^{\Gamma_2}(\pi) = 1, \ell_{\pi} = 3;$$

$$\chi^{\Gamma_2}(\pi) = -1, \ell_{\pi} = 6; \text{ and}$$

$$\chi^{\Gamma_2}(\pi/2) = -1, \ell_{\pi/2} = 6.$$

Thus $h = 24$. Using the characters from Table 4.1 for Y_3^m it is found that Γ_{2u} occurs once. The only other symmetries which occur are Γ_{4u} and Γ_{5u} , once each.

Half Integral Angular Momentum

From eq. A.8 the character of the spherical function rotated about an axis by α is

$$\chi^{(J)}(\alpha) = \frac{\sin(J + 1/2)\alpha}{\sin \alpha/2} \quad \text{A.8}$$

In eq. A.8 a rotation by $2\pi + \alpha$ results in

$$\chi^{(J)}(\alpha + 2\pi) = \frac{\sin(J + 1/2)(\alpha + 2\pi)}{\sin(\alpha/2 + \pi)} = (-1)^{2J} \chi^{(J)}(\alpha)$$

Thus if J is half integral

$$\chi^{(J)}(\alpha + 2\pi) = -\chi^{(J)}(\alpha) \quad \text{A.11}$$

The character after a 2π rotation is double valued, in fact only a rotation of 4π produces the identity. Because of the above, for half-integral angular momentum new classes must be added to the cubic group to account for the double valued nature of 2π rotations. These are in Table A.1, R for a 2π rotation of the identity class E, RC_3 , and RC_4 .

The classes RC_2 do not form new classes but double the dimensionality of the two C_2 classes.

Since the size of the 0 group has increased by three classes, new double-value irreducible representation must be added. In the Bethe notation these are Γ_6 , Γ_7 , and Γ_8 .

The character of the ${}^8S_{7/2}$ ground state of Eu can be deduced from eq. A.8 and is given in Table A.1. From eq. A.9 the dimensionality h is now 48, the $\Gamma(7/2)$ reducible representation reduced as

$$\Gamma(7/2) \rightarrow \Gamma_6 + \Gamma_7 + \Gamma_8 \quad A.12$$

Γ_6 and Γ_7 are two dimensional or two fold degenerate and Γ_8 is a four fold degenerate level. Equation A.12 says that if the physical mechanisms are present, a cubic field will split the $S_{7/2}$ ground state into two two fold levels and a four fold level. (See Chapter II).

The Generalized Spherical Functions.

When a rotation in space is performed, the bases functions transform within a $2\ell+1$ square dimensional is a unitary matrix belonging to the "rotation group." Then consecutive spatial rotations infer

$$T(g_1, g_2) = Tg_1 Tg_2; \quad A.13$$

Table A.1

(Tinkham, 1964)

$0'$	E	R	$8C_3$	$8RC_3$	$3C_2+3RC_2$	$6C_2+6RC_2$	$6C_4$	$6RC_4$
Γ_1	1	1	1	1	1	1	1	1
Γ_2	1	1	1	1	1	-1	-1	-1
Γ_3	2	2	-1	-1	2	0	0	0
Γ_4	3	3	0	0	-1	-1	1	1
Γ_5	3	3	0	0	-1	1	-1	-1
Γ_6	2	-2	1	-1	0	0	$\sqrt{2}$	$-\sqrt{2}$
Γ_7	2	-2	1	-1	0	0	$-\sqrt{2}$	$\sqrt{2}$
8	4	-4	-1	1	0	0	0	0
$\Gamma(\frac{7}{2})$	8	-8	1	-1	0	0	0	0

Where T is the matrix belonging to operation g . As a matter of convenience Euler angles are used to specify a particular orientation in space

$$T(\phi_1, \theta, \phi_2) = T_{\phi_2} T_{\theta} T_{\phi_1} \quad A.14$$

T_{ϕ_1} is a positive rotation about the x axis by ϕ_1 then T_{θ} transforms the system about the new x axis by θ , finally a rotation about the previous z axis by ϕ_2 , places the system in the desired orientation.

If initially $T_{mn}(\phi_1, \theta, \phi_2)$ are the matrix elements which transform a system by a rotation g , a second infinitesimal rotation of α about the final z axis results in a transformation expanded in a Taylor's series of

$$T_{mn}(gg_1) = T_{mn}(\phi_1, \theta, \phi_2 + \alpha) = T_{mn}(\phi_1, \theta, \phi_2) + \alpha \frac{\partial T_{mn}}{\partial \phi_2} \phi_2 + \dots \quad A.15$$

and the differential transformation operator is

$$A_3 = \partial / \partial \phi_2 \quad A.16$$

Similar operations about the x and y axes results in differential transformation operators

$$A_1 = -\cot \theta \sin \phi_2 \partial / \partial \phi_1 - \frac{\sin \phi_2}{\sin \theta} \partial / \partial \phi_2$$

and

$$A.17$$

$$A_2 = \cot \theta \cos \phi_2 \frac{\partial}{\partial \phi_2} + \frac{\cos \phi_2}{\sin \theta} \frac{\partial}{\partial \phi_1} - \sin \phi_2 \frac{\partial}{\partial \phi_2}$$

If the operators of eq. A.16 and A.17 are combined as

$$H_+ = i A_1 - A_2$$

$$H_- = i A_1 + A_2$$

and

$$H_3 = i A_3 \tag{A.18}$$

the H_+ and H_- are respectively step up and step down operators of the eigenfunctions of the z component of angular momentum divided by \hbar . (Gel'fand, Minlos, and Shapiro, 1963). The eigenvalue equation

$$H^2 u = \ell(\ell + 1)u \tag{A.19}$$

results in the differential equation

$$\begin{aligned} \frac{\partial^2 u}{\partial \theta^2} + \cot \theta \frac{\partial u}{\partial \theta} + \frac{1}{\sin^2 \theta} \left(\frac{\partial^2 u}{\partial \phi_1^2} - \frac{2 \cos \theta \partial^2 u}{\partial \phi_1 \partial \phi_2} \right. \\ \left. + \frac{\partial^2 u}{\partial \phi_2^2} \right) + \ell(\ell + 1) u = 0, \end{aligned} \tag{A.20}$$

using $H^2 = H_1^2 + H_2^2 + H_3^2$.

The H 's are the generators of the infinitesimal rotations of the spherical functions. The transformation matrices of eq. A.14 satisfy A.20. Equation A.14 can be expressed

as

$$T(\phi_1, \theta, \phi_2) = e^{-iJ_z \phi_1} e^{-iJ_x \theta} e^{-iJ_z \phi_2} \quad A.21$$

(also see Messiah, Vol. II, Chapter XIII, 1961),

Writing $e^{-iJ_z \phi_1}$ as a Taylor's series

$$e^{-iJ_z \phi_1} = 1 - iJ_z \phi_1 + \frac{J_z^2 \phi_1^2}{2!} + \dots \quad A.22$$

it can be seen that

$$e^{-iJ_z \phi_1} |JM\rangle = e^{-iM\phi} |JM\rangle \quad A.23$$

The operator $e^{-iJ_x \theta}$, however, cannot be so easily derived.

Solving eq. A.20 with $u = T_{mn}$ results in the differential equation

$$\frac{d^2 u}{d\theta^2} + \cot \theta \frac{du}{d\theta} + \left[\ell(\ell+1) - \frac{n^2 - 2mn \cos \theta + m^2}{\sin^2 \theta} \right] u = 0 \quad A.24$$

where $u = u_{mn}$ and

$$T_{mn}(\phi_1, \theta, \phi_2) = e^{-iM\phi_1} u_{mn} e^{-in\phi_2}$$

Gelfand, Minlos, and Shapiro (1963) show the solution in terms of a variable $\mu = \cos \theta$ to be

$$P_{mn}^{\ell}(u) = A(1-u)^{\frac{n-m}{2}}(1+u)^{\frac{n+m}{2}}$$

$$\frac{d^{\ell-n}}{du^{\ell-n}} \left[(1-u)^{\ell-m} (1+u)^{\ell+m} \right], \quad \text{A.26}$$

The constant A is

$$A = \frac{(1)^{\ell-m} i^{n-m}}{2^{\ell} (\ell-m)!} \sqrt{\frac{(\ell-m)! (\ell+n)!}{(\ell+m)! (\ell-n)!}}$$

In Chapter III the generalize-spherical functions for $\ell = 5/2$ are required. These are given in Table A.2. However, in Chapter III only $|P_{Mn}^{\ell}|^2$ are required. Bir and Sochava, (1964) give the $|P_{mn}^{5/2}|^2$ and present the following properties,

$$|P_{mn}^{\ell}(u)|^2 = |P_{nm}^{\ell}(u)|^2$$

$$|P_{m-n}^{\ell}(u)|^2 = |P_{nm}^{\ell}(-u)|^2 \quad \text{A.26}$$

and

$$\sum_n |P_{nm}^{\ell}(u)|^2 = 1$$

Table A.2

m	n	$ P_{mn}(\mu) ^2$
$5/2$	$5/2$	$\left(\frac{1+\mu}{2}\right)^5$
$5/2$	$3/2$	$5 \cdot \left(\frac{1-\mu}{2}\right) \cdot \left(\frac{1+\mu}{2}\right)^4$
$5/2$	$1/2$	$10 \cdot \left(\frac{1-\mu}{2}\right)^2 \left(\frac{1+\mu}{2}\right)^3$
$3/2$	$3/2$	$\left(\frac{1+\mu}{2}\right) \left(\frac{3-5\mu}{2}\right)^2$
$3/2$	$1/2$	$\left(\frac{1+\mu}{2}\right)^2 (1-\mu)^3 \left(\frac{1-5\mu}{2}\right)^2$
$1/2$	$1/2$	$\left(\frac{1+\mu}{2}\right) \left(\frac{5\mu^2-2\mu-1}{2}\right)^2$

APPENDIX B

Experimental Equipment

The E. P. R. experiment is basically stimulated absorption and emission of microwaves by the paramagnetic electrons in a sample. The absorption exceeds the emission which allows intensity measurement to be recorded. The general experiment is outlined in Pake, (1962): The microwave frequency is fixed and is oriented such that the sinusoidal H field of the electromagnetic resonance is at right angles to the field of a large electromagnet. In the Schrodinger picture, a time dependent perturbation on the Zeeman levels, induced by the electromagnet, is caused by the microwave H field. Because the microwave field is at right angles to the Zeeman field transitions of $\Delta M = \pm 1$ are allowed between levels written in terms of the Zeeman effect representation. The electromagnet's field strength is varied to examine different transitions at the fixed microwave frequency.

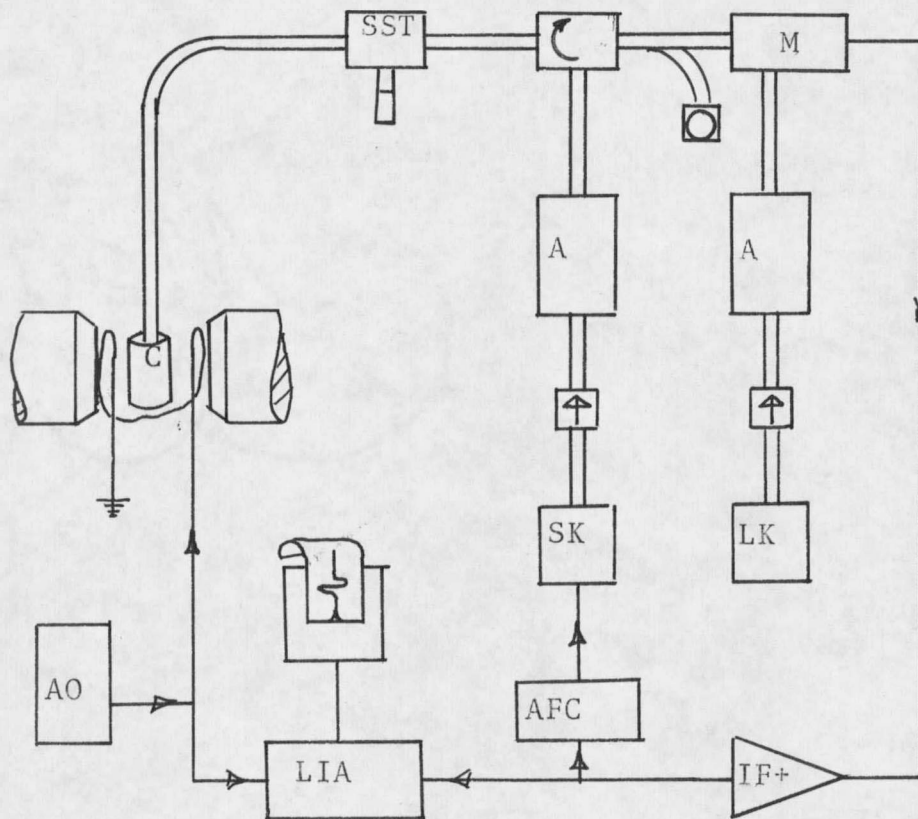
To produce the perturbation-microwave field a cylindrical cavity is designed to resonate in the TE_{011} mode. In this mode the magnetic field is directed along the center axis of the cylinder and the electric field here is zero. Thus, the center axis is placed between the poles of an

electromagnet parallel to the pole faces or perpendicular to its \vec{B} field. Most designs of equipment can be found in Poole's Electron Spin Resonance (1967).

The spectrometer may briefly be described as a super-heterodyne with balanced mixer detection and magnetic field modulation. The block diagram of Fig. B.1 shows the entire system. The basic parts are:

1. Signal and local oscillators, X-band klystron, with ferrite isolators.
2. Microwave bridge, with ferrite circulator and a slide-screw tuner.
3. Resonant cavity, TE_{011} cylindrical with sample on the axis.
4. Magnet with field-dial, adjustable 0 to 10 kilogauss.
5. Modulation coils and driving oscillator 0 to 50 gauss peak to peak at 400 Hz.
6. Microwave mixer, preamp and I. F. amplifier.
7. 400 Hz phase sensitive detector.
8. Automatic frequency control system (A.F.C.).
9. X-Y recorder, X-driven by field dial.

This spectrometer was designed by D. H. Dickey (1966, and Appendix C, 1969). The operation is generally as follows: microwave power, frequency modulated at 90 kHz, is fed into a reflection type cavity which is an arm of a balanced bridge. Balance is achieved by adjusting the size



- | | | | |
|-----|----------------------------|-----|------------------------|
| ↻ | - CIRCULATOR | ↑ | - ISOLATOR |
| SST | - SLIDE SCREW TUNER | SK | - SIGNAL KLYSTRON |
| C | - TE ₀₁₁ CAVITY | LK | - LOCAL KLYSTRON |
| M | - MIXER-PREAMPLIFIER | IF+ | - 30 MHz AMPLIFIER |
| A | - ATTENUATOR | AFC | - FREQUENCY STABILIZER |
| AO | - AUDIO OSCILLATOR | LIA | - LOCK-IN AMPLIFIER |

Fig. B-1. Block Diagram of Superheterodyne Spectrometer.

of the iris to the cavity or by an adjustable slide¹screw tuner to produce standing waves in the cavity arm. The balance can be upset by power absorption by the sample in the cavity. The cavity is in a magnetic field which is amplitude modulated at 400 Hz, so that the resonance condition is varied at that frequency. The microwave power reflected through the circulator to the mixer is thus amplitude modulated at 400 Hz. The reflected power is "beat" against the power from a local oscillator which is operated 30 MHz higher than the signal oscillator. The beat is amplified and the 90 kHz signal at which the signal oscillator was modulated is filtered and used to "lock" the signal to the resonance frequency of the cavity. The 400 Hz signal is phase-sensitive detected and the resultant dc signal is recorded. The spectra of Chapter II and III are copies of these recordings.

Table IX of Dickey's thesis (1969) is a list of the components used in the spectrometer. Additions to the list are:

2 Isolators Airtron-Pacific P/N 890350

1 X-Y Recorder Hewlett Packard 7005B

and

1 Helium Dewar System as per Dickey's design
by H. S. Martin and Son.

APPENDIX C

Phonons

The details of this appendix are expounded in the Aarhus Summer School Lectures, Phonons and Phonon Interactions, edited by T. A. Bak, (1969).

Harmonic Oscillator

Messiah, (1941) details the Dirac method for the quantum solution of the harmonic oscillator problem. A single one-dimensional harmonic oscillator is characterized by the Hamiltonian

$$H = p^2/2m + 1/2 m\omega^2 u^2, \quad C.1$$

where P and u are the momentum and displacement variables which obey the commutation relation

$$[u, p] = i \hbar. \quad C.2$$

To avoid constants in the calculation the variables

$$H = \hbar \omega H,$$

$$u = \left(\frac{\hbar}{m\omega}\right)^{1/2} Q$$

and

$$p = (m \hbar \omega)^{1/2} P \quad C.3$$

are introduced such that

$$H = 1/2 (P^2 + Q^2) \quad C.4$$

and

$$[Q, P] = i \quad C.5$$

Instead of the Hermitian operators Q and P the non-Hermitian operator a is introduced such that

$$a = 1/\sqrt{2} (Q + iP)$$

and

$$a^\dagger = 1/\sqrt{2} (Q - iP) \quad C.6$$

which from eq. C.5 have the commutation relation

$$[a, a^\dagger] = 1 \quad C.7$$

The Hamiltonian of eq. C.3 becomes

$$H = 1/2 (a a^\dagger + a^\dagger a) \quad C.8$$

and from Eq. C.7

$$H = N_{0P} + 1/2 \quad C.9$$

where $N_{0P} = a a^\dagger$.

From the wave mechanics solution to the eigenvalue problem of eq. C.1, the eigenvalues of H are

$$E_n = \hbar \omega_0 (n + 1/2). \quad C.10$$

Thus, from eq. C.3 and the eigenvalue problem

$$H|n\rangle = (n + 1/2) |n\rangle. \quad C.11$$

The definition of N is such that

$$N_{Op}|n\rangle = n|n\rangle, \quad C.12$$

The eigenvector being in occupation number space which from the commutation relation of eq. C.7 leads to the following

$$a^\dagger|n\rangle = \sqrt{n+1}|n+1\rangle \quad C.13$$

and

$$a|n\rangle = \sqrt{n}|n-1\rangle, \quad C.14$$

Because of eqs. C.13 and C.14, a^\dagger and a are called respectively creation and destruction operators.

Coupled Oscillators

A mechanical system with N degrees of freedom which has its potential energy expressible in a non-negative quadratic form in terms of the displacements can be transformed to a system of variables expressible as N decoupled harmonic oscillators. Small lattice vibration can to first order be considered by such a scheme. If only nearest neighbor interactions are considered the Hamiltonian can be expressed as

$$H = \sum_k p_k^2 / 2M_k = \frac{1}{2} \sum_{\ell, k} \phi_{k\ell} u_\ell u_k \quad C.15$$

The matrix $\phi_{k\ell}$ is symmetric, i.e.,

$$\phi_{k\ell} = \phi_{\ell k}$$

The variables B_{ℓ}^{α} are introduced as a complete set of N orthonormal eigenvectors of N -components, α labels the vector, ℓ the component. B_{ℓ}^{α} are the eigenvector of the matrix

$$D_{k\ell} = \phi_{k\ell} / \sqrt{M_k M_{\ell}} \quad \text{C.16}$$

Thus the eigenvalue problem is

$$\sum_{\ell} D_{k\ell} B_{\ell}^{\alpha} = \omega_{\alpha}^2 B_k^{\alpha} \quad \text{C.17}$$

and the eigenvalues ω_{α}^2 are real because $D_{k\ell}$ is a real symmetric matrix.

In the advent of degeneracies, the B_k^{ℓ} are allowed to be a complete orthonormal complex set such that

$$\sum_{\ell} B_{\ell}^{\alpha} B_{\ell}^{\beta*} = \delta_{\alpha\beta}, \quad \text{C.18}$$

if there is no degeneracy

$$\sum_{\alpha} B_{\ell}^{\alpha} B_{\ell}^{\beta*} = 0 \text{ for } \omega_{\alpha} \neq \omega_{\beta} \quad \text{C.19}$$

and the completeness relation is

$$\sum_{\alpha} B_k^{\alpha} B_{\ell}^{\alpha*} = \delta_{k\ell} \quad \text{C.20}$$

Now, as for the single oscillator, the inverse transformation between the conjugate u and p and the normal mode B_k^α is

$$u_k = \sum_{\alpha} \sqrt{\frac{\hbar}{2M_k \omega_{\alpha}}} (a_{\alpha} B_k^{\alpha} + a_{\alpha}^{\dagger} B_k^{\alpha*})$$

and

$$p_k = -i \sum_{\alpha} \sqrt{\frac{\hbar M_k \omega_{\alpha}}{2}} (a_{\alpha} B_k^{\alpha} - a_{\alpha}^{\dagger} B_k^{\alpha*}). \quad \text{C.21}$$

The transform or inverse transform of eq. C.21

$$a_{\alpha} = \frac{1}{\sqrt{2\hbar}} \sum_k B_k^{\alpha*} \left(M_k \omega_{\alpha} u_k + i \frac{p_k}{M_k \omega_{\alpha}} \right)$$

and

$$a_{\alpha}^{\dagger} = \frac{1}{\sqrt{2\hbar}} \sum_k B_k^{\alpha} \left(M_k \omega_{\alpha} u_k - i \frac{p_k}{M_k \omega_{\alpha}} \right). \quad \text{C.22}$$

Using eq. C.18 the commutation relations

$$[a_{\alpha}, a_{\beta}] = [a_{\alpha}^{\dagger}, a_{\beta}^{\dagger}] = 0$$

and

$$[a_{\alpha}, a_{\beta}^{\dagger}] = \delta_{\alpha\beta} \quad \text{C.23}$$

result. Then the Hamiltonian eq. C.15

$$H = \sum_{\alpha} \hbar \omega_{\alpha} \left(a_{\alpha}^{\dagger} a_{\alpha} + 1/2 \right). \quad \text{C.24}$$

The eigenvectors of the decoupled occupation number space is the product of the spaces of each oscillator

$$|n_1, n_2, \dots, n_j, \dots\rangle = |n_1\rangle |n_2\rangle \dots |n_j\rangle \dots \quad \text{C.25}$$

and the results of eq. C.12, C.13, and C.14 apply.

The Linear Chain Crystal

The potential for a linear chain of equal masses connected by springs only to the nearest neighbors has the Hamiltonian

$$H = \sum_{k=1}^k \left(\frac{p_k^2}{2M} \right) + \frac{1}{2} \phi \sum_{k=1}^{k-1} (u_{k+1} - u_k)^2 + \frac{1}{2} \phi (u_1^2 + u_N^2) \quad \text{C.26}$$

where the first and last mass are assumed fixed. Comparing eq. C.26 with eq. C.15, C.16, and C.17 for k not 1 or N

$$-B_{k-1} + 2B_k - B_{k+1} = \omega^2 / \omega_0^2 B_k \quad \text{C.27}$$

where

$$\omega_0 = \phi / M$$

The set of difference equations eq. C.27 has two solutions

$$B_k = e^{iqk} \quad \text{and} \quad e^{-iqk}$$

where b is the separation of nearest neighbors and q is

related to ω by the dispersion relation

$$\frac{\omega^2}{\omega_0^2} = 2(1 - \cos q \cdot b),$$

The Three Dimensional Crystal

If b_k is a primitive translation vector the g_k is defined such that

$$\vec{b}_i \cdot \vec{g}_k = 2\pi \delta_{ik} \quad \text{C.29}$$

or

$$\vec{g}_k = \frac{2\pi \vec{b}_\ell \times \vec{b}_m}{[\vec{b}_\ell \cdot (\vec{b}_m \times \vec{b}_k)]} \quad \text{C.30}$$

Then with

$$\vec{q} = \sum_i \frac{h_i \vec{g}_i}{N_i} \quad \text{C.31}$$

such that $N_k b_n$ is the length of the k th dimension of the crystal and h_i is an integer such that

$$\vec{q} \cdot \vec{b}_i = \frac{2\pi}{N_i} h_i \quad \text{C.32}$$

to satisfy the boundary conditions. Then for a three dimensional crystal C.21 becomes

$$\vec{u}_k = \sum_{\vec{q}} \sum_{\sigma} \frac{\hbar}{\sqrt{2MN} \omega_{\vec{q}, \sigma}} \vec{\sigma}_{\vec{q}} [a_{\vec{q}} \exp(i\vec{q} \cdot \vec{r}_k) + a_{\vec{q}}^{\dagger} \exp(-i\vec{q} \cdot \vec{r}_k)] \quad \text{C.33}$$

where MN is the mass of the crystal, \vec{r}_k is the position of atom k in the lattice and $\vec{\sigma}_{\vec{q}}$ is a polarization vector which the element can displace, two transverse and one longitudinal.

In Chapter IV the components of \vec{u}_k , eq. C.33 are required thus by dotting the α unit vector with eq. C.33

$$\alpha_k = \sum_{\vec{q}, \sigma} \frac{\hbar}{2M\omega_{\vec{q}, \sigma}} \Phi_{\vec{q}, \sigma}^{\alpha} [a_{\vec{q}} \exp(i\vec{q} \cdot \vec{r}_k) + a_{\vec{q}}^{\dagger} \exp(-i\vec{q} \cdot \vec{r}_k)] \quad \text{C.34}$$

APPENDIX D

Mechanism of The Hyperfine Interaction

A paramagnetic ion in a cubic environment has a hyperfine interaction.

$$H_{\text{hyp}} = A \vec{I} \cdot \vec{S} \quad \text{D.1}$$

where \vec{I} is the nuclear spin and \vec{S} the effective electron spin. To calculate A the matrix elements of

$$H = g g_n \beta \beta_n \sum_i \left[\frac{\vec{S}_i \cdot \vec{I}}{r_i^3} - \frac{\vec{S}_i \cdot \vec{I}}{r_i^3} + \frac{3(\vec{r}_i \cdot \vec{S}_i)(\vec{r}_i \cdot \vec{I})}{r_i^5} \right. \\ \left. + \frac{8\pi}{3} \delta(\vec{r}_i - \vec{r}_N) \vec{S}_i \cdot \vec{I} \right] \quad \text{D.2}$$

must be found. The last term in eq. D.2 is the Fermi contact term and has a value only for s electrons which have a probability of being within the nuclear volume. Hayes (1963) shows that even when the ground state is made up of f electrons, $l_i = 3$, the Fermi term can contribute to eq. D.1.

To derive D.2 Milford, (1960) began with Maxwells equation

$$\vec{H} = \text{curl } \vec{A} \quad \text{D.3}$$

where

$$\vec{A}(\mathbf{r}) = g_n \beta_n \frac{\vec{I} \times \vec{r}}{r^3} \quad \text{D.4}$$

The Hamiltonian for an electron in an electromagnetic field is

$$H = \frac{1}{2m} \left(\vec{p} + e \frac{\vec{A}}{c} \right)^2 + V(r) + 2\beta \vec{S} \cdot \vec{H} \quad \text{D.5}$$

Expansion of eq. D.5 gives

$$H = \frac{p^2}{2m} + V(\vec{r}) + \frac{e}{2mc} (\vec{p} \cdot \vec{A} + \vec{A} \cdot \vec{p}) + \frac{e^2}{2mc^2} A^2 + 2\beta \vec{S} \cdot \vec{H} \quad \text{D.6}$$

substituting eq. D.4 into D.6

$$\begin{aligned} \frac{e}{2mc} (\vec{p} \cdot \vec{A} + \vec{A} \cdot \vec{p}) &= \frac{e\beta\hbar\gamma_n}{2mc} \left[\vec{p} \cdot \frac{(\vec{I} \times \vec{r})}{r^3} + \frac{(\vec{I} \times \vec{r})}{r^3} \cdot \vec{p} \right] \\ &= \frac{e\gamma_n\hbar}{2mc} \gamma_n 2\vec{I} \cdot \frac{(\vec{r} \times \vec{p})}{r^3} \\ &= \frac{e\gamma_n\hbar^2}{mc} \frac{\vec{I} \cdot \vec{L}}{r^3} \end{aligned}$$

$\vec{r} \times \vec{p} = \hbar \vec{L}$ the orbital angular momentum of the electron.

Thus the third term on the right of eq. D.6 is

$$\hbar\gamma_n \frac{\gamma_n \vec{I} \cdot \vec{L}}{r^3} = \frac{e^2}{2mc} (\vec{p} \cdot \vec{A} + \vec{A} \cdot \vec{p}) \quad \text{D.7}$$

$$\text{Gauge } \vec{\nabla} \cdot \vec{A} = 0$$

The diamagnetic term in A^2 is very small for field less than several hundred thousand gauss.

The last term of eq. D.5 is

$$2\beta \vec{S} \cdot \vec{H} = -2\beta \vec{S} \cdot [\vec{\nabla} \times \vec{A}] \quad \text{D.8}$$

In eq. D.4 \vec{r}/r^3 can be written as $-\text{grad } 1/r$ then eq. D.8 is

$$2\beta\vec{S} \cdot \vec{\nabla} \times \vec{A} = -2\beta\vec{S} \cdot \vec{\nabla} \times (\vec{I} \cdot \vec{\nabla} 1/r) . \quad \text{D.9}$$

Singularities occur in both terms,

$$\nabla^2 1/r = 4\pi \delta(\vec{r})$$

where $\delta(\vec{r})$ is the Dirac delta function

$$\delta(\vec{r}) = 0, \quad \vec{r} \neq 0;$$

$$\int \delta(\vec{r}) d\vec{r} = 1 \quad \text{if volume of integration includes } r = 0.$$

To investigate the singularity in $(\vec{S} \cdot \vec{\nabla})(\vec{I} \cdot \vec{\nabla})1/r = K(\vec{r})$, the integral

$$N = \int_{V_\epsilon} K(\vec{r}) f(\vec{r}) d^3\vec{r} \quad \text{D.10}$$

is examined. $f(\vec{r})$ is any function which is continuous in the neighborhood V_ϵ : V_ϵ is a sphere of radius ϵ surrounding $\vec{r} = 0$. $K(\vec{r})$ contains two kinds of terms typically

$$(a) 2\gamma_n \beta S_x I_x \frac{\delta^2}{\delta x^2} 1/r \quad \text{and} \quad (b) 2\gamma_n \beta (S_x I_y + S_y I_x) \delta^2 / \delta x \delta y 1/r.$$

In $V_\epsilon f(\vec{r})$ can be expanded in a Taylor's series

$$f(\vec{r}) = f(0) + \vec{r} \cdot \vec{\nabla} f(0) + 1/2 (\vec{r} \cdot \vec{\nabla})(\vec{r} \cdot \vec{\nabla}) f(0) + \dots \quad \text{D.11}$$

where $\vec{\nabla}$ is the gradient operating only on f . All terms in D.10 are zero or of order ϵ^n , $n \geq 1$ except

$$2\gamma_n \hbar f(0) \int \left[S_x I_x \frac{\delta^2}{\delta x^2} (1/r) + S_y I_y \frac{\delta^2}{\delta y^2} (1/r) + S_z I_z \frac{\delta^2}{\delta z^2} (1/r) \right] d^3 r$$

Type (a) terms in $K(\vec{r})$ are even functions of x, y, z ; while $\vec{r} \cdot \text{grad } f$ is odd. The integral over the symmetric volume V_ϵ of odd integrands vanish. Terms resulting from products of type (a) terms and the third term of eq. D.11 are either even or odd. Odd terms integrate to zero and even terms are of order $1/r$ which by virtue of the volume $d^3 r = 4\pi r^2 dr$ integrate to terms of order ϵ^2 . Type (b) terms of $K(r)$ are odd in two variables (x and y) while $\vec{r} \cdot \text{grad } f$ contains only terms which are odd in a single variable. The products are then odd in at least one variable and integrate to zero. The oddness of type (b) terms also insure $f(0)$ times type (b) terms integrate to zero. Type (b) terms times the third term of D.11 integrate to order ϵ^2 terms. Thus

$$N = \sum_{x_i} \int_{V_\epsilon} 2\gamma_n \hbar f(0) \left[S_{x_i} I_{x_i} \frac{\delta^2}{\delta x_i^2} \right] \frac{1}{r} d^3 r + \phi(\epsilon)^2$$

Since V_e is symmetric

$$\begin{aligned} \frac{1}{3} \int_{V_e} \nabla^2 \frac{1}{r} d^3r &= \int_{V_e} \frac{\delta^2}{\delta x^2} \frac{1}{r} d^3r = \int_{V_e} \frac{\delta^2}{\delta y^2} \frac{1}{r} d^3r \\ &= \int_{V_e} \frac{\delta^2}{\delta z^2} \frac{1}{r} d^3r \end{aligned}$$

and

$$\begin{aligned} N &= 2\gamma_n \hbar \beta f(0) \int_{V_e} \vec{S} \cdot \vec{I} \frac{1}{3} \nabla^2 \frac{1}{r} d^3r = -4\pi (2\gamma_n \hbar \beta f(0)) \\ &\int_{V_e} \vec{S} \cdot \vec{I} \frac{1}{3} \nabla^2 \frac{1}{r} d^3r \end{aligned}$$

The hyperfine interaction between an electronic system of spin S and orbital momentum L and a nucleus of spin I is

$$\begin{aligned} H' &= 2\gamma_n \hbar \beta \vec{I} \cdot \vec{L} / r^3 - 2\gamma_n \hbar \beta f(\vec{S} \cdot \vec{V})(\vec{I} \cdot \vec{V}) / r \\ &+ 16\pi/3 \gamma_n \hbar \beta \vec{S} \cdot \vec{I} \delta(\vec{r}) \end{aligned} \quad \text{D.12}$$

The prime on the second term in 3.25 means matrix elements evaluated using this term exclude the origin. The second

term is more often written as

$$(\vec{S} \cdot \vec{\nabla})(\vec{I} \cdot \vec{\nabla}) \frac{1}{r} = \frac{\vec{S} \cdot \vec{I}}{r^3} - 3 \frac{(\vec{S} \cdot \vec{r})(\vec{I} \cdot \vec{r})}{r^5}$$

D.13

LIST OF LITERATURE CITED

- A. Abragam and M.H.L. Pryce, Proc. Roy. Soc. A, 205, 135 (1951).
- G. Arfken, Mathematical Methods for Physicists, Academic press, New York (1966).
- T.A. Bak, Editor, Phonons and Phonon Interactions, Benjamin, New York (1964).
- J.M. Baker, B. Bleaney and W. Hayes, Proc. Roy. Soc. A, 247, 141 (1958).
- J.M. Baker, W. Hayes, and M.C.M. O'Brien, Proc. Roy. Soc. A, 254, 273 (1960).
- D.N. Batchelder and R.O. Simmons, J. Chem. Phys. 41, 2324 (1964).
- G.L. Bir, Sov. Phys.-Solid State 5, 1628 (1964).
- G.L. Bir, E.I. Butikov, and L.S. Sochava, Sov. Phys.-Solid State 6, 1966 (1965).
- G.L. Bir and L.S. Sochava, Sov. Phys.-Solid State 5, 2637 (1964).
- M. Blume and R.O. Orbach, Phys. Rev. 127, 1587 (1966).
- M. Born and K. Huang, Dynamical Theory of Crystal Lattices, Oxford University Press, London (1954).
- L.S. Coombes, S.S. Ballard and K.A. McCarthy, J. Opt. Soc. Am. 41, 215 (1951).
- E.U. Condon and G.H. Shortley, The Theory of Atomic Spectra, Cambridge, London (1935).
- D.H. Dickey, M.S. Thesis, Montana State University (1966).
- D.H. Dickey, Ph.D. Thesis, Montana State University (1969).
- J.E. Drumheller, Unpublished Tables of $O_{\frac{1}{4}}$ and $O_{\frac{1}{6}}$, (1969).

- J.E. Drumheller and R. Rubins, *Phys. Rev.* 133 A, 1099 (1964).
- M. Fierz, *Physica* 5, 433 (1938).
- C.B.P. Finn, R. Orbach and W.P. Wolf, *Phys. Soc. (London)*, A 77, 261 (1961).
- I.M. Gel'fand, R. Minlos and Z. Shapiro, Representations of the Rotation and Lorentz Groups and their Applications, Tran. G. Cummins and T. Boddington, Macmillan, New York (1963).
- H. Goldstein, Classical Mechanics, Addison-Wesley, Reading Mass. (1959).
- J.S. Griffith, The Theory of Transition-Metal Ions, Cambridge, London (1961).
- W. Hayes, Paramagnetic Resonance of Transition Metal Ions in Crystals, unpublished lecture notes given at the University of North Carolina, Chapel Hill (1963).
- V. Heine, Group Theory in Quantum Mechanics, Pergamon Press, New York (1960).
- F. Herman and S. Skillman, Atomic Structure Calculations, Prentice-Hall, Inc., Englewood Cliffs, N. J. (1963).
- P. Ho and A. Ruoff, *Phys. Rev.* 161, 864 (1967).
- K. Horai, *J. Phys. Soc. Japan* 19, 2241 (1964).
- C. Huang and M. Inoue, *J. Phys. Chem. Solids* 25, 889 (1964)
- D. Huffman and M. Norwood, *Phys. Rev.* 117, 709 (1960).
- W. Hurren, H. Nelson, E. Larson, and J. Gardner, *Phys. Rev.* 185, 624 (1969).
- D. Jones, J. Baker, and D.F.D. Pope, *Proc. Phys. Soc.* 74, 249 (1959).
- R. de L. Kronig, *Physica* 6, 33 (1939).
- R. Lacroix, *Helv. Phys. Acta* 30, 354 (1957).

- L.D. Landau and E.M. Lifshitz, Quantum Mechanics- Non-Relativistic, Pergamon Press, London (1958).
- W. Low, Paramagnetic Resonance in Solids, Academic Press, New York (1960).
- A.A. Manenkov and R. Orbach, Spin-Lattice Relaxation in Ionic Solids, Harper and Row, New York (1966).
- T.J. Menne, Phys. Rev. 180, 350 (1969).
- T.J. Menne, D. P. Ames, and Sook Lee, Phys. Rev. 169, 333 (1968).
- A. Messiah, Quantum Mechanics Vol. I and II, Trans. G. Temmer, Wiley, London (1960).
- F.J. Milford, Am. J. Phys. 28, 521 (1960).
- G. Pake, Paramagnetic Resonance, Benjamin, New York (1962).
- C.P. Poole Jr., Electron Spin Resonance, Interscience, New York (1967).
- M.H.L. Pryce, Proc. Phys. Soc. A 63, 25 (1950).
- T. Rewaj, Sov. Phys.-Solid State 9, 2340 (1968).
- K. Shrivastava, Phys. Letters 31 A, 454 (1970).
- K. Shrivastava and J. Drumheller, Phys. Rev. 184, 271 (1969).
- E. Simanek and Nai Li Huang, Phys. Rev. Letters 17, 699 (1966).
- E. Simanek and R. Orbach, Phys. Rev. 145, 191 (1966).
- J. Stice and D. Worsencroft, Proc. Mont. Acad. Sci. 30, (1970)
- M. Tinkham, Group Theory and Quantum Mechanics, McGraw-Hill, New York (1964).
- J.H. Van Vleck, J. Chem. Phys. 7, 72 (1939).

J.H. Van Vleck, Phys. Rev. 57, 426 (1940).

J.H. Van Vleck and W.G. Penney, Phil. Mag., 19, 961 (1934).

I. Waller, Ziets. F. Physik, 79, 370 (1932).

W.M. Walsh Jr., J. Jeener, and N. Bloembergen, Phys. Rev. 139, A, 1338 (1965).

Zavoishy, J. Phys., U.S.S.R. 9, 211 (1945).

J.M. Ziman, Principles of the Theory of Solids,
Cambridge, London (1965).

